UNIVERSITÉ DE LORRAINE

école doctorale RP2E

THÈSE

présentée et soutenue publiquement le 14 Novembre 2012
pour l'obtention du grade de

Docteur de l'Université de Lorraine
Spécialité Géosciences

par

Florent LALLIER

Corrélation stratigraphique stochastique de puits

Directeur de thèse :	Jean Borgomano
Co-directeur de thèse :	Guillaume Caumon
	Sophie Viseur

Composition du jury :

Rapporteurs :	Jef Caers
	Philippe Joseph
Examinateur :	Emmanuelle Vennin
Invité :	Julien Charreau

Centre de Recherches Pétrographiques et Géochimiques
Rue du Doyen Marcel Roubault - 54500 Vandoeuvre lès Nancy

Remerciements

Voici donc venu l'heure d'écrire les dernières lignes de cette thèse.

Je tiens tout d'abord à remercier Emmanuelle Venin d'avoir accepté présider mon jury de thèse, que Jeff Caers et Philippe Joseph d'avoir accepté rapporter mes travaux de thèse, ainsi que Julien Charreau d'avoir accepté de participer à ce jury. Je vous remercie également et tout particulièrement pour la discussion qui a suivi mon exposer.

Mes remerciements vont ensuite à mes directeurs de these. Un grand merci à Guillaume Caumon qui m'a guide dans le monde de la Géomodélisation depuis mes débuts. Merci Chef pour ta confiance et pour m'avoir laissé autant de liberté. Un grand merci également à Sophie Viseur, ton enthousiasme et tes conseilles avisés m'ont été d'une grande aide. Un grand merci enfin à Jean Borgomano. Merci d'avoir accepté de diriger ma thèse et merci fait découvrir la géologie des systèmes carbonatés. Je remercie Julien Charreau pour m'avoir ouvert les portes de la magnétostratigraphie. Merci de m'avoir fait découvrir une face pour moi inconnue de la géologie. Merci également a Christophe Antoine pour tout ce tu as apporté à ce projet magneto' mais aussi pour tout ce que tu as apporté à cette thèse en général.

Je remercie aussi tous les membres de l'équipe de recherche Gocad, les CPRGiens et les Marseillais. Fatima, merci pour tout, pour les petits et les grands coups de main. Merci Pierre et encore une fois non, ce n'ai pas moi qui ai fait planter les ordinateurs. Merci Pauline (CD) pour toute les discussions, les rires et les blagues et le soutient au quotidien. Et merci à Christine, parce que tu as été ma première prof d'informatique et parce que j'aimais te croiser pour un café.
Merci aux co-thesards, compagnons de luttes gocadiennes, les anciens et les nouveaux. MarcO – le plus ancien de tous et mon premier chef ; Thomas et Vincent - les co-bureaux et champions de volleyball ; Jeanne – merci pour tes multiples relectures jusqu'à l'ultime, 30 minutes avant la soutenance ; Francois – ou Fifid'Or, et avec toi Julie et Arthur ; Romain et Jeremy ; Charline – un énorme merci pour tout ce que tu as apporté à cette thèse, Gauthier – je ne comprends toujours pas comment ils font pour prendre un bain avec simplement un mini morceau de tissus blanc ; Cécile – merci de m'avoir héberge et d'avoir supporté mon ignorance de la suisse. Merci à Nico Cherpeau, co-these et co-loc, compagnon de route tropico depuis le début, merci pour les coups de main et les à-côtés. Et puis merci à Pauline (DR), merci pour tes conseils, les innombrables relectures, ton soutient, et surtout merci d'avoir été la du début à la fin.

Je remercie également les « autres », ce qui aussi on fait le quotidien de Nancy ou de Marseille, qui ont fait que c'était chouette et que ce soit triste que ça soit fini : Michel, Chouffe, Julien aka Bidman – coloc' numéros 2 et l'homme aux meilleures histoires drôles

de la terre (ou pas...), Julien le vieux, PH, Camille, Bibi, Noémie, Laurette, Marianne, Sophie et tous les autres.

Je finirai en remerciant ce qui était là au tout début, ma sœur Pauline, mes Parents, ma et mon nourrisse et tous les autres. Merci, de m'avoir soutenu, d'avoir été la et de m'avoir laissé aller ou bon me semblais.

Merci à toutes et à tous, et à très très bientôt !

Table des matières

Table des figures

Liste des tableaux

Introduction

La représentation du sous-sol, qu'elle soit numérique ou analogique, géométrique ou physique, est construite dans deux buts : comprendre et prédire. Lors de l'étude d'un objet géologique, plusieurs représentations peuvent en être proposées en fonction de la problématique envisagée. Plusieurs exemples peuvent être donnés :

- L'étude d'un réservoir (pétrolier ou aquifère) a pour buts de prédire : (i) la capacité contenue ; et (ii) la circulation des fluides (dans une perspective de production ou de diffusion de contaminant). À chaque fois, modéliser le réservoir consistera à déterminer la répartition des hétérogénéités lithologiques ou pétrophysiques.
- Pour comprendre l'histoire du remplissage d'un bassin sédimentaire, le géologue s'intéressera à construire un modèle représentant les isochrones et ainsi sont évolution temporelle. Le remplissage d'un bassin sédimentaire étant contrôlé par des facteurs tectoniques, environnementaux et climatiques, sa représentation temporelle permet de prédire les paléoclimats, reliefs ou paysages.
- Dans une étude géotechnique, on s'intéresse à représenter les caractéristiques mécaniques du sous-sol. Cette représentation sert de base pour prédire la réponse du sous-sol lors de la construction d'un ouvrage d'art.

Depuis les années 1990 et sous l'impulsion du développement d'une nouvelle génération de logiciels dédiés aux problématiques géologiques, la représentation du sous-sol passe par la construction de modèles tridimensionnels associant géométrie des objets géologiques et propriétés physiques. Les données et informations disponibles pour la construction d'un géomodèle sont de natures diverses. On peut ainsi distinguer :

- les données d'affleurements ou issues de forages carottés. Il s'agit de données directes permettant une description lithologique à fine échelle. Les caractéristiques physiques des roches étudiées peuvent y être mesurées précisément en laboratoire sur des échantillons (appelés plugs) prélevés. Ces données, localisées et peu nombreuses, n'offrent qu'une vision limitée de la géométrie tridimensionnelle des objets étudiés ;
- Les données de puits : diagraphie et imagerie. Ces données permettent, après interprétation, d'accéder à la description des types de roches rencontrées et à certaines de leurs caractéristiques. Comme pour les affleurements, les données de puits sont localisées et souvent peu nombreuses ;
- Les données géophysiques telles que l'imagerie sismique, 2D ou 3D, les données issues de mesures gravimétriques ou électromagnétiques. Ces données sont globales mais de faible résolution et peuvent amener à des interprétations contradictoires Bond et al. [2007] ;
- Les concepts géologiques, tel que les concepts de stratigraphie séquentielle, conférant un cadre théorique à l'interprétation des données observables ;
- Les connaissances régionales ou issues d'analogues (actuels ou non).

Construire un géomodèle, c'est mettre en cohérence l'ensemble des données et connaissances disponibles. Les données disponibles sont cependant locales, de résolution inférieure au modèle souhaité, ou ambigües. De plus, les objets géologiques étudiés ont été mis en place par des processus nombreux, interdépendants et souvent mal connus voire inconnus. Il en résulte que, à partir de mêmes données et de mêmes informations, plusieurs représentations du sous-sol étudié peuvent être proposées. C'est dans ce contexte qu'intervient le concept d'incertitude en géomodélisation, c'est-à-dire lorsque le manque d'informations ou le manque de qualité de celles-ci ne permet pas d'en construire un seul et unique modèle.

Les méthodes géostatistiques telles que les simulations gaussiennes séquentielles (SGS), les simulations séquentielles d'indicatrices (SIS), les simulations par gaussiennes tronquées [Deutsch et al., 1998] et les méthodes basées objet [Deutsch and Wang, 1996, Viseur, 2004], entre autres, sont des exemples de méthodologies permettant de gérer les incertitudes en géomodélisation. Dans le cas de la modélisation de propriétés pétrophysiques, les simulations permettent de générer un grand nombre de réalisations (en théorie, un nombre infini) en tenant compte des données disponibles : valeur de propriétés au puits, données géophysiques (dans le cas de co-simulations), histogrammes et variogrammes. Dans cet exemple, plusieurs sources d'incertitudes peuvent être identifiées :

- le manque de données : seuls les puits, souvent peu nombreux, fournissent des valeurs précises de propriétés ;
- Le manque de résolution des données secondaires dans le cas de co-simulations ;
- La qualité des mesures, que ce soit pour les données géophysiques ou pour les mesures aux puits ;
- Le variogramme utilisé. En effet, dans le cas d'études de réservoir pétrolier, le variogramme est modélisé à partir de peu de points de données. Ainsi, pour être construit, le modèle de variogramme utilisé nécessite une interprétation de la part du géologue, intégrant entre autres des connaissances issues d'analogues ;
- L'espace dans lequel sont calculées les distances. En effet, dans le cas d'hétérogénéités liées aux faciès de dépôt par exemple, la distance entre des points correspond à la distance stratigraphique définie par la géométrie et la topologie des horizons et failles interprétés par le modélisateur. Cette géométrie, construite à partir des données citées précédemment, est elle-même sujette à incertitudes.

Problématique de la modélisation stratigraphique

Les travaux présentés dans ce mémoire s'inscrivent dans le contexte défini par les deux points précédent, c'est-à-dire les incertitudes liées à la subjectivité des interprétations proposées par le géologue, et celles liées à la géométrie et à la topologie des frontières des différent objets géologiques étudiés. Dans le cas de roches sédimentaires, ces frontières sont issues de deux types de processus : les processus sédimentaires contrôlent la géométrie (en partie) et la topologie des horizons stratigraphique, les processus tectoniques contrôlent la

géométrie et la topologie des réseaux de failles et des horizons stratigraphiques (directement lorsqu'on s'intéresse aux plissements et indirectement via le contrôle structural des processus sédimentaires).

Nous nous intéressons dans ce mémoire à la topologie des horizons stratigraphiques. Celle-ci est définie par la corrélation stratigraphique d'unités identifiées au niveau des puits. Cette étape de corrélation stratigraphique est l'une des premières du processus de construction d'un géomodèle dans les formations sédimentaires. Elle consiste à associer les différentes unités stratigraphiques identifiées le long des puits et affleurements disponibles. Ces unités stratigraphiques sont définies de sorte qu'elles représentent chacune un ensemble cohérent reflétant par exemple : une séquence de dépôts (cas de la stratigraphie séquentielle), une même lithologie (cas de la lithostratigraphie), un même ensemble de caractéristiques pétrophysiques ou encore une même paléo-orientation du champ magnétique terrestre (cas de la magnétostratigraphie). Dans le processus de corrélation stratigraphique, le géologue est confronté à deux choix distincts :

1. Quelle règle utiliser pour définir les unités stratigraphiques ? Ce choix est dicté par les facteurs contrôlant les caractéristiques du sous-sol que l'on cherche à représenter. Par exemple, dans le cas de l'étude d'un réservoir pétrolier, le géomodèle est utilisé pour représenter les hétérogénéités pétrophysiques des roches. Les hétérogénéités pétrophysiques peuvent être contrôlées par exemple par (i) les faciès de dépôts – les principes de stratigraphie séquentielle pourront alors être utilisés pour définir les unités stratigraphiques à corréler ; ou (ii) par la diagenèse ayant affecté les roches après leur dépôt – une approche lithostratigraphique pourra alors être choisie.
2. Comment sont associées, entre les puits, les différentes unités stratigraphiques identifiées ? Il s'agit de la problématique de corrélation stratigraphique, abordée dans ce mémoire. Cette étape clé définit la topologie et en partie la géométrie des horizons stratigraphiques correspondant aux frontières des objets géologiques étudiés. Selon le schéma de construction d'un géomodèle le plus répandu, la construction des corrélations stratigraphiques est confiée à un géologue stratigraphe qui, manuellement et de façon déterministe, définit les associations entre unités stratigraphiques. Considérant les remarques qualitatives et quantitatives faites précédemment sur les informations et connaissances disponibles pour résoudre le problème de corrélation stratigraphique, nous suggérons dans ce mémoire de le traiter de façon stochastique afin d'échantillonner les incertitudes associées.

À partir d'un algorithme général de corrélation stochastique dérivé de l'algorithme de déformation temporelle dynamique (plus connu sous le nom anglais : Dynamic Time Warping algorithm), différentes règles de corrélation stratigraphique sont proposées afin de traiter plusieurs cas naturels. Ce mémoire s'organise autour de quatre articles ayant chacun pour cadre d'étude un système naturel différent. Chacun de ces articles décrit : (i) l'algorithme général utilisé pour générer de façon stochastique les corrélations stratigraphiques ; (ii) les adaptations de cet algorithme afin de prendre en compte les

particularités de l'application ; (iii) les règles de corrélation stratigraphique utilisées.

Le premier chapitre sert d'introduction à la problématique de corrélation stratigraphique. Une première présentation de la méthode stochastique de corrélation stratigraphique est proposée. À partir de l'étude des séquences de dépôts de la plateforme carbonatée Sud-Provençale d'âge Crétacé supérieur, une méthode multi-puits et stochastique de corrélation de séquences stratigraphiques est présentée. Deux règles de corrélation des horizons bordant les séquences de dépôts sont introduites. Celles-ci s'appuient sur les caractéristiques géométriques théoriques de l'environnement de dépôt : évolution cohérente des paléo-angles et des épaisseurs de sédiments déposés ; représentation théorique de l'espace de dépôt.

Le second chapitre s'intéresse à l'impact des incertitudes liées aux corrélations stratigraphiques sur la modélisation statique et dynamique du réservoir carbonaté de Malampaya (situé au Nord-Ouest de l'île de Palawan aux Philippines). Pour ce faire, deux règles de corrélation basées sur la réponse diagraphique des unités stratigraphiques (unités diagénétiques dans ce cas) et sur le type lithologique sont proposées. Plusieurs modèles de réservoir, construits à partir de différents modèles de corrélation générés de façon stochastique, sont construits et analysés en fonction de leur comportement dynamique et de leur réponse sismique.

Une méthodologie permettant de prendre en compte les données issues de l'imagerie sismique est proposée dans le chapitre trois. Cette méthodologie, couplée à une règle de corrélation basée sur les tendances présentes au niveau des enregistrements diagraphiques, est appliquée à la corrélation stratigraphique de dépôts fluviaux deltaïques de la Mer du Nord.

Enfin, une méthode de gestion et de visualisation des incertitudes dans le cas des corrélations magnétostratigraphiques est proposée en chapitre quatre. Nous proposons alors de calculer les n meilleures corrélations entre une colonne magnétostratigraphique issue d'études de terrain et une colonne de référence, permettant ainsi de dater les sédiments étudiés et d'estimer les paléo-taux d'accumulation de sédiments et les incertitudes associées.

Chapitre 1

Stratigraphie séquentielle et méthodes stochastiques de corrélation stratigraphique de puits

Sommaire

La construction de corrélations stratigraphiques, dans le cadre d'une étude de réservoir ou de bassin, permet notamment de subdiviser le volume étudié en sous-ensembles où les variables étudiées (faciès ou propriétés pétrophysiques) répondent aux critères de stationnarités nécessaires à la plupart des méthodes géostatistiques utilisées pour simuler ces variables. Dans ce contexte, l'utilisation des concepts définis par la stratigraphie séquentielle pour construire ces corrélations apporte une aide précieuse.
Ceci est d'autant plus vrai lors de l'étude de réservoirs ou bassins carbonatés où la répartition spatiale des sédiments résulte de processus sédimentaires nombreux et interdépendants. Ainsi, compte tenu de la complexité de l'architecture stratigraphique résultante, la construction de corrélations stratigraphiques entre les différents puits ou affleurements disponibles est sujette à de nombreuses incertitudes. Nous proposons ici de prendre en compte ces incertitudes en utilisant une méthode stochastique pour générer ces corrélations stratigraphiques. Cette méthode est basée sur l'algorithme de déformation temporel (ou Dynamic Time Warping, DTW), qui a déjà été utilisé qvec succès la corrélation de séries ordonnées

en bio-informatique et en reconnaissance de la parole. Trois versions de cet algorithme sont proposées dans ce chapitre : (i) une version stochastique permettant de générer plusieurs modèles probables de corrélation ; (ii) une version multi-puits utilisant un tableau à n dimensions afin construire des modèles de corrélations stochastiques entre n puits ; (iii) une version itérative permettant corréler stochastiquement n puits. Cette dernière méthode requiert moins de mémoire vive et permet ainsi de corréler un grand nombre de puits. De plus, une approche hiérarchique est proposée, les unités stratigraphiques d'ordre inférieur sont corrélées en premier et les corrélations résultantes sont utilisées pour contraindre la corrélation des unités d'ordre supérieur. Dans ce chapitre, l'algorithme DTW est utilisé afin de construire des modèles de corrélation respectant les règles de stratigraphie séquentielle. Deux règles de corrélation sont proposées pour assurer la cohérence des paléo-angles et celle entre les faciès décrits aux puits et la paléo-géographie supposée du milieu de sédimentaire étudié.
La méthode proposée est appliquée dans ce chapitre à la corrélation d'unités stratigraphiques identifiées le long des affleurements de la marge carbonatée sud-provençale d'âge Crétacé Supérieur.

Uncertainty assessment in stratigraphic well correlation : a new stochastic method for carbonate reservoir

Article to be submitted to the AAPG Bulletin

Florent Lallier , Guillaume Caumon , Jean Borgomano , Sophie Viseur, Jean-Jacques Royer and Christophe Antoine.

Abstract

An application of well correlation is to subdivide a reservoir into stationary intervals to support geostatistical modelling of static reservoir properties. In this scope, sequence stratigraphic well correlation appears to be an efficient technique, especially in carbonate sedimentary systems resulting from numerous and interdependent genetic processes. However, due to the complexity of sedimentary layers, well correlation is a hazardous process which is subject to many uncertainties. In this work, we propose to account for these uncertainties by generating several possible realizations of well correlations. The method is based on the Dynamic Time Warping (DTW) algorithm, whose efficiency has already been demonstrated in speech recognition and bio-informatics. Three derivative versions of the DTW algorithm are introduced : a stochastic one for correlating two wells (2D DTW) ; a multi-well one, which accounts for the 3D organization of stratigraphic architectures by analysing all input wells at once. Due to computation time and memory requirements, this version is limited to the correlation of up to ten wells. To address this issue, an iterative multi-2D DTW based on well correlation propagation is proposed. In addition, the proposed algorithms integrate stratigraphic order of well markers to perform the well correlation hierarchically (low frequency stratigraphic events are correlated first, and then are used to constrain the correlation of higher-order events). To perform stratigraphic correlation with DTW algorithms, one has to compute the likelihood of each possible horizon. Because of the high significance of chronostratigraphy in siliciclastic and carbonate reservoir modeling, the presented likelihood computation is based on paleo-angles consistency and facies and sedimentary profile coherency. This stochastic correlation algorithm and the influence of stratigraphic correlation uncertainties on static reservoir modelling are demonstrated on outcrop data of the Cretaceous southern Provence Basin (Provence, S-E France).

Introduction

Well data represent 1-D information about subsurface heterogeneities. Because wells are often placed in potentally high-pay areas the set of available wells, reduced to the minimum due to drilling costs, is thus often sparsely spread over the study area and corresponds to an incomplete and possibly biased sampling of the subsurface objects and heterogeneities. As defined by Doveton [1994a] manual methods for well correlation are slow, highly labor-intensive, sometimes inconsistent and are often subject to uncertainty. Moreover, as demonstrated by Bond et al. [2007] for seismic interpretation, knowledge introduced to fill the lack of data may introduce bias depending on interpreter's background. As a consequence, well correlation is an under-constrained problem, leading to several possible results (sets of correlation).

Stratigraphic well correlation aims at linking correlative units between available wells [Doveton, 1994a] and thus helps defining the 3D structure of the studied reservoir or basin. In practice, a 3D geometrical model of the studied reservoir or basin is built from well correlations which define stratigraphic architecture and horizons and faults picked on a

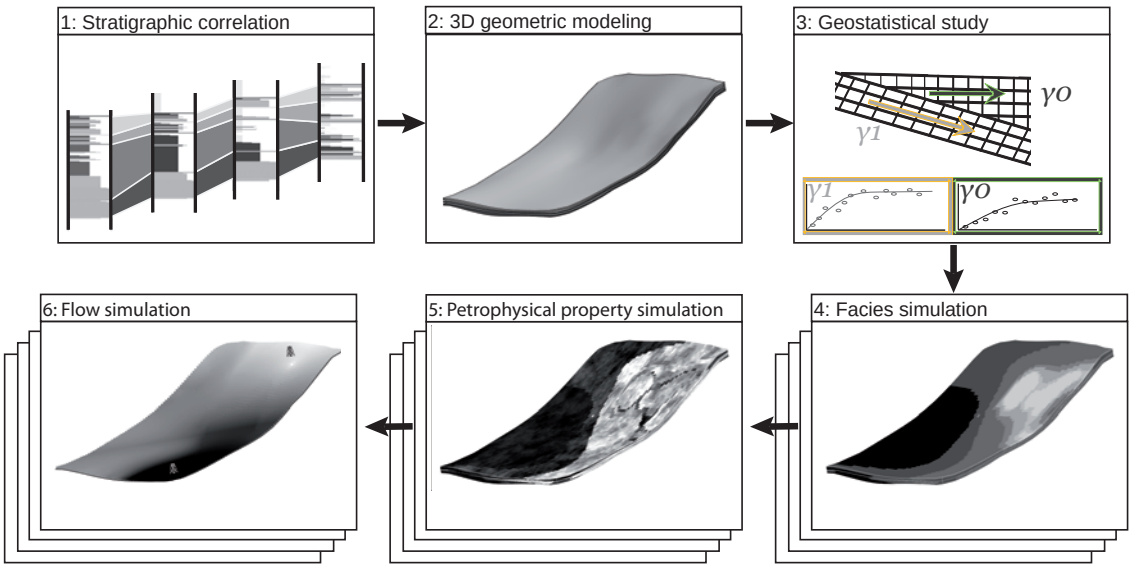

FIGURE 1.1 – Simple reservoir modeling workflow. Stratigraphic correlations constrain the geometry of the grid that will support geostatistical analysis and facies and rock property modeling.

seismic survey (Fig.1.1). This geometrical model is used to control the construction of a grid on which two types of coordinates are defined [Dubrule and Damsleth, 2001, Deutsch, 2002] : the absolute coordinates (x, y, z) and the stratigraphic coordinates (u, v, w) which are use to perform geostatistical analysis and property modelling. Uncertainties on well correlation, which affect stratigraphic coordinates result on uncertainties on petrophysical property modelling, definition of flow units and thus may have a high impact on hydrocarbon resource assessment and production prediction.

Uncertainties on a 3D reservoir model can be achieved by generating several possible models which then serve for OHIP computations or reservoir simulations [Samson et al., 1996] [Charles et al., 2001]. For example, to handle structural uncertainties, Lecour et al. [2001] propose to perturb the geometry of the reference model, Holden et al. [2003], Cherpeau et al. [2010] stochastically generate fault networks. However, for stratigraphic well correlations, in our knowledge, no stochastic method hence perturb both the model's topology and the geometry taking uncertainties into account has been proposed.

Our objective is to introduce a numerical method to build stochastically stratigraphic well correlations. Algorithm frequently used to build stratigraphic correlation automatically are reviewed in section 1.1.2. In this study, the Dynamic Time Warping algorithm [Myers and Rabiner, 1981] is used. Derivative versions of this algorithm to perform stochastic, hierarchical and multi well correlation are presented in section 1.2.

Well correlation may be achieved in different ways, and using different well descriptors (markers, facies, wireline logs, etc.). Several authors propose computer aided approaches to perform correlations between wells on the basis of logs [Zoraster, 2004] or lithostratigraphic

description [Griffiths and Bakke, 1990, Olea, 2004]. In the case of few wells spread over the area of study, the relevance of sequence stratigraphic well correlation as a basis for 3D static reservoir modelling has been demonstrated by Ainsworth et al. [1999], Ainsworth [2005] for siliciclastic settings and by Borgomano et al. [2008] for carbonate environment. Therefore, in this paper, we consider well data which correspond to sequence stratigraphic intervals identified from the depositional facies. The method proposed in this paper allows to stochastically correlate stratigraphic sequences according to sedimentological rules.

After reviewing numerical methods for well correlation problem (section 1.1), specific algorithms for multi-well stochastic stratigraphic well correlation are presented in section 1.2. Correlation rules and application of the stochastic approach to Cretaceous outcrops of the southern Provence Basin (South-East France) is presented in section 1.3.

1.1 Motivation and related works

1.1.1 Need for a stochastic approach

Combinatorial point of view. Considering two wells with respectively n and m identified stratigraphic markers and assuming that top and bottom markers of each well are correlated together, the number ($D_{n,m}$) of possible correlations between these two wells is given by the Delanoy number defined as :

$$\begin{aligned} D_{n,m} &= D_{n,m-1} + 2\sum_{i=0}^{n-1} D_{i,m-1} \\ D_{1,1} &= D_{1,n} = D_{1,m} = 1 \end{aligned} \tag{1.1}$$

This equation can be extended in d dimensions, i.e. to enumerate the number of correlations between d wells with respectively n_i markers per well as follows :

$$\begin{aligned} D_{n_1,\cdots,n_d} \;=\; & D_{n_1-1,\cdots,n_d} \;+\; D_{n_1,n_2-1,\cdots,n_d} \;+\; \cdots D_{n_1,\cdots,n_d-1} \\ & + D_{n_1-1,n_2-1,\cdots,n_d} \;+\; \cdots \;+\; D_{n_1-1,n_2,\cdots,n_d-1} \\ & \cdots \\ & + D_{n_1-1,\cdots,n_d-1} \end{aligned} \tag{1.2}$$

Two simple examples can highlight the practical meaning of these equations :

- Per equations 1.1, the number of possible correlations between two wells, with only ten markers on each well,is equal to $D_{10,10} = 1,462,563$ possible correlations.
- Stratigraphic correlation of twelve wells with respectively seven markers on each, Eq.(1.2) leads to 10^{80} possible correlation models, which is equivalent to the number of atoms in the universe.

Among this huge set of possible well correlations, only some of them are geologically sound and it is very difficult to explore and to appreciate manually the different plausible solutions of well correlation. The use of a stochastic method able to account for geological constraints to generate well correlation models would hence appear to be an appreciable tool to sample the possibly large set of plausible correlations.

A geologic point of view. In spite of sedimentological rules used to perform well correlation, interpreters often face ambiguities between many different plausible correlations. As shown by Borgomano et al. [2008] and Koehrer et al. [2011], when available wells do not allow to relate the subsurface heterogeneities several sets of well correlation may match sedimentological rules.
In the case of low average-angle carbonate ramp or platform, performing sequence stratigraphic well correlation consists in correlating meter thick sequences between kilometers-apart wells. Many stratigraphic sequences observed along borehole are beyond seismic resolution and have to be correlated on the basis of stratigraphic rules. However, due to the thickness of sequences to correlate, distances separating wells, and uncertainty on angle of paleo-sedimentary profiles, well correlation becomes uncertain (Fig.1.2). It follows that, given a range of possible average paleo angles, alternative well correlation models can be built.

1.1.2 Automatic well correlation, a review

Many authors, following the work of Sackin et al. [1965], proposed numerical methods to automatically perform well correlations. Such automatic methods are essential to handle uncertainties. A review of numerical methods used to perform well correlation is proposed by Doveton [1994a]. Three mains algorithms are described in the literature :

- The Dynamic Time Warping algorithm which is derived from bio-informatic and speech recognition [Levenshteiti, 1966, Myers and Rabiner, 1981] is used by Smith and Waterman [1980] to build the lithostratigraphic correlation of two outcrops located in Kansas.
- Neural networks are used by Bursik and Rogova [2006] to perform the lithostratigraphic correlation of volcano deposits.
- Expert systems are used by Olea [1994, 2004] for the correlation and interpretation of wireline logs.

This work focuses on the Dynamic Time Warping algorithm that is based on a representation of the correlation between two wells in a 2D table. Considering two wells W_1 and W_2 with respectively n and m stratigraphic markers, the stratigraphic correlation between these two wells is represented as a path in a cost table D (Fig.1.3A and B) built up with a series of points and transitions (respectively correlation of markers and intervals). The geological consistency of each possible correlation between markers and between units and each possible unconformity is evaluated independently thank to the computation of a cost. These costs are stored in the table as follows :

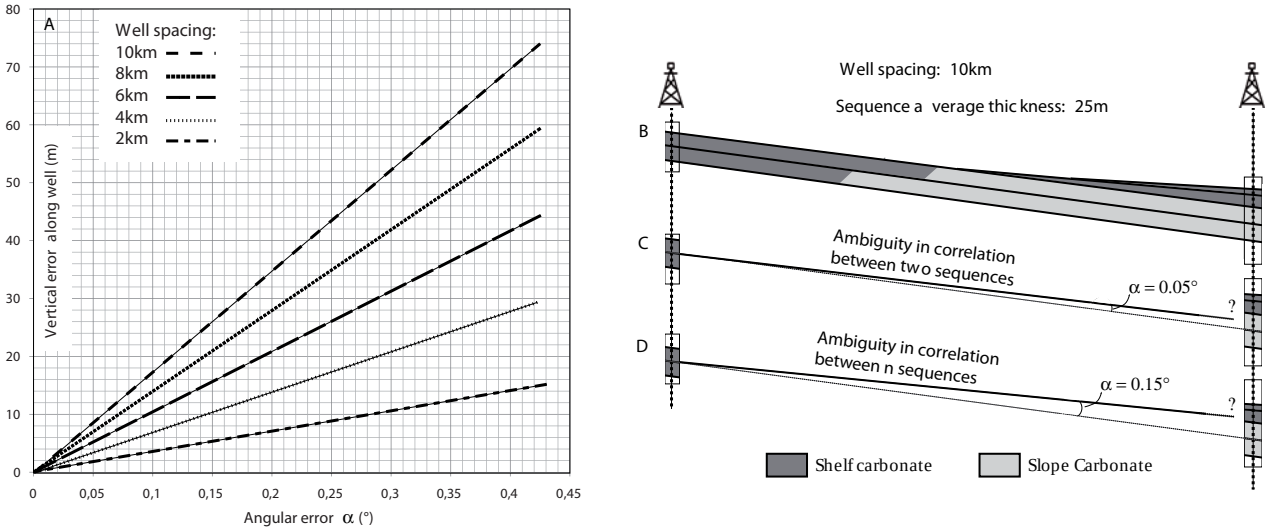

FIGURE 1.2 – In the case of carbonate ramp characterized by low average angle carbonate ramp, uncertainty α on average angle impacts well correlation. (A) Impact of errors in average paleo-angles on error in position of the horizon along the well for different well spacings. (B) Given a synthetic model of carbonate ramp (B), (C) An error of 0.5° in the evaluation of the average paleo-angle results on ambiguities on the correlation between two units 10m thick between (C). When the angular error reaches 0.15°, the ambiguity is between three units (D).

- A point at cell (i, j) corresponds to the correlation between the marker i of the first well W_1 and the marker j of the second well W_2 with a cost $c(i, j)$.
- An oblique transition corresponds to a correlation between two intervals (the interval $\{i; i-1\}$ of W_1 and the interval $\{j; j-1\}$ of W_2) with a cost noted $t_{i,i-1}^{j,j-1}$ in Eq.(1.3).
- A vertical transition between cells (i, j) and $(i-1, j)$ means that the interval $\{i; i-1\}$ of W_1 end in an unconformity between units $j; j-1$ and $j+1, j$ of W_2. This unconformity is associated to a cost noted $t_{i,i-1}^{j,j}$. An horizontal transition corresponds to an unconformity with a cost $t_{i,i}^{j,j-1}$.

The total score of a path is calculated as the sum of all the costs c and t contained in this path. The minimum cost path from the bottom left cell (bottom correlation line $[1, 1]$) to the top right cell (top correlation line $[n, m]$) corresponds to the optimal correlation between W_1 and W_2. The minimum cost correlation path through the table is obtained by computing iteratively the minimum cost path from the bottom right cell to the cell (i, j) thanks to :

$$D(i,j) = c(i,j) + \min \begin{pmatrix} t_{i,i-1}^{j,j-1} + D(i-1, j-1) \\ t_{i,i-1}^{j,j} + D(i-1, j) \\ t_{i,i}^{j,j-1} + D(i, j-1) \end{pmatrix} \tag{1.3}$$

Once the entire DTW cost table has been filled, the correlation path is searched starting at cell $[n; m]$ as shown in figure 1.3. The next cell is the one with the minimun cost, between the three adjacent cells (on the left, bottom and diagonally to the bottom-left). The search then continues from this cell, using the same rule, until the bottom left is reached. This construction method makes the correlation path unidirectional, ensuring there is no overlap. The correlation is thus consistent.

As shown by Bashore et al. [1994], the choice of the correlation strategy has a great impact on static and dynamic reservoir modelling. In DTW the obtained stratigraphic architecture depends on correlation rules use to evaluate the consistency of correlation between units or markers. Many studies on automatic well correlation based on the DTW algorithm focused on the development of these correlation rules [Smith and Waterman, 1980, Howell, 1983, Waterman and Raymond Jr., 1987, Fang et al., 1992a, Collins and Doveton, 1993]. Fang et al. [1992a] perform the correlation of stratigraphic units on the basis of wireline log attributes, Griffiths and Bakke [1990] define numerical lithologies based on gamma-ray, density, neutron and velocity log responses and perform correlation between wells using gene typing rules including the possibility of lateral facies substitution. Waterman and Raymond Jr. [1987] define rules on the basis of lithostratigraphic type, grain size and units thickness and Collins and Doveton [1993] compute the likelihood of the correlation between two units thanks to a vertical Markov transition analysis along well. These methods are mainly based on a lithostratigraphic description of facies. As a result, the probability of the correlation of two units is the same for wells 10km appart than for wells 1km apart.

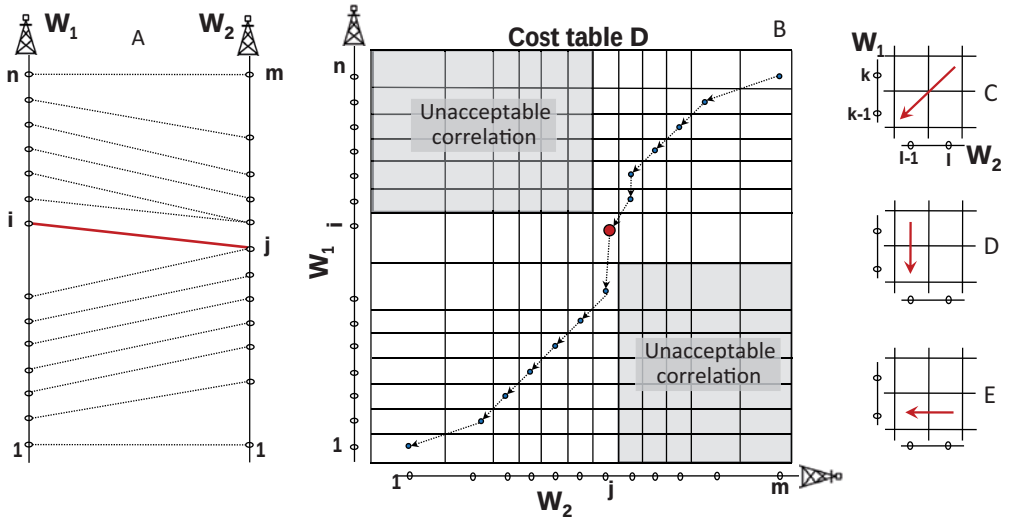

Figure 1.3 – 2D DTW for stratigraphic correlations. A) Stratigraphic correlation between two wells W_1 and W_2 containing respectively n and m markers. The thick line is the correlation between the i^{th} marker of W_1 and the j^{th} marker of W_2 (correlation line $[i; j]$) which is is assumed to be known a priori. B) DTW cost table D displaying the minimum cost correlation path. Due to the hard correlation $[i; j]$ (thick point in the table), two parts of the cost table are removed, these positions corresponding to impossible correlations. C, D and E : elements to evaluate to perform stratigraphic correlation within the DTW algorithm ; correlation between units $\{k; k-1\}$ of W_1 and $\{l; l-1\}$ of W_2, units $\{k; k-1\}$ of W_1 ends in an unconformity and units $\{l; l-1\}$ of W_2 ends in an unconformity.

1.2 Proposed framework for sequence stratigraphic correlation

1.2.1 Key points of the proposed approach

Considering well data as a ranked list of stratigraphic markers, stochastic well correlation may be seen as a method that stochastically links well markers of different wells one with another. Geologists use sedimentological rules and regional knowledge to obtain geologically sound correlations. Depending on these rules and constraints, a correlation between two well markers would appear more plausible than other ones. Similarly, in our method the correlation process first evaluates the likelihood of all possible elementary correlation lines between well markers (figure 1.4) and then, randomly chooses a set of marker correlations according to this likelihood. Therefore, several sets of correlation can emerge from the same correlation rules, which translates the imperfection of these rules while precluding unlikely correlations. Each outcome of the method, associating all markers of all considering wells, is termed a realization because it samples correlation uncertainty. The algorithm proposed in this paper relies on this key idea in the Dynamic Time Warping framework.

Unlike previous studies which assign constant value to the correlation cost between stratigraphic units (t term of the Eq.(1.3)) [Smith and Waterman, 1980, Fang et al., 1992a] or compute it as a function of units thickness [Waterman and Raymond Jr., 1987], our well correlation technique is only based on the evaluation of stratigraphic horizon consistency (term c in Eq.(1.3)). Moreover, our method considers sequence stratigraphic units identified along wells. Resulting well correlation thus defines the sequence stratigraphic architecture of the studied area.

To perform sequence stratigraphic well correlation, the first step is to formulate the sedimentological rules into a mathematical expression that estimates the cost of correlating two given markers (Section 1.3.2). The second point is the modification of the DTW algorithm to perform well correlation stochastically. Moreover the well correlation algorithm is built in order to take into account for hard constraints such as regional correlation lines and to use stratigraphic hierarchy to constrain well correlation. The well correlation algorithm should also perform multi well correlation, by taking into account the 3D structure of the studied horizons.

1.2.2 DTW for multi-well correlation

Most of the time, the well correlation problem is not limited to a simple correlation between two wells but needs to consider all available wells at once. On the basis of the Dynamic Time Warping algorithm, two strategies are proposed.

Multi-dimentional DTW

When more than two series must be correlated, Brown [1997] proposes to increase the dimension of the DTW table. The procedure is simple : a 2D cost table is used for the

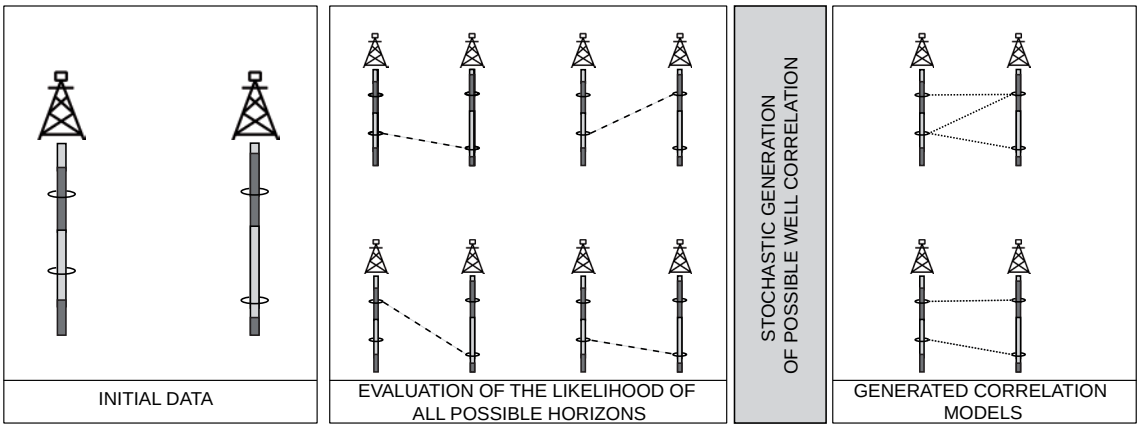

Figure 1.4 – Stochastic sequence stratigraphic correlations workflow

correlation of two wells, a 3D table for three wells and so on. In this representation, each cell of the table corresponds to the association of one marker of each well. This approach offers the possibility to correlate all available wells at once. Hence, it can take into account the 3D geometry of the deposition environment for each correlation likelihood computation. However, the time and memory complexity $O(n^m)$, with n the number of markers per well and m the number of wells, is prohibitive, and limits its applicability to a dozen of wells. Moreover, with a simple implementation of this algorithm, the correlation of 12 wells with 10 stratigraphic markers on each requires 4 Gigabytes of RAM to store the cost table. In bioinformatic applications it was proposed to reduce the computational time of the procedure by assuming that the minimum score path is close to the main diagonal of the cost table (see [Brown, 1997] for an application to stratigraphic correlation and Fullen [1997] for a review of optimization methods). In our case, this optimization is possible only in a globally conformable stratigraphic setting.

Multi 2D DTW

A way to decrease the computational time and the memory requirement of the multi well correlation is to correlate all wells two at a time by considering each pair independently. To achieve this, a correlation path is built to define the pairs of wells that are to be correlated. In addition, loops are prohibited to avoid conflicting results (Fig. 1.6). In practice, the correlation path is computed by extracting the minimum spanning tree between studied wells. This strategy has the asset of the time performance but can only be done for simple elementary correlation cost and to not allow to account for global trends to perform stratigraphic correlation. Indeed, when correlating wells i and j correlations of i and j with all other available wells contains information that are not contained in i and j only. Therefore, we have developed an iterative DTW (Fig. 1.7). First all pairs of wells of the correlation path are correlated. So that, for each pair p of the correlation path, all previously correlated pairs (i from 1 to $p-1$) are known and used to compute the current

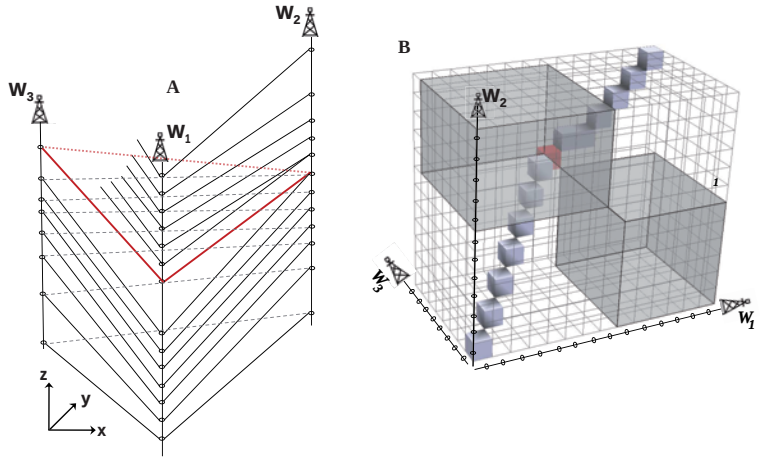

FIGURE 1.5 – DTW based on a 3D table A) 3D representation of the wells correlation. B) 3D DTW Cost Table and correlation path for the correlation of the three wells.

correlation. Then, the computed correlation of a randomly drawn pair of the path is deleted and rebuilt taking into account all other correlations. This ensures that every correlation is generated knowing the whole 3D stratigraphic structure.

1.2.3 Integrating geological constraints

Three levels of constraints can be used to perform well correlation using the DTW algorithm.

- A correlation line interpreted by a geologist can be an input constraint. This constraint is represented as a fixed point in the DTW table (see thick line and point on Fig.1.3A and B). Due to the correlation path construction and to the input correlation line $[i, j]$ in Fig.1.3B), some positions become unacceptable in the table. As a result, the correlation problem is divided in two and two DTW tables are used : one to compute the correlation path from $[1, 1]$ to $[i, j]$, and another one to compute the correlation path from $[i, j]$ to $[n, m]$ (Fig. 1.3B). The correlation path is thus constrained to pass through this point, and the overall performance of the algorithm is significantly improved.
- Stratigraphic sequences identified along the well bore can be ordered using stratigraphic sequence hierarchy [Vail et al., 1977] or fractal nature [Schlager, 2004, Neal, 2009, Schlager, 2009]. Lowest stratigraphic orders markers (*sensu* Vail et al. [1977]) are correlated first to constrain higher order markers correlation. To introduce such a capability, first stratigraphic order markers are correlated thanks to the DTW algorithm, and resulting correlation lines are used as input correlation line in the DTW for the correlation of higher stratigraphic orders markers.
- Correlation rules used to compute cost within the DTW algorithm are a third level of constraint because they drive the way correlation likelihoods of n markers are

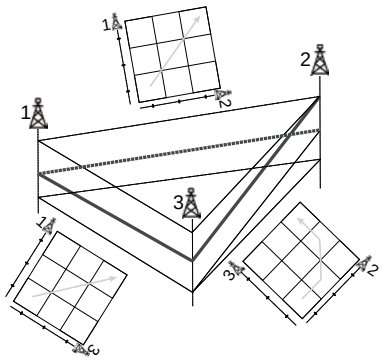

FIGURE 1.6 – Exemple of inconsistent well correlation (thick line) generated using three classical DTW. This inconcistency is due to the loop (1 2 3) described by the correlation path

evaluated.

1.2.4 Uncertainty management

As discussed in section 1.1, well correlation is a complex problem and Waterman and Raymond Jr. [1987] and Griffiths and Bakke [1990] propose to generate several realizations of correlations by modifying cost computation rules, leading to generate a model per geological scenario. Our method may not only use several senarios, bur also generates various models from one single scenario using a stochastic function to fill the DTW Cost Table. From the current location (i, j) in the DTW cost table, we propose to randomly draw the next location by replacing Eq.(1.3) by : $D(i,j) = f(a,b,c,d)$ where p is a random value drawn from a uniform distribution $U[0,1]$, and a (respectively b and c) is the probability of making an oblique (respectively vertical or horizontal) transition in the DTW table (Eq.1.4).

$$f(a,b,c,p) = \begin{pmatrix} 1/a \text{ if } p \in \left[0, \frac{a}{a+b+c}\right[\\ 1/b \text{ if } p \in \left[\frac{a}{a+b+c}, \frac{a+b}{a+b+c}\right[\\ 1/c \text{ if } p \in \left[\frac{a+b}{a+b+c}, 1\right] \end{pmatrix} \quad \text{with} \quad \begin{aligned} a &= 1/\Big(c(i,j) + t_{i,i-1}^{j,j-1} + D(i-1,j-1)\Big) \\ b &= 1/\Big(c(i,j) + t_{i,i-1}^{j,j} + D(i-1,j)\Big) \\ c &= 1/\Big(c(i,j) + t_{i,i}^{j,j-1} + D(i,j-1)\Big) \end{aligned} \tag{1.4}$$

1.3 Application to outcrop data of the Beauset Bassin

1.3.1 Geological settings and material

The Beausset basin is located in Basse-Provence, southeastern France (Fig. 1.8 a). The studied area corresponds to a carbonate platform, aged Cenomanian-Middle Turonian, which developed on the southern part of the "Durance swell" [Philip, 1974]. These

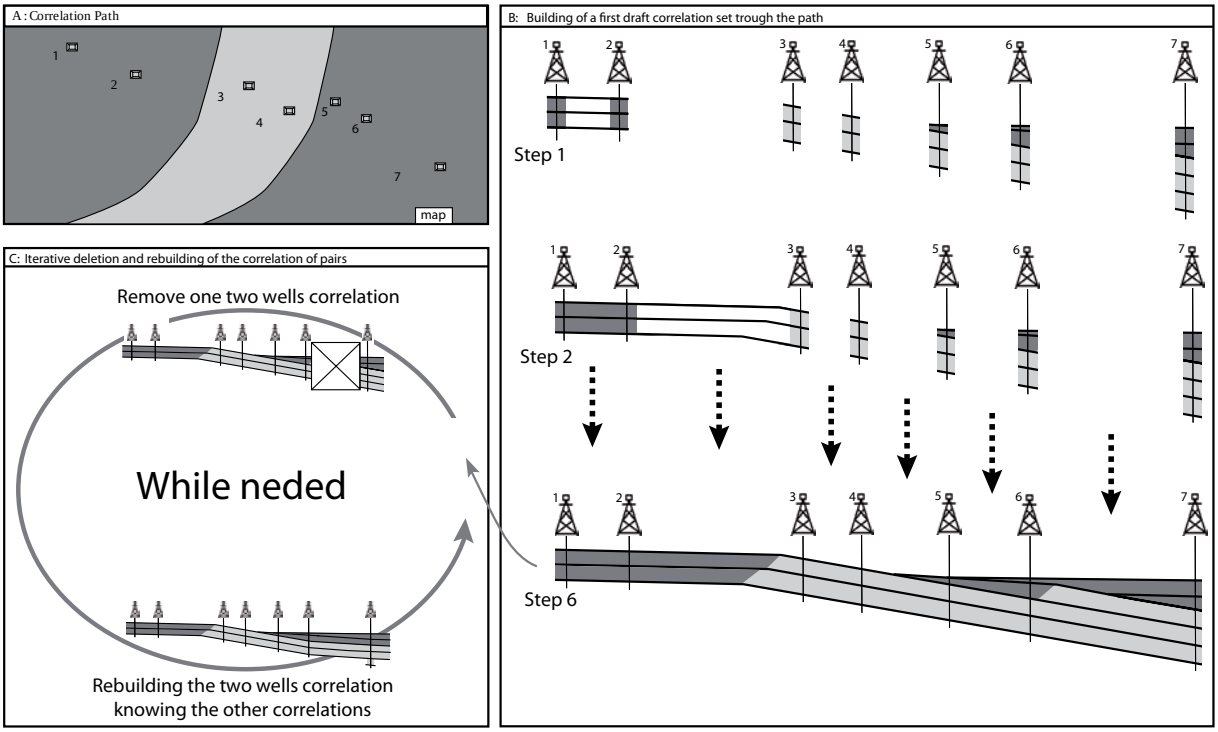

FIGURE 1.7 – Iterative DTW algorithm. From a correlation path (A), a first correlation draft between wells is built (B) using a sequential 2D DTW. At each step of (B), the previously built correlations are known and used as a constraint. Then, to ensure the 3D consistency of the correlation, a random correlation between two wells is removed and rebuilt given all other correlations (C). In the deterministic DTW, this process is performed until sum of the pair-wise scores alonf the spanning tree is no longer modified by the iterative loop. In the case of stochastic DTW the number of loops to perform is defined empirically.

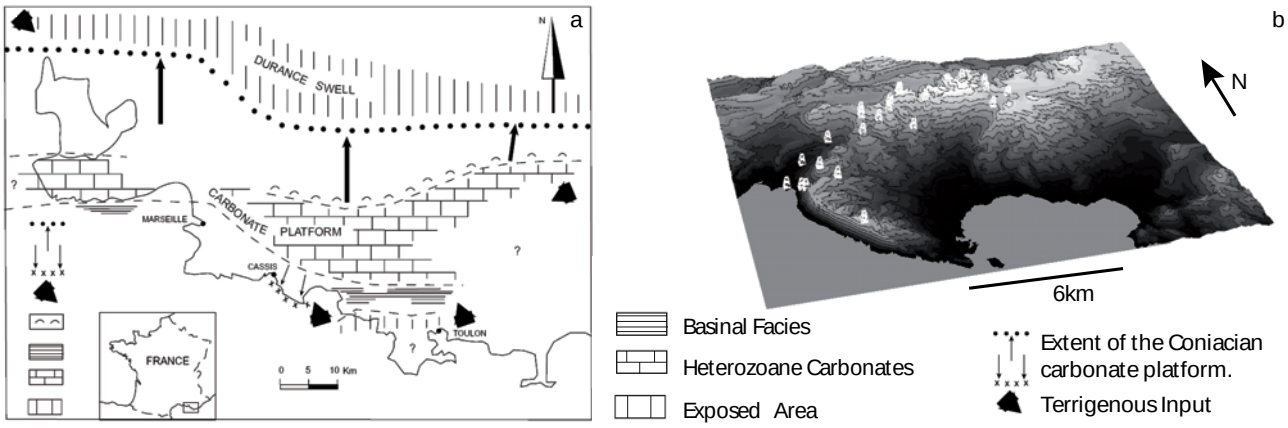

FIGURE 1.8 – a) Geographic and paleogeographic settings of the study area. After Philip [1993]. b) Location of studied outcrops

deposits display terrigenous inputs from a crystalline Hercynian basement corresponding to the southeastern limit of the basin (Fig. 1.8). Multiple outcrops have been described in this area [Philip, 1974, 1993, Philip and Gari, 2005, Gari, 2007]. These almost continuous outcrops from platform to basin deposits allowed previous authors to build well constrained geometrical model and sequence stratigraphic correlations.

Outcrop data

The studied outcrops are aged lower Cenomanian to middle Turonian (Fig.1.9). Nine outcrops sections covering the entire studied interval, are used in this study (Fig. 1.8). The studied interval is subdivided in two primary stratigraphic units : U.I and U.II [Gari, 2007]. U.I, aged Cenomanian, correspond to the transgressive part of a second order, *sensu* Vail et al. [1991], transgressive regressive cycle ending mid Turonian [Philip, 1998]. This unit is divided into six secondary stratigraphic units (U.I 1 to U.I 6), bounded by conspicuous surfaces or abrupt facies changes corresponding to 3^{rd} and 4^{th} order cycles. The U.II primary stratigraphic unit, aged lower to mid Turonian, is the regressive part of the 2^{nd} order cycle started in U.I. This unit is also divided into six secondary stratigraphic units (U.II 1 to U.II 6). Following the outcrop description and study proposed by Gari [2007], eight facies have been distinguished according to the depositional depth range, bioclastic content and deposition style (Table 1.1).

1.3.2 Stochastic well correlation

Correlation rules

Two methods for the evaluation of the consistency of a horizon are used : (i) a paleoangle based rule which compares markers by pairs and (ii) a depositional facies based rule which uses all available markers of the considered horizon at once.

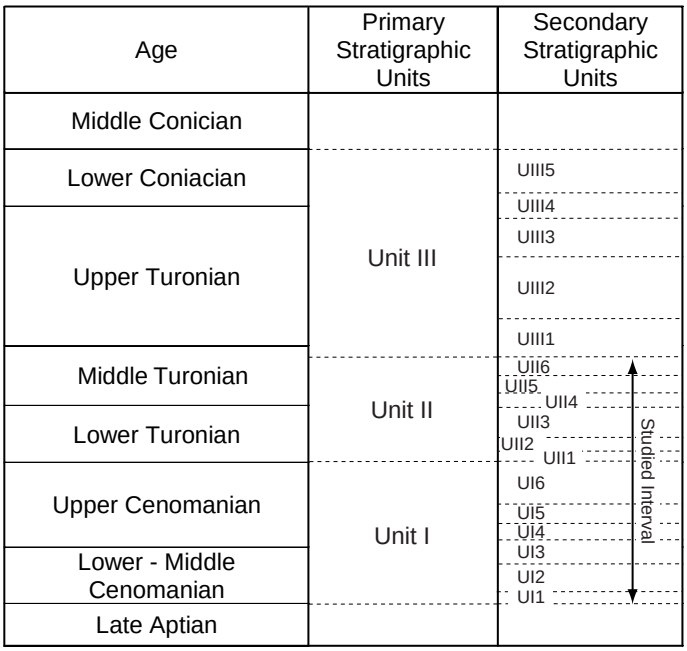

FIGURE 1.9 – Chronostratigraphic and sequence stratigraphic subdivision of the Cretaceous southern Provence Basin. The studied interval is composed of twelve fourth order hemicycles.

1.3.2.1 Paleoangle consistency

To check the consistency of a stratigraphic correlation of a carbonate ramp, Borgomano et al. [2008] introduce trigonometric relationships between average paleo-angles (α and β) of two considered horizons and sediment thicknesses (e_1 and e_2 respectively on wells 1 and 2) according to (Fig. 1.10) :

$$(tan(\beta) - tan(\alpha)) = (\frac{e_1 - e_2}{L}) \tag{1.5}$$

This formalism is adapted to compute a cost of stratigraphic correlation between two markers using a prior defined correlation line, extracted for instance from seismic data. From the paleobathymetry at markers *a priori* correlated (pb_a^1 and pb_a^2), the paleobathymetry of the studied markers (pb_b^1 and pb_b^2) and the sediment thicknesses (e_1 and e_2), we compute the cost C as the degree of violation of the theoretical formula 1.5 when computing the terms using paleo-bathymetric data as follows :

$$C = (pb_a^1 - pb_a^2) - (pb_b^1 - pb_b^2) - (e_1 - e_2) \tag{1.6}$$

This method is valid in the case of a regular accommodation increase between the two correlated wells. In the case of a differential subsidence, a rotation angle has to be added to Eq.(1.6) [Borgomano et al., 2008].

Facies	Minimun bathymetry of deposition		Maximum bathymetry of deposition	
	value	uncertainty	value	uncertainty
F0 : Charophyte Limestones	-50	0	0	0
F1 : Micritic Limestones	0	-5	1	5
F2 : Bioclastic Limestones with Rudists	5	3	10	5
F3 : Bioclastic Limestones with Rudists and Corals	7	4	15	5
F4 : Bioclastic Limestones with fragment of Rudists and Corals	15	5	50	10
F5 : Argilous Limestones	50	25	100	25
F6 : Marl and Marly Limestones	125	25	175	–
F7 : Brecia, Lobe, Grainflow and Debris flow	40	10	175	–

Table 1.1 – Facies described by their possible depositional bathymetry. This description is used to build the depositional space presented in figure 1.12 and to interpolate bathymetry along wells. Modified after Gari [2007].

This correlation rule relies on a well log describing the bathymetry of deposition. The method used to compute this curve in this study has been proposed by Kedzierski et al. [2008] : it uses interpolation method Mallet [2002] constrained by facies depositional depths described in table 1.1.

1.3.2.2 Sedimentary profile consistency

Boundaries of stratigraphic sequences identified on wells could be considered as time significant [Catuneanu et al., 1998]. Consequently, markers bounding stratigraphic sequences could be taken as a sparse sampling of the geography (*i.e.* sedimentary profile) at the time of deposition. Evaluating the likelihood of a correlation line then boils down to checking whether this sampling is consistent with the paleogeography.
In practice, the cost of the considered horizon, *i.e.* a set of correlated stratigraphic markers (one per well) is computed as follow :

1. A map representing the theoretical paleogeography is built. The probability of deposition of each facies is defined on the map.
2. The considered correlation horizon is set back into the depositional space using for instance a map restoration method. Each considered marker is thus defined by its facies and its deposition space coordinates.

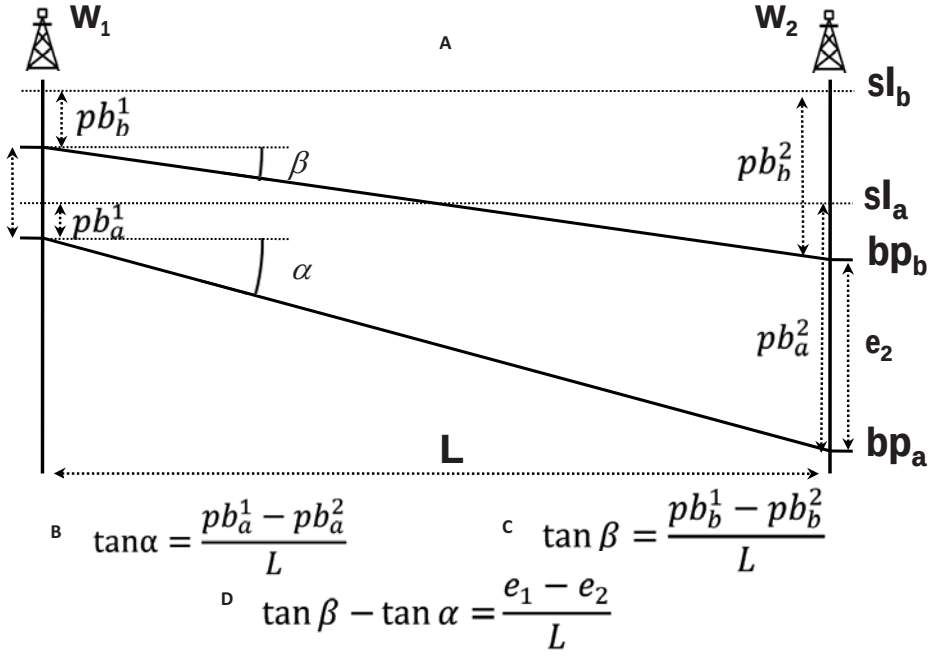

FIGURE 1.10 – Trigonometric relationships on a carbonate ramp system (from Borgomano et al. [2008]). These relations are used to check the consistency of a marker correlation : using measurement in A and relations B and C, the equality D is true if the correlation is good. Notations : *pb* is the paleobathymetry at the current marker ; *sl* the sea level ; L the well spacing ; *bp* the base profile ; e_1, e_2 the decompacted sediment thicknesses ; α, β the angles between the base profile and the sea level.

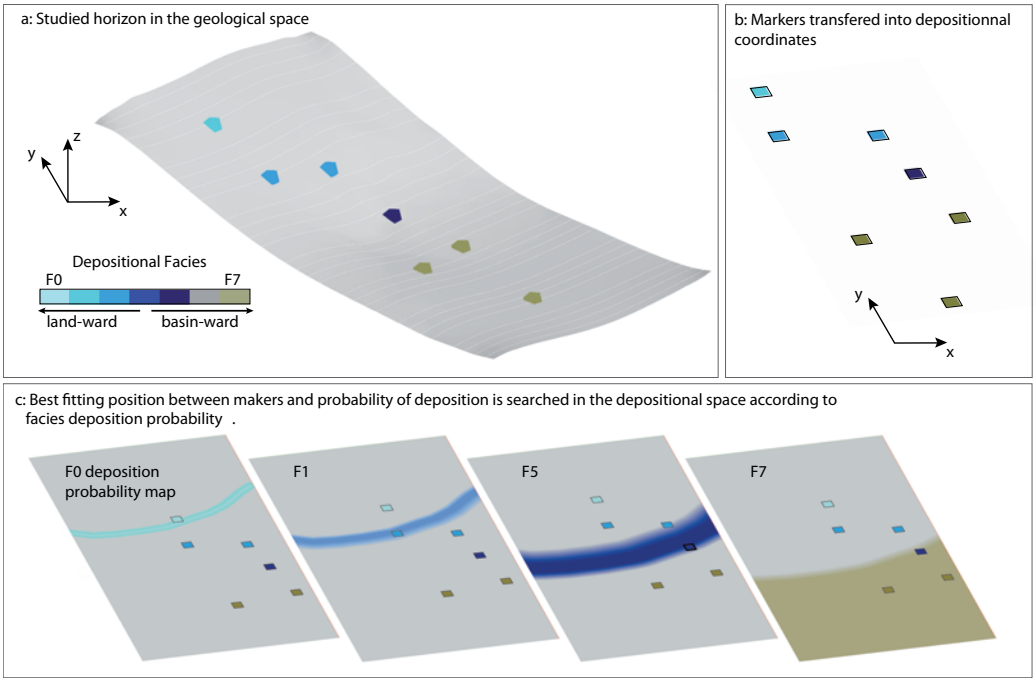

Figure 1.11 – Likelihood computation using theoretical sedimentary profile. a) Studied horizon and markers displaying depositional facies in the geological space. b) Studied markers transferred into the depositional space coordinate system. c) Likelihood computation : the best location of the set of markers is searched in the depositional space (see Fig.1.12) according to the deposition probability of each facies. The likelihood is computed as the sum of these probabilities.

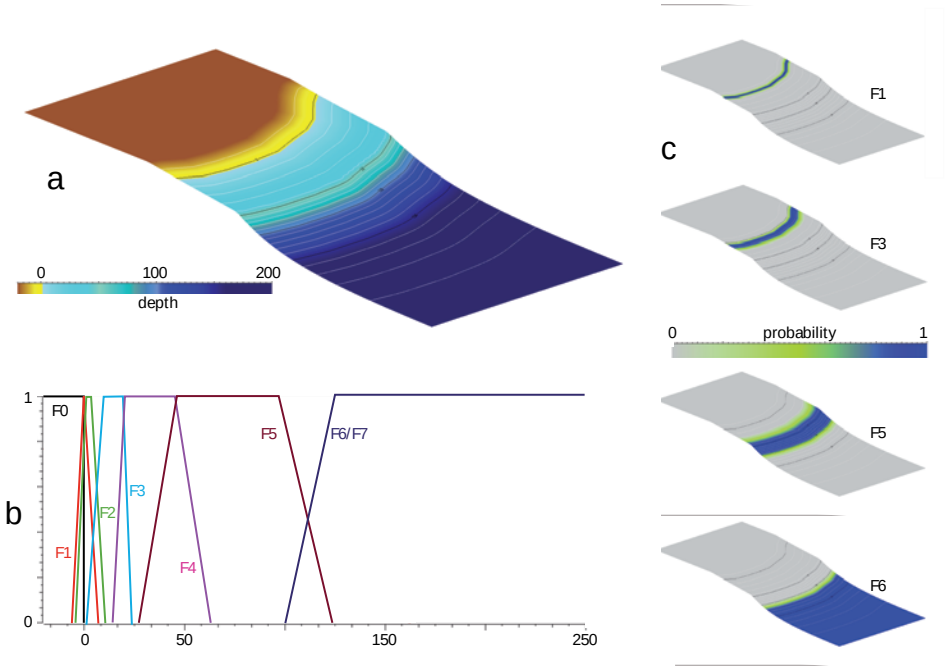

FIGURE 1.12 – Construction of a map describing the palaeography using equations of slope geometry [Adams and Schlager, 2000] and membership function. a) sedimentary profile built from shoreline, regular increase of bathymetry in the shelf with an angle = 0.5°, a shelfbreak at 40 meter depth and a slope described using exponential equation. b) Membership functions for the description of the location of facies using bathymetry (see Table 1.1). c) Examples of possible location of deposition for facies 1, 3, 5 and 6.

3. The best fitting configuration of this set of markers in the theoretical deposition space is searched so that it maximizes the sum of facies probabilities at markers. Due to the low degree of roughness of the considered map, we use the gradient descent method.
4. The cost is computed as the inverse of the facies probabilities sum (Fig.1.11).

The theoretical deposition space may be built using seismic attributes computed on derived from 3D high resolution seismic volumes [Baaske et al., 2007]. When seismic imaging is poor, we propose to build it using membership functions [Mallet, 2002] describing the bathymetry of deposition of each facies (Fig. 1.12). Membership functions, coupled to a sedimentary profile geometry built from 2D seismic lines or using equations proposed by Adams and Schlager [2000], allow to build probabilistic pictures of the depositional environment. However, in most depositional settings, facies type is not controlled by the bathymetry only. Membership functions allow addressing this by defining facies deposition location as a probability range.

1.3.2.3 Constraints

The top and bottom horizons of the studied interval (U.I 1 and U.II 6 in Fig.1.9) are input as known correlations to constraint the stochastic well correlation process. These horizons are also used as *a priori* known correlations to compute correlation costs based on paleoangles (section 1.3.2.1).

1.3.2.4 Results and discussions

Geometrical model and grid building Four alternative models are built (Fig.1.13 B, C, D, and E) : a reference model built from the deterministic correlation proposed by Gari [2007] (Fig.1.13 B) and three models built from the stochastically generated correlations (see Section 1.2.4) using the iterative DTW algorithm (see Section 1.2.2).
The geometry of these four models is constrained by the geometry of the top and the bottom horizon of the studied interval (U.I 1 and U.II 6 in Fig.1.9)). These two horizons have been built by Gari [2007] using intersections with the topography and dip and strike measurements on field. Internal horizons corresponding to well correlations, are build so that they respect well markers and the thickness variations of units defined by surfaces are smoothed [Mallet, 2002]. A conformable stratigraphic grid is then built for the reference model and the stochastic ones.

Facies distribution analysis Vertical proportions of facies are calculated for each stratigraphic model (Fig.1.13). This vertical proportion of facies can be analyzed in terms of reservoir facies distribution, assuming that facies F0 to F4 are potentially reservoir and facies F5 to F7 are flow barriers. Because outcrops located on the North side of the basin display a continuous record of reservoir facies, any model built from the stochastic correlations results in compartmentalization of the reservoir. However, the four models

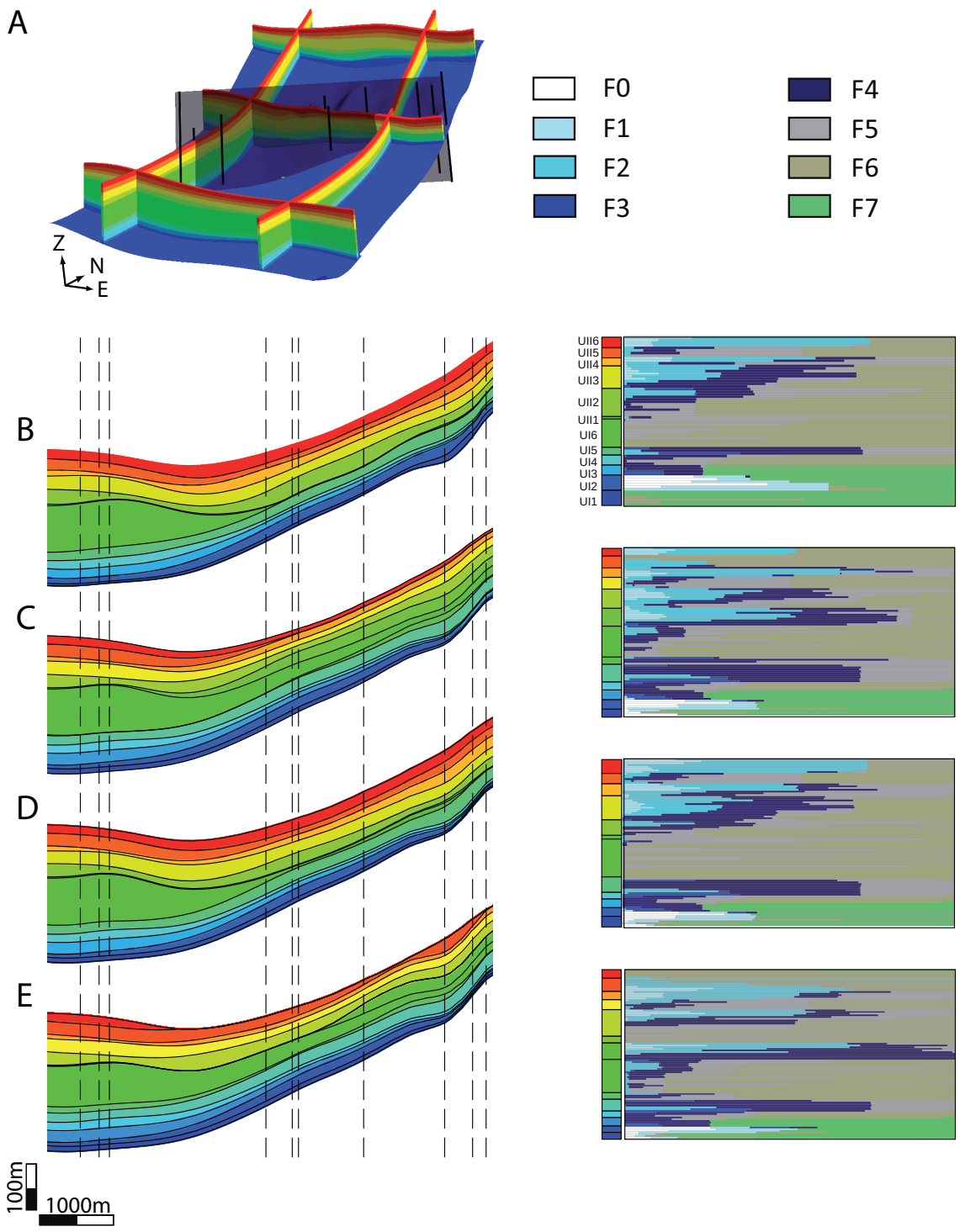

FIGURE 1.13 – Set of possible stratigraphic models of the Cretaceous southern Provence basin. A : 3D deterministic stratigraphic model of the basin (from Gari [2007]). The black lines indicate the location of the studied outcrops ; the shaded surface the location of the cross-sections presented in B to E. B : Stratigraphic correlation model proposed by Gari [2007] and associated vertical proportions of facies. The dash lines are the projected locations of the used outcrops. C, D and E : Stratigraphic models built from three different stochastic stratigraphic correlations.

presented in figure 1.13 (representing a small subset of the possible stratigraphic correlation models) show two alternative views of the distribution of reservoir rocks : in the models B and D, reservoir facies are concentrated into two main groups whereas in models C and E, reservoir facies are divided into several units (6 in the model C and 5 in the model D) separated by flow barriers. Alternative stratigraphic correlation models thus result in different reservoir compartmentalization scenarios. Additional information coming from well production, such as well PLT could be used to select stratigraphic correlation models.
Alternative stratigraphic correlation models may also interpretations of the sedimentary and tectonic history of the stlead to different udied area. For instance, Gari [2007] interprets the unit U.I 6 as a prism constituted of marls whose deposition is due to a tectonic tilting. In relation with this tectonic activity, the production of carbonate is stopped on the platform, suggesting a confinement and hypoxic event. In contrast, such a hypoxic event could not be interpreted if the model E is considered, because the equivalent prism is correlated to platform deposits.‘

Conclusions

The presented algorithms offer the possibility to generate several possible stratigraphic correlations of a study area. These automatic methods offer reliable computation of correlation parameters (paleoangle, distance). Several stratigraphic correlations can be quickly generated, which was challenging when manually performing the correlations. Moreover, the generated correlation sets can be constrained by prior knowledge such as correlation lines extracted from seismic data or/and hypothetical base profile geometry. Several geological senarios may be tested in agreement with prior geological knowledge.
Stochastic stratigraphic correlation, combined with geostatistical facies simulation, is a better way to handle uncertainties on reservoir and basin modeling than multiple facies simulation on a unique grid. Indeed, it allows propagating the correlation uncertainties down to facies and flow simulations.

Chapitre 2

Corrélation d'unités diagénétiques à partir de données diagraphiques : des incertitudes sur l'interprétation d'une sismique haute résolution à leur impact sur les écoulements de fluides

Sommaire

Lors de la construction d'un modèle de réservoir, les corrélations stratigraphiques permettent de construire une trame pour la modélisation tridimensionnelle des propriétés pétrophysiques. Dans le cas du réservoir à gaz Malampaya, la distribution de ces propriétés résulte de la diagénèse de roches carbonatées. Modéliser un tel réservoir nécessite de : (1) identifier le long des puits les différentes unités diagénétiques constitutives du réservoir, ces unités étant des ensembles cohérents de transformations diagénétiques affectant les roches ; (2) corréler spatialement ces unités diagénétiques, ce qui permet de déterminer la répartition spatiale des différentes unites diagénétiques. Dans ce chapitre, une méthode de corrélation d'unites diagénétiques est proposée. Elle est basée sur l'algorithme DTW présenté dans le

Chapitre 1. Les corrélations entre unités diagénétiques sont construites de sorte que : deux unités sont corrélées si elles ont un type diagénétique équivalent ; deux unités sont corrélées si elles présentent un enregistrement diagraphique comparable. Quatre modèles stratigraphiques du réservoir Malampaya sont construits à partir de corrélations générées de façon stochastique (trois modèles) ou de façon déterministe (un modèle). Le modèle déterministe de corrélation correspond au modèle le plus probable compte tenu des règles de corrélations proposées. Ces quatre modèles sont utilisés pour étudier les origines et les conséquences des incertitudes liées aux corrélations stratigraphiques :

- Est-ce que, lorsque qu'une imagerie sismique haute résolution est disponible différents modèles stratigraphiques doivent être considérés ?
- Quel est l'impact des incertitudes liées aux corrélations stratigraphiques sur la production d'un réservoir pétrolier ?

Relevance of the stochastic stratigraphic well correlation approach for the study of complex carbonate settings : Application to the Malampaya buildup (Offshore Palawan, Philippines

Geological Society, London, Special Publications
2012

Florent Lallier, Guillaume Caumon, Jean Borgomano, Sophie Viseur, Francois Fournier, Christophe Antoine and Théophile Gentilhomme

Abstract

The stochastic stratigraphic well correlation method considers the stratigraphic correlation of well data as a set of possible models to sample and manage uncertainty in subsurface studies. This method addresses the incompleteness of typical subsurface data, e.g. limited seismic resolution, seismic blindness due to the lack of impedance contrast between distinct stratigraphic formations, borehole preferential location, *etc.*

The stochastic stratigraphic well correlation method is applied to the Malampaya buildup (a well documented offshore gas field located North-West of the Palawan Island, Philippines), aged upper Eocene to lower Miocene and developed on the crest of a tilt-block. Among the available data, ten wells, seven of which are cored, have been drilled and a high resolution 3D seismic survey has been acquired by Shell Philippines in 2002. Previous studies highlight that rock petrophysical properties are mainly controlled by diagenesis. Correlation rules are thus developed in order to adapt the stochastic stratigraphic well correlation method to the study of diagenetic units. These rules are based on wireline log shape and diagenetic units types.

Four stratigraphic correlation models are generated using the proposed correlation method : a deterministic one corresponding to the most probable model considering only well data and three stochastic ones. These correlation models are bound with geostatistical methods to build static reservoir models. Synthetic seismic profiles are computed from facies models conditioned to acoustic impedance models. It leads to comparable seismic amplitude images, highlighting the importance of considering several well correlation models for one given seismic survey. Stochastic stratigraphic correlations are shown to have a first order impact on reservoir unit characterization, rock volumes and fluid flow response on the reservoir model.

2.1 Introduction

The Malampaya gas field is a well-documented carbonate buildup located NW of the Palawan Island, Philippines [Grötsch and Mercadier, 1999, Neuhaus et al., 2004, Fournier et al., 2004, 2005, Fournier and Borgomano, 2007](Fig.2.1). Reservoir rocks belong to the Upper Eocene- to Lower Miocene-aged Nido Limestone formation [Sales et al., 1997, Williams, 1997]. Deposition of the Nido limestone occurred on the edge of a tilted block resulting from the rifting phase of the China sea (Upper Eocene to Lower Oligocene). The development history, palaeo-environments and diagenesis of the Malampaya buildup has been studied by Fournier et al. [2005, 2004]. Meter-scale, 4^{th} to 5^{th} order subtidal cycle bounded by exposure surfaces are interpreted as constitutive of the buildup.

Fournier and Borgomano [2007] studied petrophysical properties of the Nido limestone of the Malampaya buildup and showed that reservoir properties are mainly controlled by diagenetic processes affecting carbonate rocks. They defined five types of diagenetic units (Ia, Ib, II, IIIa, IIIb) characterized by : a coherent set of diagenetic transformations (meteoric diagenesis and late burial cementation and leaching) ; specific statistical porosity and acous-

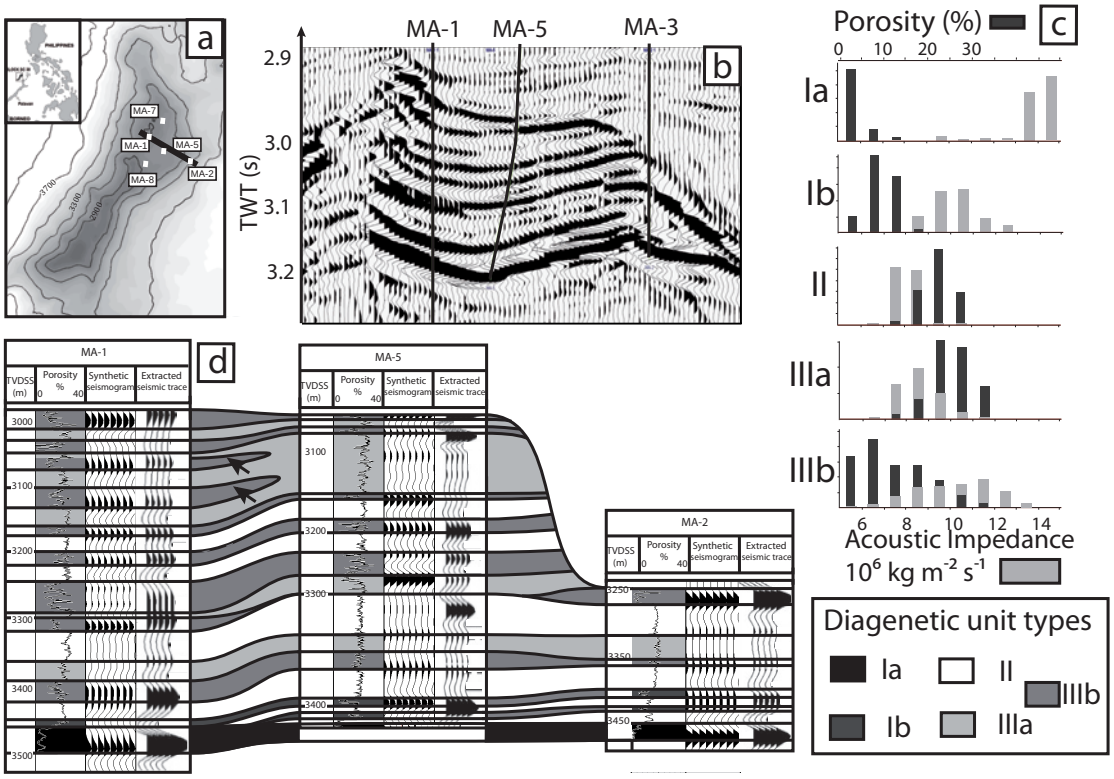

FIGURE 2.1 – (a) Topographic map (in meter sub-sea) of the top horizon of the Malampaya gas reservoir located offshore western Palawan island, Philippines. (b) Seismic line between wells MA-1 and MA-2 displaying Malampaya interior reflector. (c) Porosity and acoustic impedance histogram for the different diagenetic unit types. (d) Stratigraphic model proposed by [Fournier and Borgomano, 2007] on the basis of wells and seismic interpretation. Modified after [Grötsch and Mercadier, 1999] and [Fournier and Borgomano, 2007].

tic impedance distributions (Fig.2.1) ; pore types ; porosity-permeability relationships ; and well-log signatures. From well-to-seismic ties, Fournier and Borgomano [2007] showed that the main seismic reflectors within the buildup image the boundary of diagenetic units. The 3D picking of the reflectors and well correlation of diagenetic units thus provide an envelope of geobodies characterized by specific pore type and reservoir properties. Diagenetic units also define the layering of the reservoir and impact the 3D architecture, showing in particular an alternation of porous and tight diagenetic units. Hence, this impacts the understanding of the reservoir flow behaviour on fluid flow modelling.

Fournier and Borgomano [2007] proposed a stratigraphic model of seismo-diagenetic units of the Malampaya buildup on the basis of well logs and interpretation of a high-resolution seismic survey (Fig.2.1d). However, in common subsurface studies the well-to-well stratigraphic correlation process is subject to uncertainties owing to limited seismic resolution, ambiguity between rock types and well logs and inherent variability between boreholes. The objectives of this study were to question if the seismic response of the Malampaya buildup may be explained by alternative well-towell stratigraphic correlation models of diagenetic units and to assess the impact of well correlation uncertainty on reservoir description and dynamic behaviour. Different possible sets of diagenetic units were automatically generated by a stochastic well correlation process and used to produce a static and dynamic model of the Malampaya buildup.

Different approaches and well descriptors (markers, facies, wireline logs, *etc.*) have been proposed to perform computer-aided stratigraphic well correlations. For instance, deterministic methods have been proposed to correlate wells on the basis of logs [Zoraster, 2004] or lithostratigraphic description [Griffiths and Bakke, 1990]. Recently, Lallier et al. [2009] have presented a stochastic procedure for generating several plausible stratigraphic well correlations from a given set of wells, described by depositional facies.

In the first part of this study, an adaptation of the stochastic method proposed by Lallier et al. [2009] to the stratigraphic correlation of diagenetic units is presented. It relies on the correlation rules proposed by Fang et al. (1992). Using this proposed approach, four stratigraphic correlation models of diagenetic units were generated and used to construct cross-sectional models of these units. Geostatistical simulations of porosity, permeability and acoustic impedance were then performed. The impact of stochastic stratigraphic correlation was then evaluated on the basis of synthetic seismic computation and fluid flow modelling.

2.2 Stratigraphic correlation method

2.2.1 Correlation rules

Two rules were used here to perform stratigraphic well correlation of diagenetic units identified by Fournier and Borgomano [2007] along well from thin-section, cuttings, cores and well logs : (1) Two units were correlated only if they are of the same diagenetic type. This rule implies that diagenetic units are correlated as geological bodies ; (2) Two units were correlated if they display a comparable well log pattern as explain below.

2.2.2 Evaluation of the value of a correlation between two units

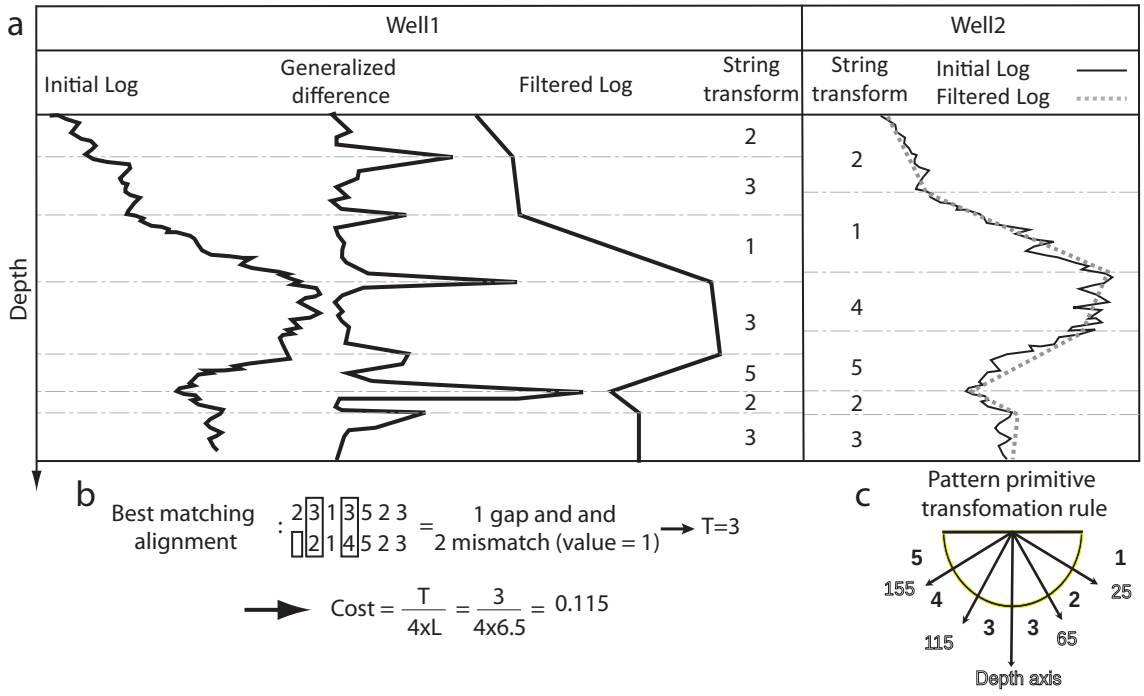

FIGURE 2.2 – Evaluation of similarity between log responses of two units. Well log are first filtered using generalized difference (a) and transformed into string of pattern primitives according to dip angle of filtered log segments (c). Cost is computed as the difference between the two strings representing the two considered units (b). After Fang et al. [1992a]

An automatic method of well correlation requires a mathematical formulation of correlation rules. Several methods have been proposed to evaluate the similarity between two well log curves. Olea [2004] used the product between the standardized similarity coefficient and Pearson's correlation coefficient to evaluate the similarity between two parts of a wireline log. These two coefficients suppose that for the two considered units the same number of points is sampled, and hence may call for re-sampling the well log for the considered unit.

Moreover, in the case of lithostratigraphic correlation, the use of this correlation coefficient assumes a globally constant preservation rate between the two wells (*i.e.* no distortion in the signal). The sedimentary record is also assumed to be quasi-complete between the two units, that is, there is no erosion on a studied stratigraphic unit that is not recorded in the other unit.
In this study, we used the method proposed by Fang et al. [1992a] to evaluate similarity between well logs of two diagenetic units. This method, based on the dynamic programming approach, follows workflow with two steps (Fig.2.2) :
Transformation of well logs into pattern primitives. Well log curves are filtered to extract points that are representative of a log pattern. This method is called "adaptive" by Fu [1980] and is performed in two steps. First, a generalized difference log **d** is computed along the well at each point at depth i :

$$d_i^2 = (s_{i-\alpha} - s_{i+\alpha})^2, \tag{2.1}$$

where d_i is the value of the generalized difference log **d** at depth i ; $s_{i-\alpha}$ the slope of the considered well log between the point at depths i and $i-\alpha$; and $s_{i+\alpha}$ the slope between the point at i and $i+\alpha$. The half-window α is be defined according to the well log resolution and noise characteristics. Then for each peak of the generalized difference log, the value of the studied log at peak depth is selected and used to build a filtered log. Finally, the obtained simplified log is transformed into a string of pattern primitives according to the dip angle of the filtered log segment.
Similarity evaluation. Considering two stratigraphic units a and b transformed into two strings of pattern primitives (respectively $[a^1, ..., a^i, ...a^n]$ and $[b^1, ..., b^i, ...b^m]$), the best match is searched between a and b using dynamic programming [Levenshteiti, 1966] where the penalty of an insertion and a deletion equals 1 and the penalty of a mismatch is equal to the difference between a^i and b^j. Finally, the similarity between the two units a and b has a value C which equals 0 if a and b are similar and increases with the difference between a and b :

$$C = \frac{T}{(4 \times L)} \tag{2.2}$$

where L is the mean length of the strings and T the cumulative penalty of association between a and b. This method has two main advantages : (1) it handles possible distortions of the initial signal through a string of pattern primitives ; (2) it manages missing event in a unit with regard to the other unit through the use of dynamic programming.

Most of the time, more than one well log is available. Given n wireline logs noted $\lambda_\mathbf{1}$ to $\lambda_\mathbf{n}$ (for instance a density log, a porosity log and a sonic log), the possibility of a correlation between two considered units can be evaluated using a weighted sum of cost $C^{\lambda \mathbf{i}}$ computed for each available well log :

$$C^{\lambda_\mathbf{1},...,\lambda_\mathbf{n}} = \sum_{i=0}^{n} w_i C^{\lambda_\mathbf{i}} \tag{2.3}$$

where w_i are weights defined according to : (i) the redundancy of information contained in the wireline log ; (ii) the relevance of the rock property recorded by the log.

2.2.3 Automatic stratigraphic correlation between two wells

Once the similarity between stratigraphic units has been computed, the global correlation between the considered wells can be built. The goal of this study was to handle uncertainties on stratigraphic well correlation and to stochastically generate correlation models constrained by well logs. Lallier et al. [2009] propose to use a stochastic variation of the Dynamic Time Warping algorithm (DTW) [Levenshteiti, 1966, Myers and Rabiner, 1981] which automatically builds correlations between two ordered series. The correlation between two wells u and v, on which stratigraphic units u^1 to u^n and v^1 to v^m are defined, is determined with a recursive function $D(u^i, v^j)$:

$$D\left(u^i, v^j\right) = S\left(\begin{array}{c} \alpha = m(u^i, v^j) + D\left(u^{i-1}, v^{j-1}\right), \\ \beta = g(u^i) + D\left(u^{i-1}, v^j\right), \\ \gamma = g(v^j) + D\left(u^i, v^{j-1}\right) \end{array}\right) \tag{2.4}$$

where :

(a) $D(u^i, v^j)$ is the cost of the correlation between units u^1 to u^i of w_1 and units v^1 to v^j of w_2 ;

(b) $m(u^i, v^j)$ is the cost of a correlation (match) between the units u^i and v^j ;

(c) $g(u^i)$ is the cost of a gap of unit u^i, *i.e.* the unit u^i of the well u is not recorded on well v and end as a stratigraphic gap between the two wells ;

(d) $g(v^i)$ is a cost of a gap of units v^j of v ;

(e) $S(\alpha, \beta, \gamma)$ is a value equal to cost α (respectively β or γ) with a probability inversely proportional to the relative cost $\frac{\alpha}{\alpha+\beta+\gamma}$ (respectively $\frac{\beta}{\alpha+\beta+\gamma}$ or $\frac{\gamma}{\alpha+\beta+\gamma}$).

Applying equation 2.4 from $i = 1$ to n and $j = 1$ to m enables to minimize the cost $D(u^n, v^m)$ of the correlation between wells u and v and thus to build correlations which are consistent with rules used to compute $m(u^i, v^j)$, $g(u^i)$ and $g(v^i)$. In the original deterministic version of the DTW [Myers and Rabiner, 1981], the S function is not a stochastic one and returns the minimum value of α, β and γ ensuring that the DTW algorithm builds the minimum cost correlation between wells u and v. This correlation is called deterministic.

In this study, the correlation between two diagenetic units was considered only if they are of the same diagenetic type. Considering two units u^i and v^j of a diagenetic type respectively $t(u^i)$ and $t(v^j)$, the cost of a match was computed as following :

$$\begin{array}{c} m(u^i, v^j) = \infty \text{ if } t(u^i) \neq t(v^j) \\ \text{else} \\ m(u^i, v^j) = C^{\lambda\mathbf{1},\ldots,\lambda\mathbf{n}}, \text{ as defined by Fang et al. [1992a]} \end{array} \tag{2.5}$$

The analysis of the match function $C^{\lambda\mathbf{1},\ldots,\lambda\mathbf{n}}$ highlights that the cost of a match between two units has a cost lower than 1 if log patterns of u^i and v^j are similar and higher than

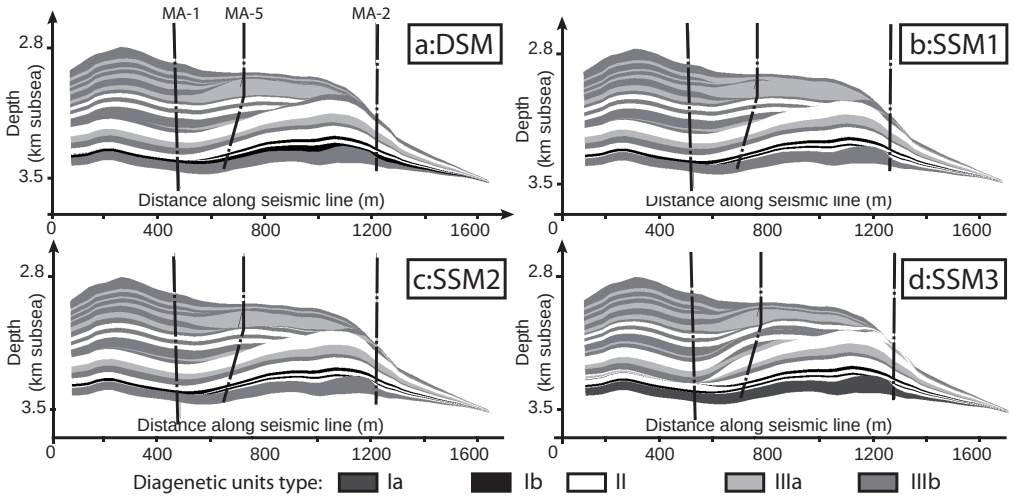

FIGURE 2.3 – Sections of diagenetic units model built from stratigraphic correlation computed using the proposed algorithm. The deterministic model is the minimum cost one. For reference, wells MA-1, 2 and 5 are projected on the section.

1 if no similarity appears between the considered units. Therefore, we set the gap costs $g(u^i)$ and $g(v^j)$ to 1 so that units with comparable log patterns have a higher chance to be correlated than to be pinched out.

2.3 Results and discussions

2.3.1 Stratigraphic correlation models

Four stratigraphic correlation models (Fig.2.3) were built between wells MA-1, 2, 5, 7 and 8 : a stratigraphic correlation model (DSM) corresponding to the minimum cost correlation ($S(\bullet) \equiv Min(\bullet)$) and three stochastic stratigraphic correlation models (SSM1, 2 and 3).

Validity of the well correlation method. The confrontation of our DSM (*i.e.* the most probable stratigraphic correlation model regarding used correlation rules, Fig.2.3a) with the stratigraphic model proposed by Fournier and Borgomano [2007] (Fig.2.1d) serves as validation of the method. Several points could be highlighted : (i) all the diagenetic units correlated by Fournier and Borgomano [2007] are also correlated in the DSM ; (ii) hiatuses interpreted by Fournier and Borgomano [2007] are also present in the DSM ; (iii) the only difference between the two models is the interpretation of the units marked with an arrow on figure 2.1d which are interpreted as pinching out diagenetic lenses by Fournier and Borgomano [2007](Fig.2.1B) and top-lap in the DSM. This difference comes from modelling

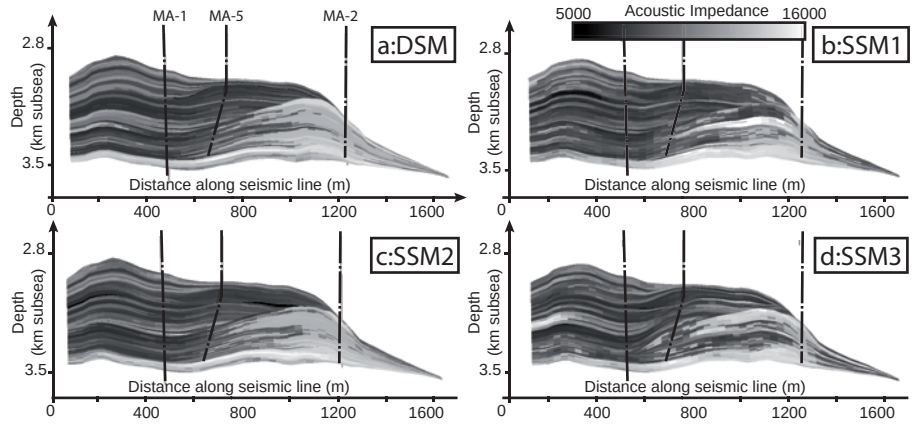

FIGURE 2.4 – MA-1 to MA-2 cross-section of acoustic impedance models generated on grids built from DSM (a), SSM1(b), 2(c) and 3(d) using Sequential Gaussian Simulation.

decision we made : the presence of diagenetic lenses has been interpreted by Fournier and Borgomano [2007] based on a high resolution seismic survey on which abrupt disappearance of seismic reflector corresponding to this diagenetic units indicates pinch out. In our case, only well log data on which no indication of such pinch out could be identified, were considered to preform stratigraphic well correlation. As a consequence, we did not design our stratigraphic correlation algorithm to manage units pinch out. However, the likeness between the DSM and the stratigraphic model proposed by Fournier and Borgomano [2007] suggests that our algorithm generates an acceptable stratigraphic well correlation.

Geometrical model building. The four possible stratigraphic correlation models were combined with top and bottom Nido horizon geometry interpreted from 3D seismic to build 3D stratigraphic grids [Mallet, 2002] conforming to diagenetic units (sections of these grids are shown in Fig.2.3). In addition to the uncertainties owing to the correlations, there were uncertainties owing to the way horizons were interpolated between the correlated markers [Goff, 2000, Caumon et al., 2007, Seiler et al., 2010]. To limit the influence of this geometric uncertainty, we focused on the neighbourhood of wells MA-1, 2 and 5 (Fig.2.1a). This restriction was necessary since the internal geometry of the reservoir is only constrained by well marker positions and by the top and bottom reservoir horizons.

2.3.2 Property modelling

Three-dimensional stratigraphic grids were populated with porosities property using sequential Gaussian simulation (SGS) conditioned by well porosity logs on wells MA-1, 2, 5, 7 and 8. As shown by Fournier and Borgomano [2007], petrophysical properties were controlled by diagenetic history and thus diagenetic unit type. Therefore, in this study, petrophysical properties were considered second-order stationary on each diagenetic unit type. Univariate, bivariate and spatial analyses were performed for each diagenetic type. Experimental histograms (Fig. 2.1c) were used as target distributions for the SGS. Owing

to lack of information (data are provided by five wells), the variogram model could not discriminate between diagenetic units as expected theoretically. A unique spherical variogram model was thus built and used to perform SGS with a range of 950 m horizontally and 40 m vertically. Porosity was then simulated on each stratigraphic grid. The same process was used to simulate acoustic impedance.

2.3.3 Seismic response to alternative stratigraphic models

The value of a stochastic correlation model can be questioned when high-quality seismic data allow us to follow stratigraphic units between wells. Moreover, since the petrophysical properties distribution through the Nido Limestone is controlled by the geometry of tight and porous diagenetic units imaged by seismic survey, we could question if the seismic response of the Malampaya buildup can be explained by alternative internal architectures.

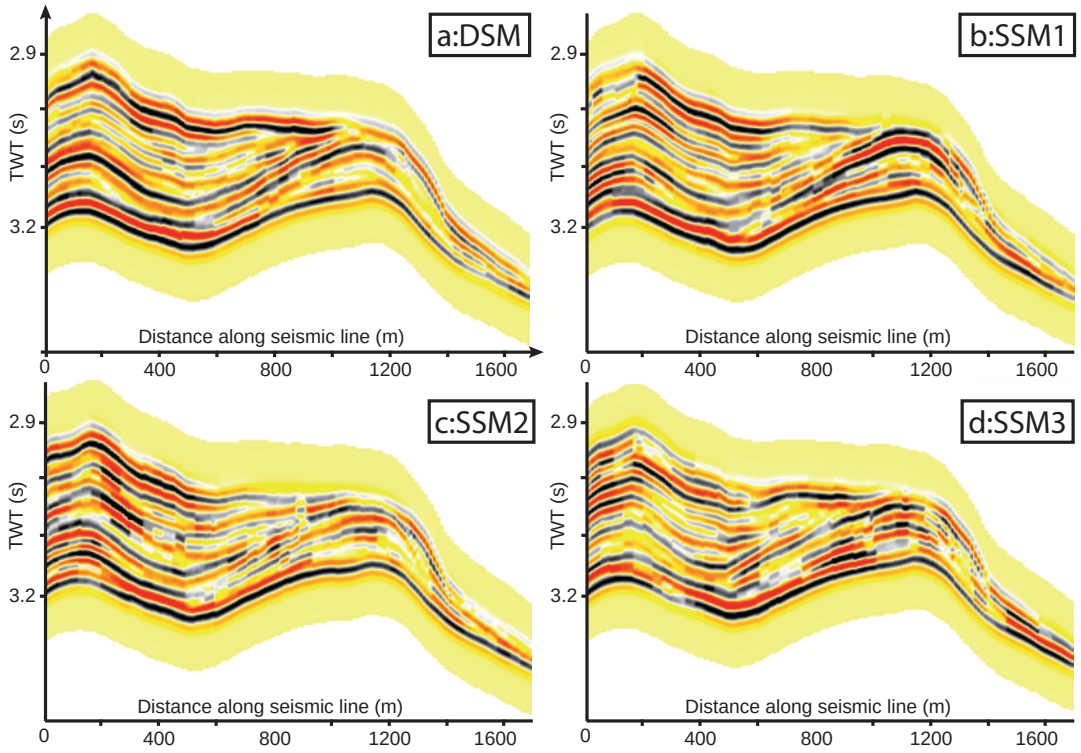

FIGURE 2.5 – MA-1 to MA-2 cross-section of synthetic seismic computed by convolution of acoustic impedance model (Fig.2.4) with a 50hz Ricker wavelet. All of the four seismic sections display comparable internal reflector and may result in similar stratigraphic interpretation.

Synthetic seismic computation. A realisation of acoustic impedance is presented for each correlation model in figure 2.4. Synthetic seismic were computed by convolving the acoustic impedance models (DSM, SSM1, 2 and 3) with a Ricker 50Hz wavelet extracted from the

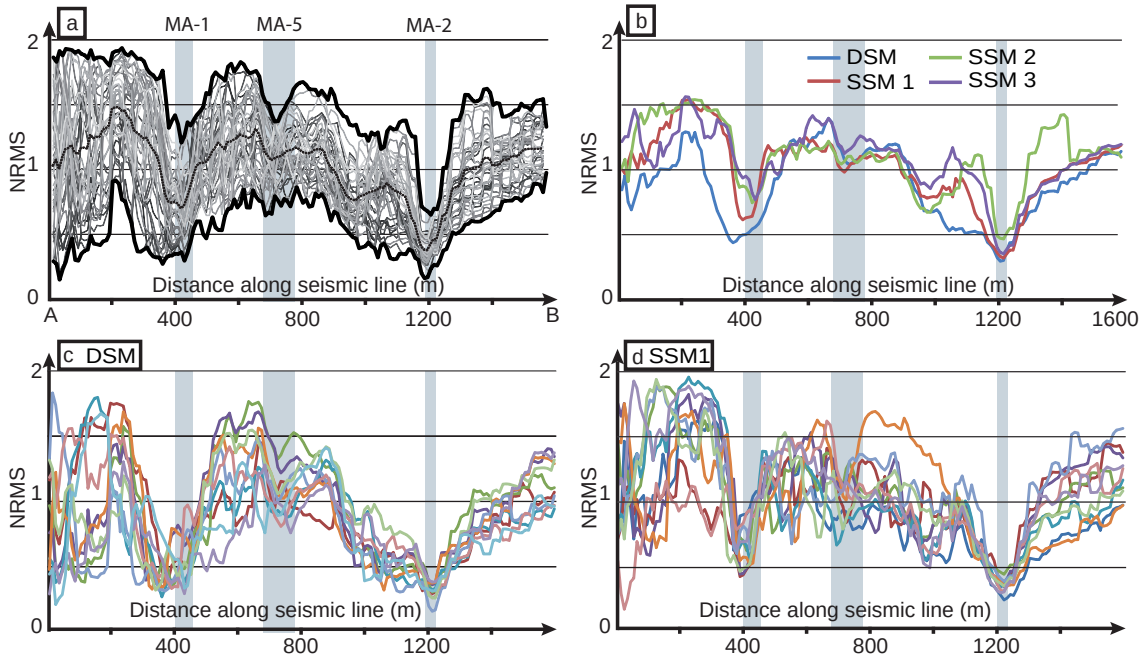

FIGURE 2.6 – NRMS computed along the MA-1 to MA-2 section between one reference seismic amplitude model computed on DSM and forty alternative seismic models computed on DSM, SSM1, 2 and 3 (ten on each). On (a) are displayed all the forty computed NRMS, maximum and minimum values (thick line) and mean values. (b) Mean values of NRMS for each stratigraphic correlation model show comparable values. The ten NRMS computed on DSM (c) and SSM1 (d) show comparable variations. NRMS dispersion observed at well location (grey zones) are due to well path deviation. The well MA-5 trajectory is projected on the studied cross section which explain the amplitude of dispersion at its location.

seismic data by Fournier and Borgomano [2007](Fig.2.4). A realisation of convolution is presented for each correlation model in figure 2.5.

Qualitative comparison of synthetic seimic. Synthetic seismic were visually compared with MA-1 to MA-2 section of high resolution 3D seismic presented by Fournier et al. [2005] and Fournier and Borgomano [2007] (Fig.2.1b). Synthetic seismic showed a good visual correlation with original reflectivity data. The major features of the original high resolution seismic data (Fig.2.5A) were present on the synthetic seismic section : top and bottom reservoir reflectors, major internal reflectors and antiform located on the eastern part of the buildup [Fournier et al., 2005]. This visual comparison allowed to validate our reservoir model on a first order. When comparing synthetic seismic together, it is hard to discriminate which geometrical model (Fig.2.3) or acoustic impedance model (Fg.2.4) has been used to generate the synthetic seismic model in figure 2.5. It appears that even when good quality reflection data are available, internal architecture of the Malampaya buildup can be explained by several stratigraphic correlation models of diagenetic units.

Quantitative comparison of synthetic seismic. The normalized root mean squared difference (NRMS) of the MA-1 to MA-2 cross-section was computed to evaluate the likeness between synthetic seismic models. Considering one reference seismic model r and one alternative synthetic seismic model a, the NRMS at a seismic trace between top (t) and bottom (b) reflectors is defined by :

$$NRMS = \frac{2 \times RMS(r_i - a_i)}{RMS(r_i) - RMS(a_i)}$$
$$\text{with } RMS(x_i) = \sqrt{\frac{\sum_{i=t}^{i=b} (x_i)^2}{N}} \tag{2.6}$$
$$\text{where } N \text{ is the number of samples between } t \text{ and } b$$

We define the synthetic seismic computed from the convolution of one realisation of acoustic impedance on the DSM as our reference seismic. From ten simulations of acoustic impedance, ten synthetic seismic models were computed on each stratigraphic correlation model (DSM, SSM1, 2 and 3). Figure 2.6 shows the NRMS computed between our reference model and each of the forty alternative synthetic seismic models. The mean value of NRMS of each stratigraphic correlation model (Fig.2.6b) shows that the difference between the reference seismic model and DSM-based alternative models is comparable with the difference between the reference model and SSM-based seismic models. Moreover, the figure 2.6c and 2.6d show that the NRMS variability is similar for DSM-based and SSM1-based models, both reaching minimum and maximum values of the envelope of all the realizations. Dispersion at well location observed on figure 2.6 are explained by well deviation and grid rescaling between acoustic impedance simulation and synthetic seismic computation.
From this quantitative analysis, it appears that synthetic seismic data computed from different stratigraphic correlation models are comparable. One of the consequences of this observation is that several stratigraphic correlation models should ideally be considered when performing seismic interpretation.

2.3.4 Implications on fluid flow modelling

Flow simulation were performed on MA-1 to MA-2 cross-section model, using GPRS flow simulator, to evaluate the impact of alternative stratigraphic frameworks on flow response.

The porosity wwas simulated with SGS conditioned by wells MA-1, 2, 5, 7 and 8, using the same random walk that the one used to simulate acoustic impedance and synthetic seismic models(respectively Fig.2.4 and Fig.2.5). The permeability was modelled using porosity-permeability cross-plots presented by Fournier and Borgomano [2007]. To highlight the influence of correlation uncertainty on the recovery in a classical reservoir setting, we considered : (i) Malampaya as a black oil reservoir without an aquifer ; (ii) a water injector close to well MA-2 ; (iii) a productor well close to well MA-1 ; and (iv) an initial oil saturation of 0.8. Figure 7 shows permeability models and oil saturation at four different time steps. The visual evaluation of saturation at different time steps showed that the use of alternative stratigraphic correlation models significantly impacts connectivity between

porous/permeable units. This results in different drainage areas and may impact decision-making in reservoir development. The stratigraphic correlation models generated with our approach could be used to generate an a priori set of models representing reservoir stratigraphic uncertainties. A model screening method based on production data[Suzuki et al., 2008] could be then used to efficiently select acceptable stratigraphic correlation models with regard to observed reservoir flow behaviour.

2.4 Conclusions

The stratigraphic well correlation of units identified along-section is a hazardous task even if high quality data are available. This study shows that different stratigraphic correlation models may produce similar seismic images, and hence several stratigraphic well correlations models may be considered from the initial data (including in, our case, five wells and seismic data). As shown by the computed synthetic seismic models, seismic data may not discriminate stratigraphic correlation models. However, stratigraphic correlation models have a significant impact on fluid flow.
This paper demonstrates the necessity and the technical feasibility of numerical management of uncertainty on stratigraphic well correlation. Additionally, model screening approaches could be used to select only stratigraphic models compatible with production data or well tests.
Limits of the proposed approach should be pointed out, in particular, the inability of our stratigraphic well correlation method to deal with diagenetic lenses. A way to manage this issue could be found in using improvement of the DTW algorithm proposed by Waterman and Raymond Jr. [1987]. In the version of the DTW we use, a stratigraphic unit can be correlated to only one other unit ("one to one correlation") excluding diagenetic lenses. The "one to many correlation" configuration proposed by Waterman and Raymond Jr. [1987] allows to correlate several successive stratigraphic units of one well to one unit on another well and thus to manage lenses. However, such a configuration requires to compute a correlation cost associated to the "one to many correlation". The mathematical expression of this cost is not easy to formulate honestly and still requires developments.
As highlighted by Bashore et al. [1994], the choice of the well correlation strategy affects not only the geometrical model used to guide the geostatistical simulations, but also reservoir models and fluid flow behaviour. This study corroborates their conclusions and points out that even when stratigraphic well correlation rules are defined, several well correlation models have to be considered. In the presented case study, diagenetic units are correlated using lithostratigraphic rules. However, in other geological settings, such as carbonate ramps, reservoir modelling requires to build stratigraphic well correlation in environment with significant lateral facies variability. In such a case, correlation rules presented in this study are unsuitable. The DTW algorithm should thus be associated to correlation rules managing lateral facies transitions as proposed by Lallier et al. [2009].

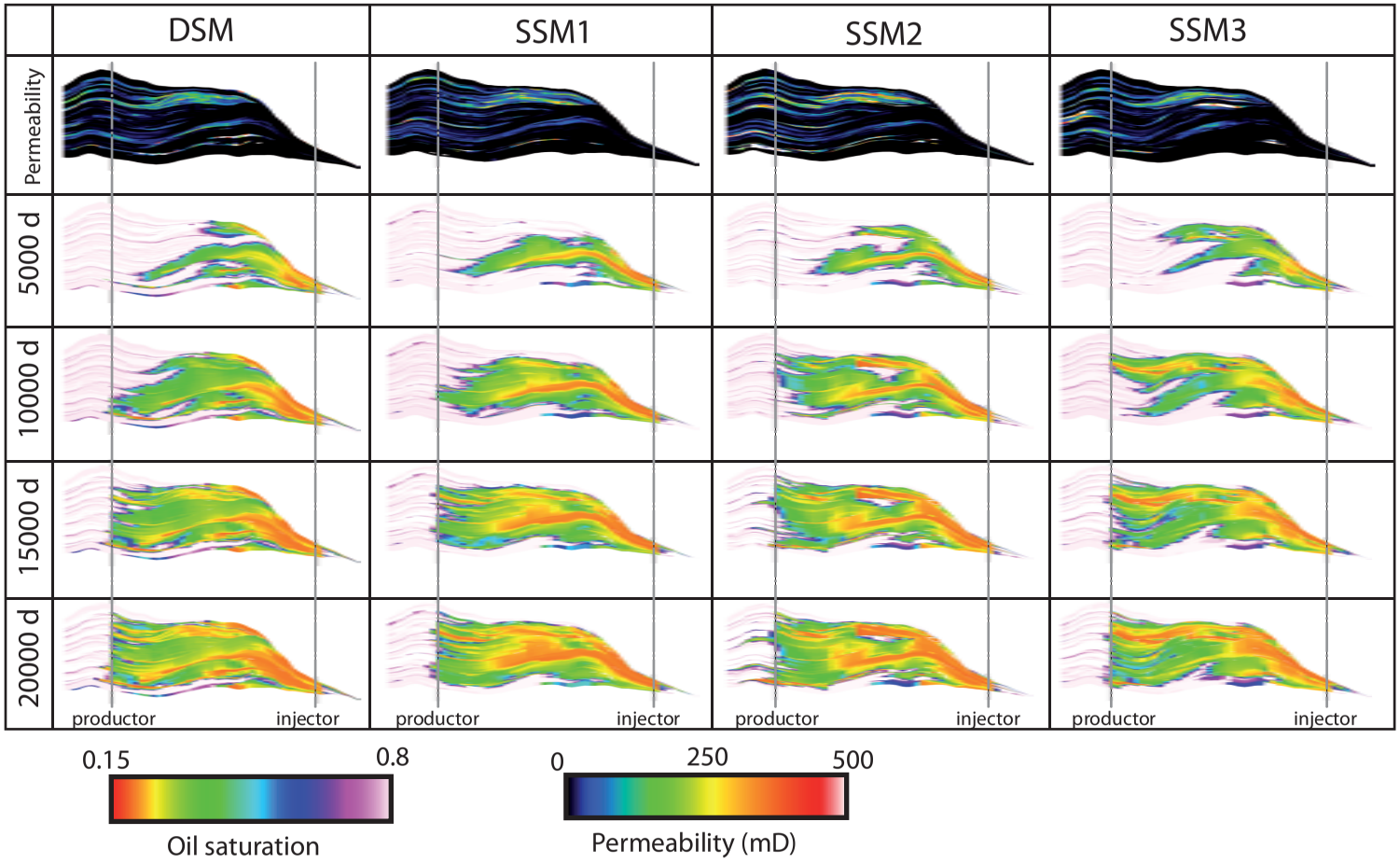

FIGURE 2.7 – Permeability models and oil saturation at different time steps (d = days) show that stratigraphic correlation uncertainty impacts fluid flow patterns

Chapitre 3

Utilisation de l'imagerie sismique comme contrainte dans le processus de corrélation stochastique de puits

Sommaire

Accounting for seismic trends in stochastic well correlation

Article accepted to the 9th Internationnal Geostatistical congress

Charline JULIO, Florent LALLIER and Guillaume CAUMON

Abstract

Stratigraphic well correlation is a critical step of basin and reservoir analysis and modeling workflows. In this paper, we propose an automatic stratigraphic well correlation method which is based on both borehole data and interwell information extracted from poststack seismic data to constrain stratigraphic well correlation. The presented stratigraphic well correlation method uses the Dynamic Time Warping algorithm. Global correlations are built by combining elementary correlation costs between stratigraphic units or markers identified along studying wells. Whereas various rules can be used to compute the correlation likelihood between well sections, a significant challenge is to compute the cost for an unconformity to occur. Therefore, we use first-order trends extracted from seismic data : (1) a rule based on a 3D scalar field whose gradient is orthogonal to horizons, (2) a rule based on a seismic attribute which highlights the convergence of seismic reflectors.

3.1 Introduction

Well data provide a great deal of information on physical and geological properties of underlying rocks. This relatively precise information, sparsely distributed over the study area, does not allow to build stratigraphic correlations of units identified along wells without making strong subjective assumptions [Doveton, 1994b]. This results in correlation uncertainties that may significantly affect the geometry of the model used for geostatistical studies.

Numerous reproducible automated correlation methods which require a mathematical formalisation of the correlation rules have been developed [Lallier et al., 2009, Waterman and Raymond Jr., 1987]. To take into account uncertainties, some algorithms present a stochastic approach aiming at generating numerous correlation models [Lallier et al., 2009]. However, both stochastic and deterministic methods consider only information along the wellbore to establish the stratigraphic correlation rules. Because well data are not sufficient to significantly reduce correlation ambiguities due to the incompleteness of the observations along the borehole and long distances between wells, we introduce new correlation rules based on seismic data which provide interwell information on the continuity of the sedimentary bodies. Due to the difference of resolution between well and seismic data, these rules exploit first-order trends inferred from seismic and should not be substituted to higher order rules between well sections.

In this paper, we introduce a new workflow for stratigraphic well correlation based on the Dynamic Time Warping algorithm which allows to compute likely correlations according to correlation rules built from both borehole and seismic data (Fig. 3.1, Sect. 3.2). A first correlation rule (noted $\mathbf{R}_1$) consider gamma ray trends recorded on stratigraphic units in order to evaluate the likelihood of the stratigraphic correlation (Sect. 3.3). Aiming at integrating seismic information, two additional rules are developed : (1) a rule $\mathbf{R}_2$ built from a 3D draft geometric model, (2) a rule $\mathbf{R}_3$ based on a seismic attribute enhancing stratigraphic sequences (Sect. 3.4). The proposed stratigraphic correlation method is applied to

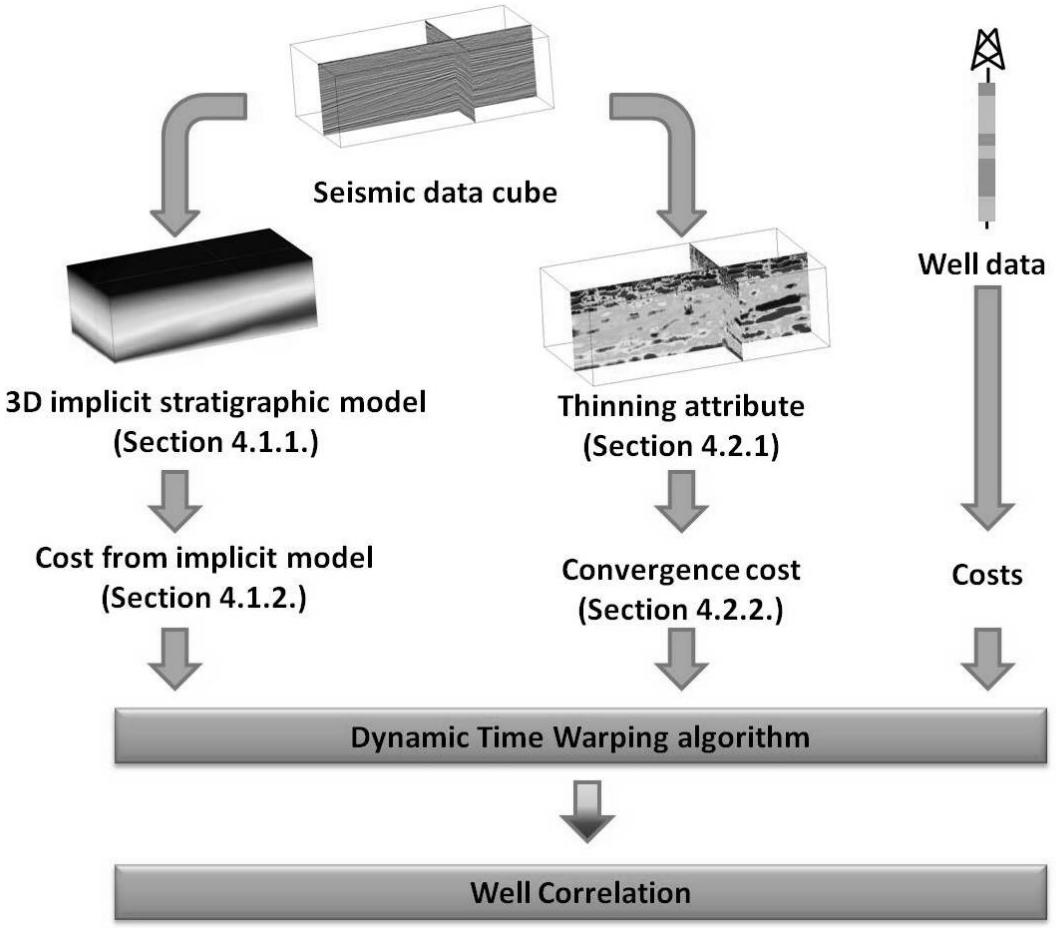

Figure 3.1 – The successive steps of a proposed worflow which takes interwell information from seismic data into account.

the sequence stratigraphic correlation of Miocene, Pliocene, and Pleistocene fluvio-deltaic deposits of the Dutch sector of the North Sea (Fig. 3.8, Sect. 3.5).

3.2 One Algorithm for Stratigraphic Correlation

Dynamic Time Warping (DTW) is a simple and rapid algorithm to compute the optimal correlation between two sequences according to elementary correlation rules often used for stratigraphic well correlations [Doveton, 1994b, Fang et al., 1992b, Waterman and Raymond Jr., 1987].

$\mathbf{a} = \{a_1, ..., a_n\}$ and $\mathbf{b} = \{b_1, ..., b_m\}$ denote two sequences of stratigraphic units, with respectively n and m strata. The dynamic programming framework uses the two sequences $\mathbf{a}$ and $\mathbf{b}$ as axes of a cost matrix D containing all the possibilities of correlation between

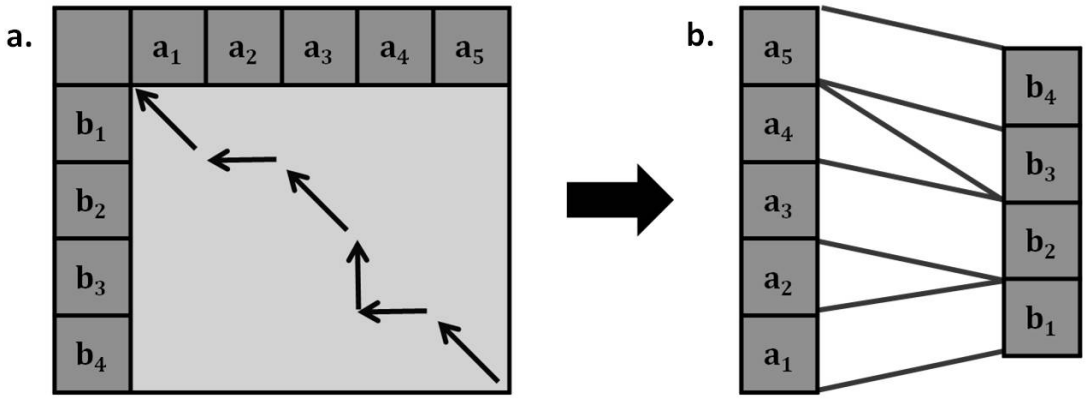

FIGURE 3.2 – The DTW algorithm. **a** Correlation pathway computed within the matrix D whose axes correspond to the stratigraphic sequences **a** and **b**. **b** Optimum correlation between the two stratigraphic sequences.

stratigraphic units (Fig. 3.2). Indeed, between two stratigraphic units a_i and b_j, there are three possibilities of correlation : a_i and b_j match, a_i is gapped or b_j is gapped. The gap of the unit a_i (respectively b_j) corresponds to the non association of this unit with any unit of the sequence **b** (respectively **a**) (e.g., units a_2, a_4 and b_3 in Fig. 3.2). Gaps are associated to the occurrence of stratigraphic unconformities. A cost is associated to each possibility of correlation (match or gap) reflecting its likelihood (i.e. the higher the cost, the lower the correlation likelihood) and is computed according to specific correlation rules (lithostratigraphy, sequence stratigraphy, chemiostratigraphy for instance). Then, the matrix D whose axes correspond to the possible well sections is filled with these costs (Fig. 3.2).

The algorithm computes the least-cost pathway through the matrix corresponding to the most probable correlation. For this, the search of the minimal cost is applied recursively at each cell location.

Waterman and Raymond Jr. [1987] define three functions :

- d : distance function which associates a cost to the matching between two units. For instance, if lithostratigraphic correlation rule is considered, d may be equal to the difference of the average grain size between the studied units.
- g : gap function which associates the cost of a gap to each stratigraphic unit. This cost may be stationary or inversely proportional to the unit thickness [Waterman and Raymond Jr., 1987].
- D_{ij} : minimal distance function which associates the minimal sum of costs to the correlation between the strata $a_1, a_2, ..., a_i$ and $b_1, b_2, ..., b_j$. This cost is defined as [Waterman and Raymond Jr., 1987] :

$$D_{ij} = min(D_{i-1,j} + g(a_i), D_{i,j-1} + g(b_j), D_{i-1,j-1} + d(ai, bj)) \tag{3.1}$$

with : $D_{00} = 0$, $D_{i0} = \sum_{l=1}^{i} g(a_i)$ and $D_{0j} = \sum_{k=1}^{j} g(b_j)$.

To handle uncertainties on stratigraphic well correlation, a stochastic variation of the Dynamic Time Warping algorithm can be considered [Lallier et al., 2009]. The expression of D_{ij} becomes :

$$D_{ij} = S \begin{pmatrix} \alpha = D_{i-1,j} + g(a_i), \\ \beta = D_{i,j-1} + g(b_j), \\ \gamma = D_{i-1,j-1} + d(ai, bj) \end{pmatrix} \tag{3.2}$$

where : $S(\alpha, \beta, \gamma)$ is a value equal to cost α (respectively β or γ) with a probability inversely proportional to the relative cost $\frac{\alpha}{\alpha+\beta+\gamma}$ (respectively $\frac{\beta}{\alpha+\beta+\gamma}$ or $\frac{\gamma}{\alpha+\beta+\gamma}$).

Thus, the DTW algorithm allows either to find the optimal correlation, or to stochastically generate correlation models. In Sect. 3.3, a cost function based on well log trends is proposed and in Sect. 3.4 we present correlation rules computed from seismic reflection data for stratigraphic interpretation. The objective is threefold : (1) try to exploit the inter-well information provided by seismic data to guide correlation ; (2) use higher order trends extracted from the seismic data to define non stationary gap cost functions ; (3) combine both borehole and seismic data to build stratigraphic well correlations.

3.3 Correlation Rule $\mathbf{R}_1$ased on Well Log

The well logging tools are very useful to characterise underlying rocks. Several methods based on the comparison of well logs have been proposed to automatically correlate stratigraphic units [Doveton, 1994b, Fang et al., 1992b].

In the context of fluvio-deltaic sediments, sequence stratigraphic units could be correlated on the basis of vertical trends of shale contents and thus on gamma ray variation. Therefore, we propose a correlation rule $\mathbf{R}_1$ with a matching cost defined as : $d(a_i, b_j) = |s_i^a - s_j^b|$, where s_i^a (respectively s_j^b) is the linear regression slope of the gamma ray values in function of depth for the unit a_i (respectively b_j). The gap cost is defined constant and equal to the mean of all matching costs computed between considered units.

3.4 Correlation Rules from Seismic Data

Seismic reflection methods provide a low-resolution and noisy representation of subsurface heterogeneities. The seismic reflectors, that are often modeled as the convolution of sediment acoustic impedance contrast with a wavelet could, in many cases, be interpreted as bounding horizons of stratigraphic sequences [Vail, 1987]. Over the last decade, the development of seismic attributes and automated horizon extraction methods has considerably facilitated the seismic interpretation task. Using these tools, we propose two correlation rules to evaluate the likelihood of the correlation between stratigraphic units and the possibility of unconformities.

3.4.1 Correlation Rule R_2ased on a Draft Stratigraphic Model

Seismic reflector tracking is a common way to perform well to well stratigraphic correlation. This requires preliminary seismic-to-well tie (e.g. using checkshot data). However, the integration of horizon auto-tracking into automatic well correlation methods may not be simply done. Indeed automatic reflector tracking methods are sensitive to seismic quality and thus do not ensure building continuous horizon between considered wells. We propose to use the geometric information provided by the reflectors extraction to build a draft stratigraphic model to compute correlation cost.

3.4.1.1 Implicit Draft Stratigraphic Modeling from Seismic Data

The objective is the creation of continuous data between wells characterising the geometry of the sedimentary deposits. To this end, we model the stratigraphy of the subsurface with an implicit approach, which considers geological interfaces as iso-surfaces of a 3D scalar field [Frank et al., 2007, Moyen et al., 2004]. Creating a 3D implicit stratigraphic model from seismic amplitude calls for two main steps (Fig. 3.3) :

- The extraction of horizon segments from seismic cubes [Bouchet et al., 2002, Mallet et al., 2002](Fig. 3.3.a).
- Implicit model building. The top and the bottom of the seismic cube are assigned constant scalar value, respectively 0 and 1. Then, a scalar field is built in such way that it respects two types of constraints : (1) a constant gradient, (2) isovalue constraints at the top and the bottom of the seismic cube, and at the extracted horizons segments (Fig. 3.3.b).

The implicit stratigraphic model reflects the 3D large-scale variations of the thicknesses of the stratigraphic units. In this paper, we suppose that no large-scale erosion occurred in the studied area, since the computation of the scalar field assumes continuous variation of thickness. However, erosions clearly visible at the seismic scale can be handled by using several scalar fields for each conformable sequence [Calcagno et al., 2008, Durand-Riard et al., 2010].

This modeling method presents three main advantages : an implicit stratigraphic model can be rapidly created and only partial seismic interpretation is required. Furthermore, the implicit modeling makes easy to refine or to update the model with additional data.

3.4.1.2 Correlation Cost from Draft Stratigraphic Model

The 3D implicit stratigraphic model reflects the 3D geometry of the stratigraphic horizons, so two units with close values in the scalar field are probably nearer in the stratigraphic sequence than units with very different values.

We use this property to establish a new correlation rule allowing to estimate the likelihood of match, $d(a_i, b_j)$ (Eqs. 3.1 and 3.2) : the closer the scalar field values of the units a_i and b_j, the lower the correlation cost between a_i and b_j is. The correlation cost between two stratigraphic units is defined as the absolute value of the difference of the mean va-

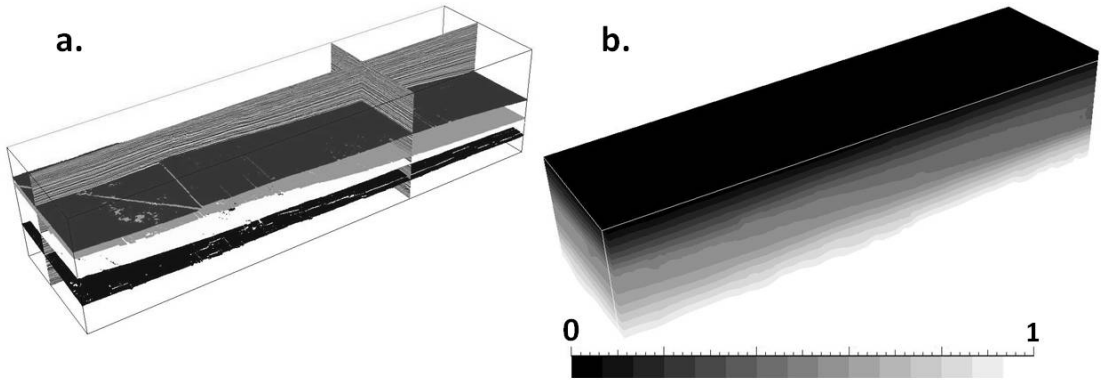

Figure 3.3 – Building an implicit 3D stratigraphic model highlighting the reflector geometry. **a** Extraction of horizons segments from seismic data. **b** Computation of the scalar field constrained by the extracted segments.

lues of the normalized scalar field in the two units. This rule provides a coarse geometric framework to guide well correlations.

3.4.2 Correlation Rule R$_3$ased on a Stratigraphic Seismic Attribute

The identification of the seismic reflection terminations (onlap, downlap, toplap, erosional truncation) allows to define reflection packages that delimit seismic sequences and systems tracts [Vail, 1987]. However, the exhaustive identification of reflection terminations is a tedious manual work. To facilitate the stratigraphic seismic interpretation, Van Hoek et al. [2010] introduce the thinning attribute which quantifies the degree of seismic reflection convergence (or divergence) of a seismic package over a moderate-to-large scale hence relates to unconformities. We propose using the convergence of seismic reflectors to compute non-stationary gap likelihood.

3.4.2.1 The thinning attribute

As pointed out by Van Hoek et al. [2010], the dip variations reflect the degree of convergence (respectively divergence) of the seismic reflectors. The reflection terminations are specifically highlighted as a result of the important variations of reflector inclinations.

At each point of a seismic section, we compute the value of the thinning attribute in three steps :

1. **Computation of the dip mean $\bar{\alpha}$ in the neighbourhood of the point.**
2. **Computation of the oriented variation of dip (relative to $\bar{\alpha}$).** A new basis B is created. Its origin is the study point. The x and z axes of B are respectively equivalent to the horizontal and vertical axes, both rotated by $\bar{\alpha}$ (Fig. 3.4.a–c).

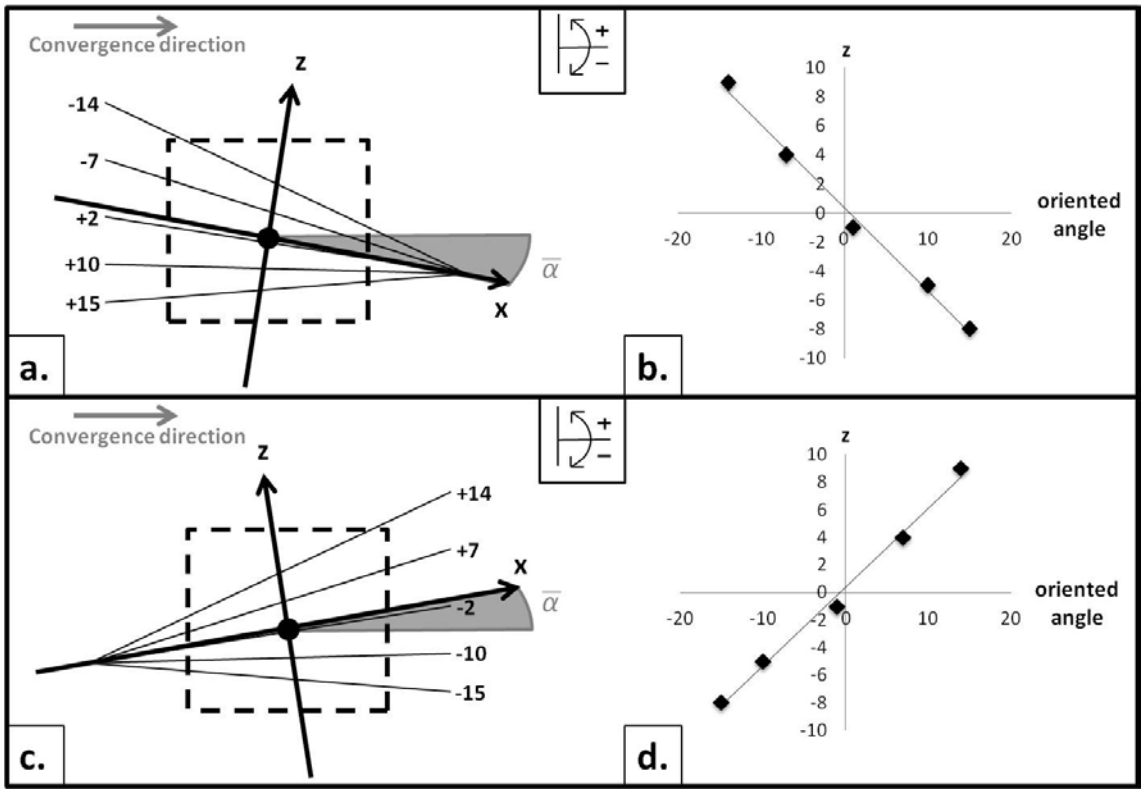

FIGURE 3.4 – Computation of the thinning attribute. **a. and c.** The mean dip value $\bar{\alpha}$ is computed in the neighbourhood (*dotted square*) of the studied point (*black dot*). The axis x and z are obtained rotating respectively the horizontal and vertical axes by $\bar{\alpha}$. The *arrows* show the direction considered as convergent. **b. and d.** The oriented variations of the dip, relative to the dip mean, along the axis z are plotted. For the convergent case (b), the slope of the linear regression line is negative. Conversely, in divergent situations (d), the slope of the linear regression line is positive.

3. **Computation of the degree of convergence (or divergence).** An arbitrary direction is chosen to differentiate the convergence case from the divergence case (e.g., *the arrows* in Fig. 3.4 show the direction considered as convergent). From a dip vs. depth plot, the sign of the slope of the regression line allows to differentiate convergent strata from divergent strata. Moreover, the degree of convergence (divergence) is proportional to the slope of the regression line (Fig. 3.4.b–d).

The thinning attribute computed on a synthetic version of Vail's systems tract is presented in Fig. 3.5.

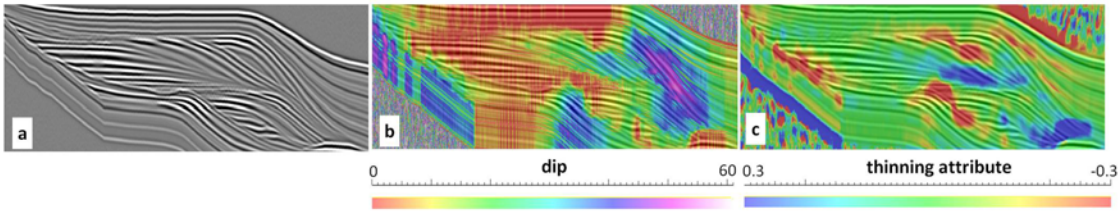

FIGURE 3.5 – **a** Synthetic version of Vail's [1987] systems tract, from Van Hoek et al. [2010]. **b** The dip field. **c** The thinning attribute highlighting reflection terminations (i.e., onlap, downlap).

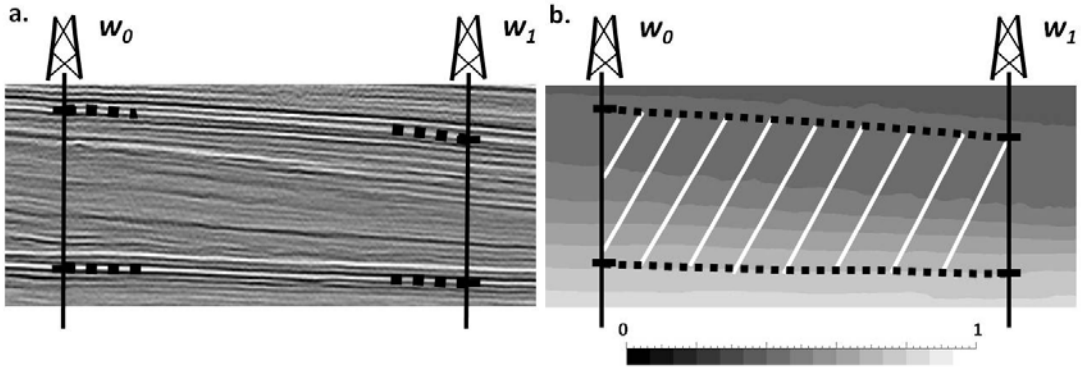

FIGURE 3.6 – Building study zone to compute the cost between two units. **a** The reflectors located at the top and the bottom of the two units are extracted locally (*black dotted lines*). The top reflectors are assigned the value v_1. The bottom reflectors are assigned the value v_2. **b** The gradient of the built scalar field is orthogonal to the extracted horizons. Vertically the study zone is delimited by the isovalues v_1 and v_2 (*white hatched area*).

3.4.2.2 Correlation Cost from Thinning Attribute

In opposition to the cost of match which is naturally constrained by the data along the wellbore, the cost of a gap is often difficult to estimate. For instance, Waterman and Raymond Jr. [1987] define that a gap cost for a unit a_i (or b_j) is proportional to its thickness. However, many field examples show thin units spread over a wide area and thick units with a relatively small lateral extension.

We propose to establish a cost rule relating the likelihood of a gap between two units to the convergence degree in a zone of interest. The definition of this zone is performed for each calculation of cost between units a_i and b_j.

Consider two wells w_0 and w_1 where the stratigraphic units $\{a_1, ..., a_i, .., a_n\}$ are identified along w_0 and $\{b_1, ..., b_j, ..., b_m\}$ along w_1. Currently, we use the following methodology to compute the costs for correlating the units a_i and b_j :

1. **Delimitation of the 2D study zone.** Laterally, the study zone is bounded by the

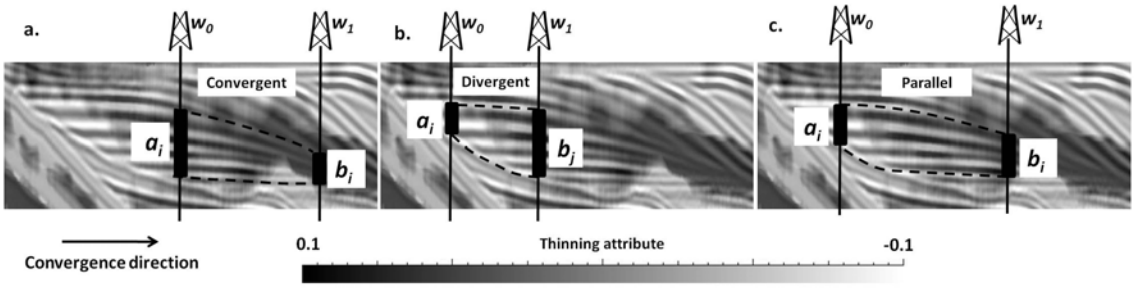

FIGURE 3.7 – The three cases for the calculation of a cost. The *arrow* shows the direction considered as convergent. **a** In the convergent case, the unit b_j is significantly thinner than the unit a_i. **b** In the divergent case, the unit a_i is significantly thinner than the unit b_j. **c** In the parallel case, the units a_i and b_j have approximately the same thickness.

two wells w_0 and w_1. To bound it vertically, the implicit modeling approach is used. For this, the seismic reflectors located at the top and the bottom of the two units are extracted locally (Fig. 3.6.a). The top horizons of units a_i and b_j are assigned the value v_1 and the bottom horizons are assigned the value v_2. Then, we build a scalar field whose gradient is orthogonal to the horizons previously extracted. Vertically, the study zone is delimited by the isovalues v_1 and v_2 of this scalar field (Fig. 3.6.b).

2. **Cost computation.** The direction of the convergence is assumed from w_0 towards w_1. The ratio between the thickness of a_i and the thickness of b_j is noted r_{ij} and a cut-off value α for r_{ij} is chosen in the interval $]0;1]$. This value α allows to distinguish three cases :

   – $r_{ij} > \frac{1}{\alpha}$: the unit b_j is significantly thinner than the unit a_i. This case is considered as a convergent case (Fig. 3.7.a).
   – $r_{ij} < \alpha$: the unit a_i is significantly thinner than the unit b_j. This case is considered as a divergent case (Fig. 3.7.b).
   – $r_{ij} \leq \frac{1}{\alpha}$ and $r_{ij} \geq \alpha$: The units a_i and b_j have approximately the same thickness. This case is considered as a parallel case (Fig. 3.7.c).

   The total area of the study zone defined between the units a_i and b_j is noted $\mathbf{A}_{ij}^t$. Within this zone, the areas of the convergent, divergent and parallel zones, respectively noted $\mathbf{A}_{ij}^c$, $\mathbf{A}_{ij}^d$ and $\mathbf{A}_{ij}^p$, are defined by two thinning attribute cut-off values β and γ. According to the values of r_{ij} and α, the costs of gap and matching between

a_i and b_j are computed as follows :

$$(3)\begin{cases} d(a_i,b_j) = 1 - \dfrac{\mathbf{A}^c_{ij}}{\mathbf{A}^t_{ij}} \\ g(a_i) = 1 - \dfrac{\mathbf{A}^c_{ij}}{\mathbf{A}^t_{ij}} \\ g(b_j) = 1 - \dfrac{\mathbf{A}^d_{ij}}{\mathbf{A}^t_{ij}} \end{cases} (4)\begin{cases} d(a_i,b_j) = 1 - \dfrac{\mathbf{A}^d_{ij}}{\mathbf{A}^t_{ij}} \\ g(a_i) = 1 - \dfrac{\mathbf{A}^c_{ij}}{\mathbf{A}^t_{ij}} \\ g(b_j) = 1 - \dfrac{\mathbf{A}^d_{ij}}{\mathbf{A}^t_{ij}} \end{cases} (5)\begin{cases} d(a_i,b_j) = 1 - \dfrac{\mathbf{A}^p_{ij}}{\mathbf{A}^t_{ij}} \\ g(a_i) = 1 - \dfrac{\mathbf{A}^c_{ij}}{\mathbf{A}^t_{ij}} \\ g(b_j) = 1 - \dfrac{\mathbf{A}^d_{ij}}{\mathbf{A}^t_{ij}} \end{cases}$$

where the Eqs. 3, 4 and 5 correspond respectively to the convergent, divergent and parallel cases. These costs estimate the likelihood of the matching or gap of two units for each case (convergent, divergent or parallel). For instance, in the convergent case, the likelihood of matching between a_i and b_j is function of the proportion of the convergent area within the study zone. The same reasoning is applied to the other cases.

The computation of costs assumes a precise seismic-to-well calibration to limit uncertainties at the step where seismic horizons are extracted at the top and the bottom of units. The seismic is also assumed to have a reasonable quality so that the area of interest is determined with confidence.

However, we can question the relevance of the computation of a correlation cost between two units far apart in the sedimentary sequences, and so with a likelihood of correlation very low. Indeed, the defined study zone can intersect the seismic reflectors, and in this case, the defined zone is not representative of the lateral variation of the units. Therefore, we only apply the rule $\mathbf{R}_3$ when the likelihood given by the rule $\mathbf{R}_2$ is deemed acceptable.

3.5 Application

The study is based on the Dutch North Sea data set provided by the seismic open repository (http ://www.opendtect.org/osr/Main/NetherlandsOffshoreF3Block Complete4GB). Two wells w_1 and w_2 are considered, where respectively 13 and 11 sequence stratigraphic units are identified [De Bruin and Bouanga, 2007]. Along the two boreholes, the gamma ray has been recorded. The stratigraphic model proposed by De Bruin and Bouanga [2007] serve as a base case (Fig. 3.8).

First, the rule $\mathbf{R}_1$ is applied to the wells w_1 and w_2 in a deterministic way (Eq. 3.1). The obtained stratigraphic correlation differs substantially from the base case (Fig. 3.9.a–b). The gaps are particularly improperly positioned. The well-based correlation does not respect the clinoform structures, clearly identifiable on the seismic data (Fig. 3.8).

Second, the seismic rules $\mathbf{R}_2$ and $\mathbf{R}_3$, and the well rule $\mathbf{R}_1$, are simultaneously used to compute deterministic, and stochastic, correlations (Eqs. 3.1 and 3.2) between the two wells w_1 and w_2. Each stratigraphic correlation is equally weighted by the three rules. The deterministic correlation is close to the base case (Fig. 3.9.a–c). The clinoform structures

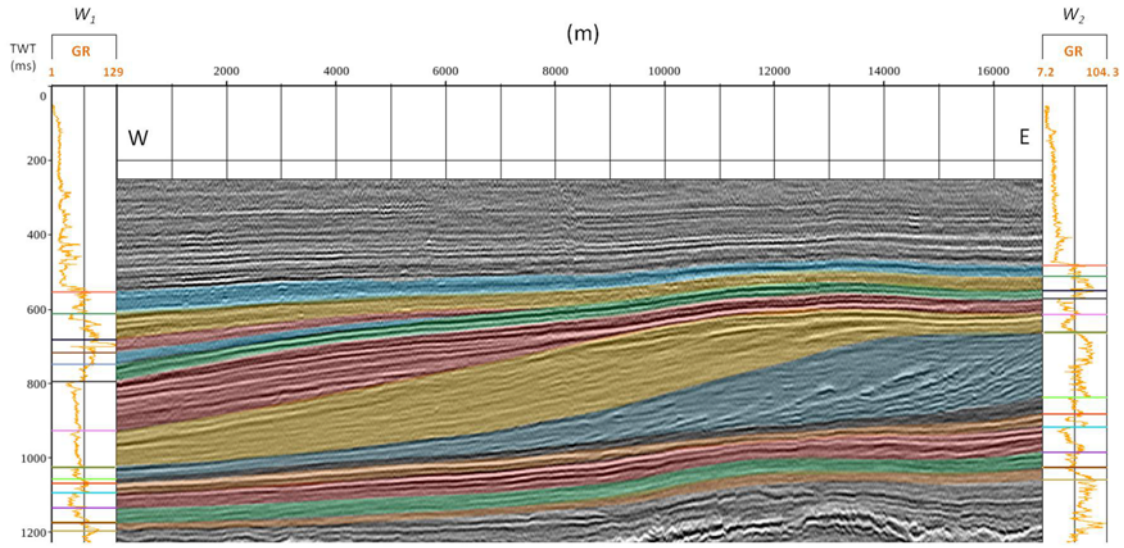

FIGURE 3.8 – Reference correlation proposed after the interpretation of well and seismic data. Along the wells w_1 and w_2, respectively 14 and 12 markers are identified.

are respected. However, between 500 ms and 700 ms (TWT), the correlation is shifted by gaps improperly positioned. This slight shift highlights the difficulty to precisely correlate close markers from seismic information due to the difference of resolution between well and seismic data. Then different possibilities of stratigraphic correlations are computed with the stochastic approach (Fig. 3.9.d–e). The various realisations preserve the main sedimentary trends, although a high variability is observed for relatively thin stratigraphic units.

3.6 Conclusion

The main objective of our correlation method is to use interwell data to constrain the well stratigraphic correlation. The development of this method is made possible thanks to a new generation of geometric seismic attributes. Taking into account seismic data allows to discriminate possible stratigraphic correlation models. Then the use of a stochastic approach provides a sampling of these possibilities, and thus allows to better estimate the parameters characterising both basin and reservoir.

A number of possible improvements for the seismic-based correlation method can be considered. In terms of uncertainty management, an obvious topic would be to account for well-to-seismic calibration uncertainty and more generally for velocity uncertainty. From a structural standpoint, the proposed method has currently no specific management of faults. A major way of improvement would then be to have a tighter coupling of this method to full-featured seismic interpretation tools so that fault could be handled. Hence, with slight modifications of the cost computation methodology, the cost based on the thinning attribute and the cost from the draft stratigraphic model would become applicable to the

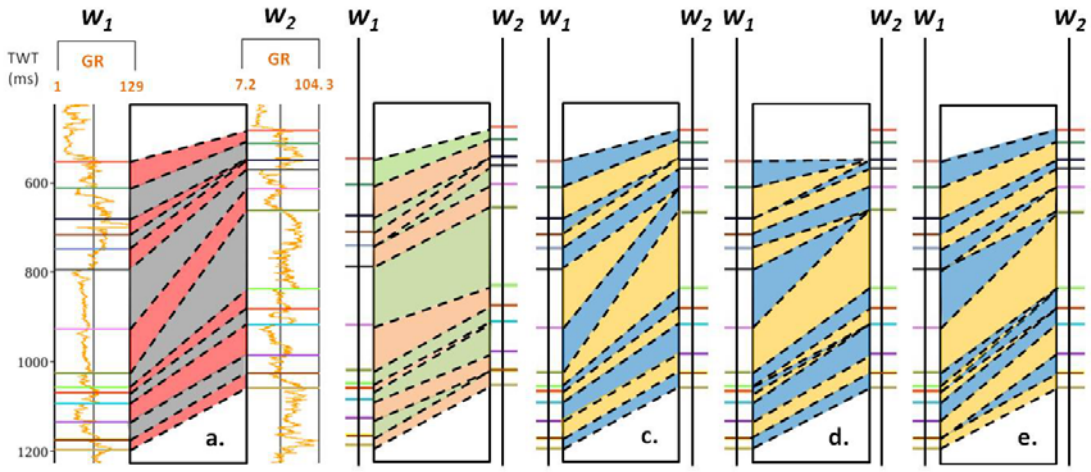

FIGURE 3.9 – Stratigraphic well correlations between the wells w_1 and w_2. **a** The reference stratigraphic correlation model [De Bruin and Bouanga, 2007]. **b** The most likely correlation built from the wellbore-based rule $\mathbf{R}_1$. **c** The most likely correlation built from the wellbore-based rule $\mathbf{R}_1$, and the seismic-based rules $\mathbf{R}_2$ and $\mathbf{R}_3$. **d-e** Two possible correlations stochastically built from the well-based rule $\mathbf{R}_1$, and the seismic-based rules $\mathbf{R}_2$ and $\mathbf{R}_3$.

case of faulted data set. The poor quality of the seismic data, for instance in the context of highly fractured underlying rocks, remains a limiting factor.

Chapitre 4

Magnétostratigraphie automatique : Méthode de gestion des incertitudes sur l'âge des roches et sur les taux d'accumulation de sédiments

Sommaire

L'étude de bassins sédimentaires, depuis le dépôt des sédiments jusqu'à la tectonique les affectant, bénéficie d'une réelle plus-value lorsque l'âge absolu des roches en présence est déterminé. En effet, dater une colonne stratigraphique permet entre autres d'accéder aux taux d'accumulation de sédiments et d'érosion, à la chronologie de déformation et d'enfouissement et de contraindre l'histoire thermique d'un bassin. La datation des roches permet également de tracer des lignes temps à travers un bassin sédimentaire étudié et ainsi de reconstituer l'évolution spatiale et temporelle des environnements de dépôts. Celle-ci est cruciale pour la compréhension de la dynamique d'un bassin sédimentaire et des forçages

externes qui la contrôle (climat, flux sédimentaire, subsidence).
Plusieurs méthodes de datation des roches sont envisageables (biostratigraphie, thermochronologie, isotopes cosmogéniques) mais ne sont applicables que dans certains cas précis ou sont difficilement applicables pour la datation continue de plusieurs milliers de mètres de sédiments. Ainsi, lors de l'étude des dépôts continentaux où la présence de fossiles est rare, l'utilisation des méthodes biostratigraphiques ne peut apporter qu'une information ponctuelle sur l'âge des roches et ne permet pas une datation continue. De plus, dans un contexte continental, l'estimation des âges de dépôts basée sur des corrélations d'unité lithostratigraphiques reste dangereuse. Les sédiments déposés sont en effet fortement contrôlés par des migrations diachrones des environnements de dépôts en réponse aux forçages externes.
La magnétostratigraphie est une méthode de corrélation stratigraphique basée sur l'enregistrement par les sédiments, au moment de leur dépôt, du champ magnétique terrestre. Les inversions passées du champ magnétique terrestre étant connues, datées, et compilées dans une colonne de référence, la GPTS (Geomagnetic Polarity Time Scale), la magnétostratigraphie permet ainsi une datation absolue des colonnes stratigraphiques étudiées par corrélation de la séquence d'inversions du champ magnétique terrestre enregistrée dans les sédiments à la GPTS. Cependant, en raison de la nature des données magnétostratigraphiques, la corrélation d'une colonne magnétostratigraphique à la GPTS peut être incertaine et sujette à débat entre différents auteurs (voir Gilder et al. [2001], Yin et al. [2002] et Wang et al. [2003]).
Nous proposons dans ce chapitre une méthode de corrélation magnétostratigraphique permettant la gestion des incertitudes associées. Après un bref rappel des concepts de magnétostratigraphie (Section 4.1), un algorithme de corrélation automatique basé sur le principe de la déformation temporelle dynamique (algorithme DTW) est proposé.

4.1 Le champ magnétique terrestre et son enregistrement dans les roches

4.1.1 Description et origine du champ magnétique terrestre

La Terre émet un champ magnétique pouvant être approximé au premier ordre à celui émis par un dipôle axial géocentré. Un champ magnétique terrestre (noté par convention H et exprimé par convention en A/m) se définit en tout point de la surface du globe par deux composantes (Fig.4.1a) : D la déclinaison (égale à zéro en tout point dans l'hypothèse d'un dipôle géocentré) correspond à l'angle entre le Nord géographique et le Nord magnétique (qui est la composante horizontale $\mathsf{H_v}$ de $\mathbf{H}$) ; I l'inclinaison (Fig.4.1b), angle entre $\mathsf{H_v}$ et $\mathbf{H}$, est liée à la latitude (λ) du point considéré par : $tan\mathsf{I} = 2 \times tan\lambda$.
Le champ magnétique terrestre a pour caractéristique d'être perpétuel et de voir ses pôles s'inverser à des intervalles de temps allant de 10 000 à 100 000 ans en moyenne. L'origine du champ magnétique et les mécanismes de son inversion restent largement débattus. Le modèle actuellement le plus admis, suppose que ce champ est généré par le principe de la dynamo auto-excitée, le mouvement de convection de matériaux riches en fer siégeant

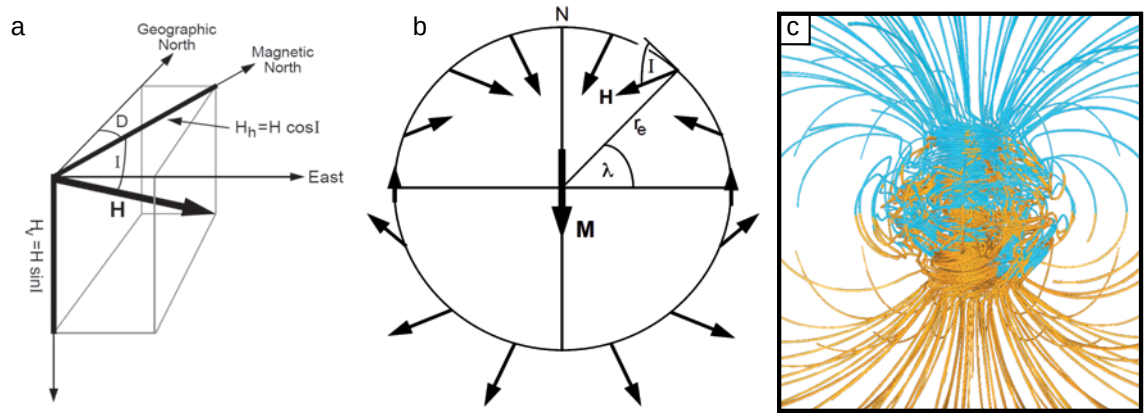

FIGURE 4.1 – (a) Composantes horizontale H_h et verticale H_v du champ magnétique terrestre H et définition géométrique de l'inclinaison I et de la déclinaison D, d'après Butler [1992] ; (b) Direction et orientation du champ magnétique dans un modèle de dipôle axial géocentré, d'après Butler [1992] ; (c) Simulation numérique du champ magnétique terrestre à partir des équations de magnétohydrodynamique, d'après Glatzmaier and Clune [2000]

dans le noyau externe générant le champ magnétique terrestre. Glatzmaier and Roberts [1995] proposent un modèle numérique basé sur les équations de magnétohydrodynamique permettant de simuler le champ magnétique terrestre ainsi que ses inversions (Fig.4.1c).

4.1.2 L'alimentation rémanante détritique

Les minéraux ont la propriété de s'aimanter sous l'action d'un champ magnétique et certains d'entre eux conservent cette aimantation une fois le champ magnétique absent, on parle alors d'aimantation rémanente. Cette propriété des minéraux dit ferromagnétiques est liée à la nature des éléments qui les composent (Fe entre autres) ainsi qu'à l'organisation de leur réseau cristallin (exemple de l'hématite ou de la magnétite). Ainsi, lors du dépôt de roches détritiques sédimentaires en milieu aquatique, les grains ferromagnétiques possédant un moment magnétique **m**, sont soumis à une force magnétique, en plus des forces hydrodynamiques, gravitaires ou liées à l'intéraction entre grains. Si les forces magnétiques dominent, il en résulte une orientation des grains ferromagnétiques selon le champ magnétique auquel ils sont soumis au moment de leur sédimentation et une rémanence de cette orientation après consolidation de la roche (Fig.4.2a). Pour permettre ce processus d'orientation, les forces hydrodynamiques doivent donc êtres négligeables et les conditions suivantes respectées : le milieu de dépôt est suffisamment calme, les grains ferromagnétiques sont suffisamment petits. Enfin les roches considérées ne doivent pas être réaimantées *a posteriori*.
Du phénomène d'orientation des grains des roches sédimentaires détritiques, appelé aimantation rémanente détritique (ARD ou DRM pour Detrital Remanent Magnetization), résulte la mise en place de colonnes de sédiments au sein desquelles la direction et l'orien-

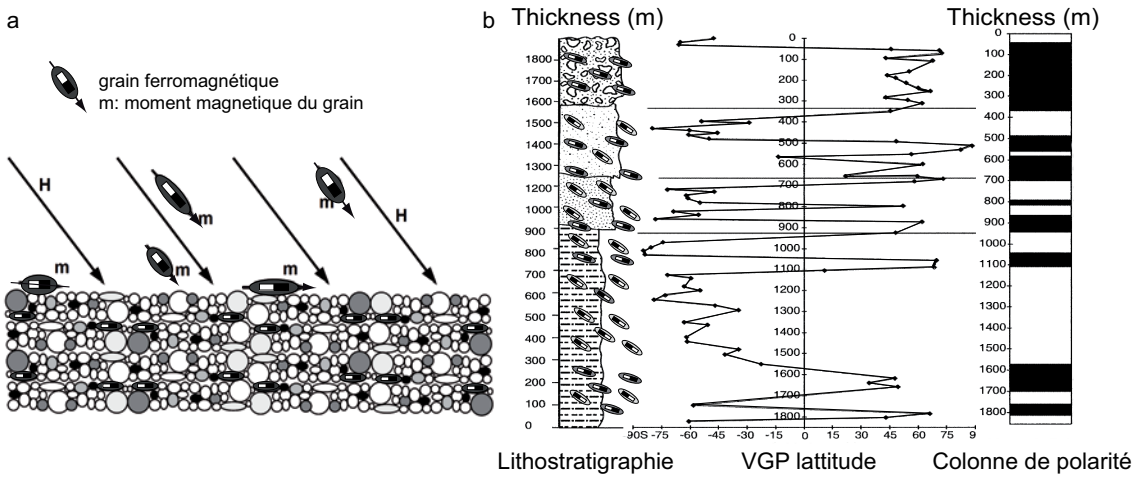

FIGURE 4.2 – (a) Orientation des grains ferromagnétiques possédant un moment magnétique **m** lors de la sédimentation de roches détritiques. Les grains ferromagnétiques soumis au champ magnétique terrestre **H** s'orientent au moment de leur dépôt selon la direction et l'orientation de **H**. Cette orientation est ensuite conservée, ce qui constitue le principe de L'Aimantation Rémanente Détritique. D'après Butler [1992]. (b) Principe de construction d'une colonne de polarité paléomagnétique. Les sédiments ayant enregistré l'orientation du champ magnétique terrestre au moment de leur dépôt, sont échantillonnés et permettent de connaitre la position du pôle magnétique à cette époque (VGP, Vitual Geomagnetic Pole). Les périodes dites Normales sont par convention représentées en noir (VGP proche du Nord géographique) et les périodes de polarité inverse (VGP proche du pole Sud) en blanc. Modifié d'après Yin et al. [2002].

tation du champ magnétique terrestre au moment du dépôt sont enregistrées (Fig.4.2b), ce qui donne accès aux variations du champ magnétique au cours du temps.

4.1.3 Reconstruction de l'histoire des inversions du champ magnétique terrestre : l'échelle de référence

La GPTS est construite par le recoupement de datations obtenues par différentes méthodes dont :

- L'étude des anomalies magnétiques enregistrées de part et d'autre des dorsales médio-océaniques, au taux d'accrétion du plancher océanique et à la durée des inversions (Fig.4.3A) ;
- La datation directe de sédiments déposés en milieu marin par méthode biostratigraphique ou analyse isotopique. Cette datation permet de disposer de points de calage pour la datation des roches de la croûte océanique ainsi que pour l'estimation du taux d'accrétion de cette même croûte (Fig.4.3B et D) ;
- La mesure de l'aimantation thermorémanente de roches volcaniques et de l'aimanta-

tion rémanente détritique de colonnes stratigraphiques de référence par ailleurs datées par méthode isotopique ou biostratigraphique.

La mise en commun de ces informations permet de contraindre l'âge des inversions du champ magnétique terrestre. Cependant, différentes incertitudes sont à prendre en compte telles que : (i) l'incertitude sur l'âge des points de calage (notée (b) et (d) sur la figure 4.3B) ; (ii) l'incertitude sur la taille des anomalies enregistrées au niveau de la crôute océanique (notée (a) sur la figure 4.3B et illustrée par la figure 4.3C) ; (iii) l'incertitude sur les taux d'accrétion de la croûte océanique au cours des temps géologiques.

Il en résulte plusieurs GPTS, proposées par différents auteurs (Fig.4.3D) et une référence fréquemment remise à jour. Pour tenir compte de ces incertitudes, Agrinier et al. [1999] proposent une approche probabiliste de construction de la GPTS (Fig. 4.3E), basée sur le théorème de Bayes. L'âge des points de calage est donné par une fonction de distribution. L'âge des évènements non datés par méthode isotopique ou biostratigraphique est déterminé en utilisant le théorème de Bayes, l'ordre des inversions étant connu.

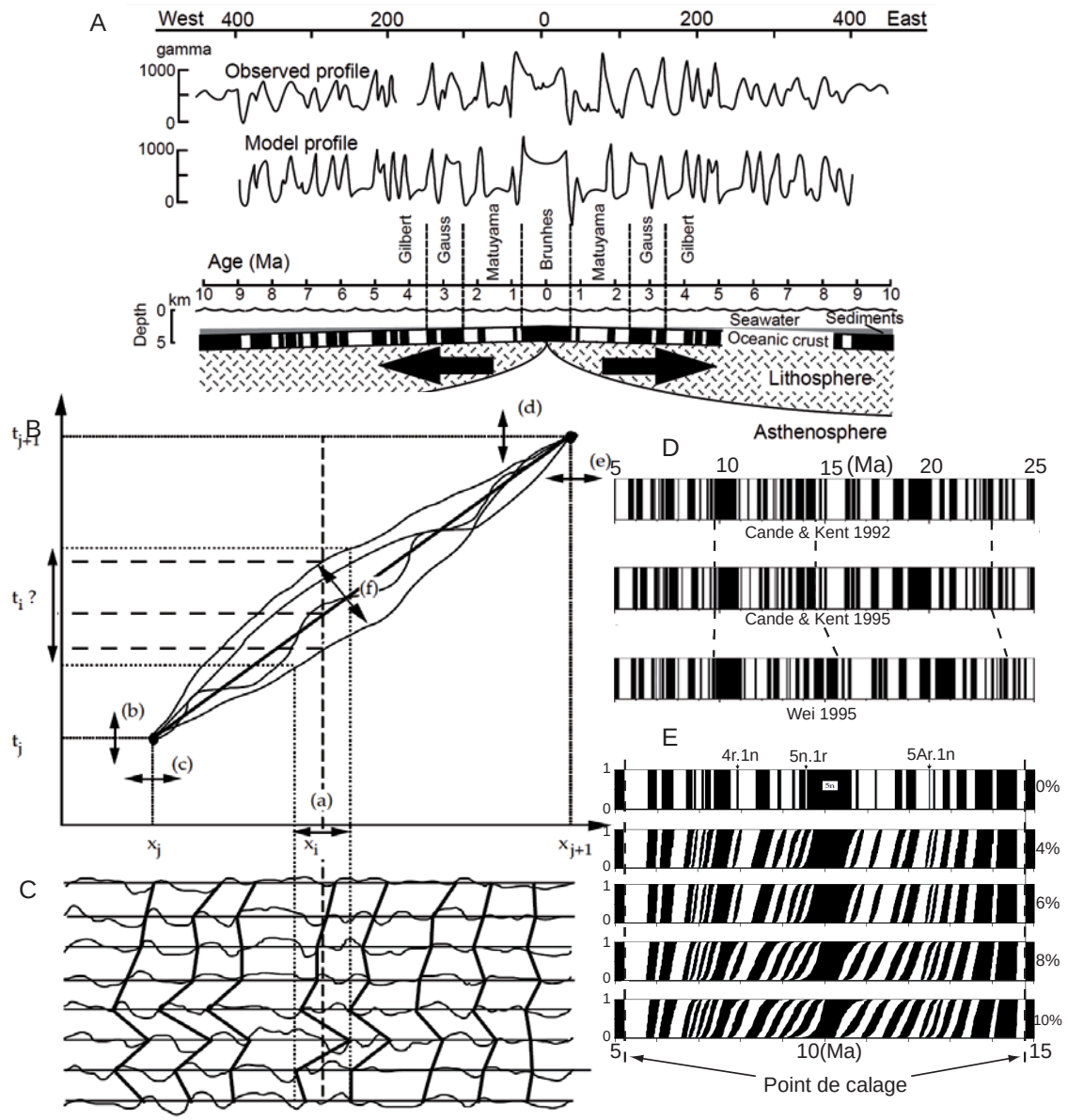

Figure 4.3 – Légende sur la page suivante

FIGURE 4.3 – (A) Enregistrement de l'orientation du champ magnétique au moment de la mise en place de la croûte océanique : les variations entre le profil d'anomalies mesuré (Observed profile) et le profil théorique (Model profile) s'expliquent en partie par l'acquisition d'une aimantation rémanente par les sédiments se déposant sur la crôute océanique. D'après Cox and Hart [1986]. Les âges des inversions sont déterminés par analyse des anomalies magnétiques enregistrées au niveau des dorsales océaniques. Le taux d'expansion des fonds océaniques varie le long d'une même dorsale : (C) exemple des anomalies enregistrées le long de différentes sections de la dorsale sud Atlantique. Il en résulte les incertitudes présentées en (B) sur : (i) la position ((*c*),(*e*)) des inversions x_j et x_{j+1} datées par des méthodes annexes et permettant de caler l'âge des points médians x_i ; (ii) sur la position (*a*), l'âge (t_i) et les taux d'expansions (*f*) au niveau des points (x_i) non calés par méthodes annexes. (D) Comparaison entre plusieurs échelles d'âge des inversions géomagnétiques. (E) Vue probabiliste de la GPTS tenant compte des incertitudes sur le taux d'accrétion de la croûte océanique. Les incertitudes ici prises en compte sont de 0, 4,. . . , 10% du taux d'accrétion moyen. Modifié d'après Cande and Kent [1992, 1995], Wei [1995], Agrinier et al. [1999]

4.2 Magnétostratigraphie : principes et méthodes

4.2.1 Construction d'une colonne magnétostratigraphique

La méthode la plus répandue de construction d'une colonne magnétostratigraphique est basée sur le prélèvement, le long d'un affleurement, d'échantillons orientés de roches. L'aimantation rémanante des échantillons est ensuite caractérisée (inclinaison et déclinaision) par désaimantation thermique ou par champ alternatif. Celles-ci permettent d'isoler les directions caractéristiques portées par des minéraux fortement coercitifs (c'est-à-dire difficilement réaimantables, exemple de l'hématite, la magnétite. . .) et de nettoyer celles acquise *a posteriori* par des minéraux faiblement coercitifs. Grâce à un échantillonnage dense et orienté, on peut ainsi déterminer l'évolution de l'inclinaison et de la direction du champ magnétique terrestre au moment du dépôt, et par conséquent reconstruire la position virtuelle des pôles et identifier les périodes de polarité normale et inverse (Fig.4.2b). Sur des séries sédimentaires de plusieurs milliers de mètres, la mesure de l'aimantation rémanente ne peut se faire en continu et s'appuiera donc sur un échantillonnage discret dont la fréquence est le paramètre clé de la qualité d'une corrélation.
Une méthode alternative pour mesurer l'aimantation rémanante des roches est proposée par Bouisset and Augustin [1993]. Celle-ci est basée sur la mesure *in situ* de l'aimantation rémanante des roches au niveau de puits en combinant les mesures effectu/'ee par deux outils de logging.

4.2.2 Corrélation à l'échelle de référence

Le principe de base de la datation des roches par méthode magnétostratigraphique est la corrélation de la colonne de polarités construite à partir d'échantillons prélevés sur le terrain avec la GPTS. Cette corrélation est basée sur l'identification de similarités entre les séquences d'inversion enregistrées dans les sédiments, et celle présentes dans la GPTS. Cette étape n'est possible que si :

- La colonne sédimentaire étudiée est quasi continue sur une séquence suffisamment importante d'inversions afin de pouvoir être reconnue sur la GPTS. La présence de failles, ou de nombreuses et importantes périodes d'érosion entrecoupant la série étudiée, sont notamment susceptibles de rendre toutes corrélations hasardeuses ;
- La colonne sédimentaire a été échantillonnée suffisamment densément de sorte que la majorité des inversions enregistrées dans les sédiments ait été observée ;
- Le taux d'accumulation est stationnaire sur une période suffisamment longue. La séquence d'inversions enregistrée ne doit pas être trop fortement déformée et être ainsi reconnaissable dans la GPTS ;
- Le champ magnétique terrestre a bien été enregistré au moment de la sédimentation et les sédiments n'ont pas été remaniés ou démagnétisés.

La corrélation entre la colonne de polarité et la GPTS effectuée manuellement est par essence subjective et il est fréquent que plusieurs auteurs proposent une datation différente pour une même série sédimentaire. L'étude de fossiles ou de pollens, ou encore l'analyse isotopique de coulées de lave entrecoupant la série étudiée, peuvent apporter des indices sur la position de la colonne étudiée dans la GPTS ; ces informations ne sont cependant pas toujours disponibles.

4.3 Gestion des ambiguités lors de corrélations magnétostratigraphiques

Afin de gérer les incertitudes qu'un tel processus engendre, nous proposons une méthode de corrélation automatique entre une colonne de polarité issue d'études de terrain et la GPTS. Cette méthode n'enlève en rien la subjectivité des corrélations produites ; en effet la méthode de corrélation est basée sur des fonctions mathématiques dont le choix est lui même subjectif. Cependant, plusieurs avantages sont à tirer de l'utilisation d'une méthode numérique pour les corrélations magnétostratigraphiques :

- Le débat entre auteurs sur la validité d'une corrélation ne se situe plus sur une interprétation mais sur des règles mathématiques formulées explicitement.
- Plusieurs corrélations possibles pour une même série sédimentaire peuvent être calculées, ce qui permet en peu de temps d'envisager de nombreux scénarios de corrélations possibles. Un auteur peut alors présenter dans son étude l'ensemble des datations possibles et apporter des arguments en faveur de celle lui semblant la plus probable. Ceci a pour avantage de limiter le nombre de publications sur une même série sédimentaire comme c'est le cas par exemple pour la colonne de Xishuigou (aussi appelée colonne

de Subei) qui a été reprise et datée différemment dans trois études : Yin et al. [2002] datant la section entre 33.5-27 Ma, Gilder et al. [2001] entre 26-19 Ma et Wang et al. [2003] entre 20-9 Ma.

– Les corrélations calculées automatiquement sont associées à une valeur représentative de leur plausibilité, ce qui permet de les ordonner et de pondérer leur participation dans des études statistiques sur l'âge des roches et les différents paramètres qui en découlent (taux d'accumulation ou de déformation par exemple). Ce type d'études statistiques est particulièrement utile lorsque peu de points de calage permettent de contraindre l'âge des roches.

La méthode de corrélation que nous proposons est basée sur l'algorithme DTW et fait l'objet d'un article soumis à la revue Earth and Planetary Science Letter.

Management of ambiguities in magnetostratigraphic correlation

Article to be submitted to the Earth and Planetary Science Letter

Florent Lallier, Christophe Antoine, Julien Charreau, Guillaume Caumon, Jeremy Ruiu

Abstract

Magnetostratigraphy is a powerful tool to provide absolute dating of sediments enabling good and detailed chronostratigraphic correlations. It is based on the correlation of a magnetic polarity column, observed and measured in a given sediment section, to a magnetic polarity reference scale where polarity changes are well dated *via* other independent methods. However, magnetostratigraphic correlations are loose because only constrained by binary magnetic chrons (*i.e* normal or reversal) and their thickness, which are both defined from depth variations of the magnetic remanent directions. The thickness of a given magnetic chron is a function of time and sediment accumulation rate, which may not be stationary, leading to ambiguities when performing the correlations.
To address these ambiguities, a numerical method based on the Dynamic Time Warping algorithm is proposed. Magnetostratigraphic correlations are computed in order to minimize the local variation of accumulation rate. The main advantage of the proposed method is to automatically provide a set of reasonably likely correlations. This set can then be scrutinized for further analysis and interpretation. However, the likelihood of a correlation should be handled carefully. It depends on the information content of the magnetotratigraphic section itself and remains ultimately valid by ancillary constraint. Nevertheless, the method is shown to present consistent results on difficult synthetic cases simulating abrupt variations of the sedimentation rate, and provides interesting insights on true sections debated by previous authors.

Introduction

Sedimentary basins provide key records of many earth processes including tectonics, climate and erosion. They may also host large resources of ore deposits (e.g gold, U...), hydrocarbon and fresh water. Good and detailed chronostratigraphy is critical to bear quantitative constraints on the wide variety of interactions that may exist between these processes. This observation holds for reservoir and basin modeling which are also based on stratigraphic correlation and request reliable chronology. Sediment dating is thus a fundamental step for a broad community in Earth sciences. Various techniques have been developed such as radio-isotopic dating (e.g K-Ar, Fission Tracks), biostratigraphy, cosmonucleid isotopes (10Be/26Al), astronomical records, palynology, 14C, varves etc. All these methods enable the dating of sediments in a large range of environments and for time scales ranging from years to 10^7 years. However, in continental areas, due to the paucity of biostratigraphic markers, reliable dating via classic methods remains challenging. The depositional ages are therefore mainly inferred from loose lithostratigraphic correlation, which suffers from many flaws in the presence of strong lateral facies variations and diachronous deposition (e.g. Charreau et al. [2009b]).Yet, continental sediments may record the Earth magnetic field and its polarity at the time of deposition via Detrital Remanent Magnetization (DRM) mechanism (e.g Tauxe [2006]). Given a sedimentary section or a log, one can measure the depth variation of the remanent magnetic directions and identify the polarity changes of the Earth magnetic field. A polarity column can then be reconstructed as a succession of

polarity chrons (or reversal) characterised by their length in meters or duration in years and their polarity (normal or reverse). A normal polarity chron is represented in black in a polarity column and corresponds to a period where the Earth magnetic dipole is similar to the present one with the magnetic North close to the geographic North. A reverse polarity chron is shown in white and corresponds to a period where the dipole has been switched with its magnetic North close to the southern Earth's pole.

Magnetostratigraphy is based on the correlation of a polarity column observed and measured in a sediment section to the geomagnetic polarity time scales (GPTS [Lourens et al., 2004]) where polarity changes are well dated via independent methods (astronomical constraints, spreading of the oceanic floor, thermochronology). This powerful technique enables the dating of sediments in many areas where other approaches have failed. However, magnetostratigraphy is based on several assumptions : (1) the Earth magnetic field is bipolar, (2) the sedimentary section is continuous with no depositional hiatus nor erosion and (3) the accumulation rates are constant at short time scales ($<$ few Ma). This method is particularly well suited for the Cenozoic Era and Jurassic Period in which numerous polarity changes have been documented.

Nevertheless, the major drawback of this dating technique is that the correlation between the observed polarity column to the reference scale is subjective as only based on eyes, and provides a single dating with no assessment of uncertainty. Other datings, for example from fossil or lava flows observed in the studied section, are therefore very useful to independently constrain the correlation and reduce uncertainty. In many cases, the absence of such data yield controversial debate between authors and leave magnetostratigraphic correlation results to doubts and critics. For example in the Subei section in Western China, three different authors have proposed different correlations with ages ranging between 33.5-27 Ma [Yin et al., 2002], 26-19 Ma [Gilder et al., 2001], 20-9 Ma [Wang et al., 2003], leading to conflicting interpretations about the tectono-climatic history of the Northeast Tibet Plateau (section 4.3.2.1).

A magnetic polarity column only provides an incomplete view of the sedimentary record. It is therefore almost impossible to find "the right" correlation model which would require a huge amount of independent data impossible to acquire in practice. Instead, we suggest to automatically generate possible correlation models by using well-established rules and principles in order to cope with uncertainty. In the proposed algorithm (section 4.3.1.4), each correlation is associated with a cost, which is used to rank the various proposed solutions according to specified rules. Moreover, the proposed approach provides estimate on the instantaneous accumulation rate and their uncertainties on the basis of several possible solutions while classic "eye-based" correlation only gives the 90-95% confidence limit from basic linear regression built on a unique dating.

Tests carried out on synthetic polarity columns (Section 4.3.1.6) attest that the algorithm can handle sedimentary hiatus and sharp variations of the accumulation rate. The method is therefore applied to the Subei and Yaha magnetostratigraphic sections in Central Asia (section 4.3.2) where a debate still remain on the depositional ages though they represent standard sections for tectonics and climate in this region. The analysis of the 10,000 mi-

nimum cost correlations, covering many acceptable possibilities for these sections provides interesting insights about the correlations discussed in the literature.

4.3.1 Computer method for magnetostratigraphic correlation

4.3.1.1 Problem Settings

Computing correlations between magnetic polarity section and polarity reference scale is challenging since :(i) the magnetic record is binary information (ii) the studied section represents only a part of the whole polarity reference scale and has potentially been transformed by changes in the accumulation and compaction rates and (iii) under-sampling may yield unrecorded polarity changes.
Moreover, in a sedimentary section, the correlation to the reference scale strongly depends on the thickness of each polarity zone, which is a function of three parameters : (i) the duration of the polarity chrons $i(t)$; (ii) the accumulation rate $p(t)$ and (iii) the compaction rate c. From a mathematical analysis, Lowrie and Kent [2004] show that the geomagnetic polarity time serie is not stationary but is composed of stationary periods. They also reveal that the duration of the polarity chrons follows a Poisson law.
The accumulation rate is also a non-stationary process as it is driven by the nature of the depositional environment and erosion processes, which may rapidly (i.e. few kyr) and strongly varies. However, authors often consider the accumulation rate to change stepwise between long stationary periods. For example, from magnetostratigraphic study of the Jingou He section in northern Tianshan piedmont, Charreau et al. [2009a] found that the mean accumulation rate was 0.10 mm/yr, 0.18mm/yr and 0.29mm/yr from 23 Ma to 16Ma, from 16Ma to 11Ma and from 11Ma to 1Ma, respectively. Finally, the compaction rate may vary along a given section due to rock lithology and burial leading to distortion of the observed accumulation rate.
To provide robust, relevant and trustworthy correlations, computer based methods will be required to handle distortion in the time signal of the magnetic chrons induced by these processes (accumulation rate, compaction rate...).

4.3.1.2 Previous works

Man [2011] proposes an interesting computer method which correlates a given polarity column to the reference scale under the following assumptions : (i) the thickness of the observed polarity zone is supposed stationary, (ii) the polarity column is supposed complete (all polarity changes have been recorded and sampled in the section), (iii) the age of the studied column is *a priori* roughly known and (iv) the geomagnetic reversal process is supposed to follow a Gaussian law. As pointed out above, these assumptions can be discussed when working on long sedimentary sections. First, the chron thickness and duration are mainly non-stationary. Second, due to non-depositional and/or erosional periods, several magnetic polarity changes may be missed in the sediment record. Moreover, non-amenable lithology for sampling (e.g conglomerate) may sometimes impose low sampling density in-

sufficient to identify all magnetic reversals. And finally, in continental areas it is sometimes very difficult to assess the age of a given section from sedimentology only, due to the absence of biostratigraphic markers. For example, in Central Asia, thick conglomerate lying at the top of the basin sedimentary piles, have long been assigned to the Plio-pleistocene whereas recent magnetostratigraphic studies have shown that their deposition could start during the middle Miocene (Charreau et al., 2009).
Another way to correlate a given polarity column to the reference scale was proposed by Man [2008]. This method is based on a preprocessing step which transforms both the polarity column and the reference scale to dimensionless data by calculating the logarithm of the thickness (or the duration) of a given magnetic chron minus the logarithm of the thickness (or the duration) of the underlying chron. Thanks to this transformation, accumulation rate and chron duration can be supposed locally stationary. The correlation between the reference scale and the studied polarity column is then computed using a cross correlation function. This method is less sensitive to the non-stationarity of the data but still requires that all reversals have been recorded and sampled in the sediments. In this paper, we similarly use thickness ratios to relax the global assumption of stationary preservation rate.

4.3.1.3 Proposed approach

Our approach has been designed to manage non-stationary data, unrecorded chrons in the polarity column (sedimentary hiatus and/or erosion) and to support independent constraints derived from biostratigraphy or geochemical dating techniques. This method is based on the Dynamic Time Warping (DTW) algorithm described in section 4.3.1.4 [Levenshteiti, 1966]. The DTW algorithm is modified to output not only the "*best*" correlation between the studied polarity column and the GPTS, but also the "*n best*" correlations in order to manage uncertainties on sediment dating and accumulation rate. The Python implementation used in this paper is available at the address `http://www.gocad.org/w4/index.php/research/free-software`, at which new versions will be posted. Input data are : (*i*) the reference polarity section which is supposed exhaustive (i.e. there is no polarity change in the recorded section which is not in the reference scale) ; (*ii*) the thickness of polarity zones observed in the sediment section.

4.3.1.4 The Dynamic Time Warping algorithm

The Dynamic Time Warping (DTW) algorithm has been introduced by Levenshteiti [1966] and found many applications for automatic signal correlation in speech recognition [Myers and Rabiner, 1981], bioinformatic and geoscience for the correlation of magnetic susceptibility stratigraphic sections [Hladil et al., 2010], lithostratigraphic correlation [Smith and Waterman, 1980] or for the correlation of well logs [Fang et al., 1992a]. Lisiecki and Lisiecki [2002] propose to correlate paleoclimate record using a dynamic programming method comparable to the DTW algorithm.
Consider two columns **a** and **b** presented in Fig.4.4, composed of polarity zones noted from

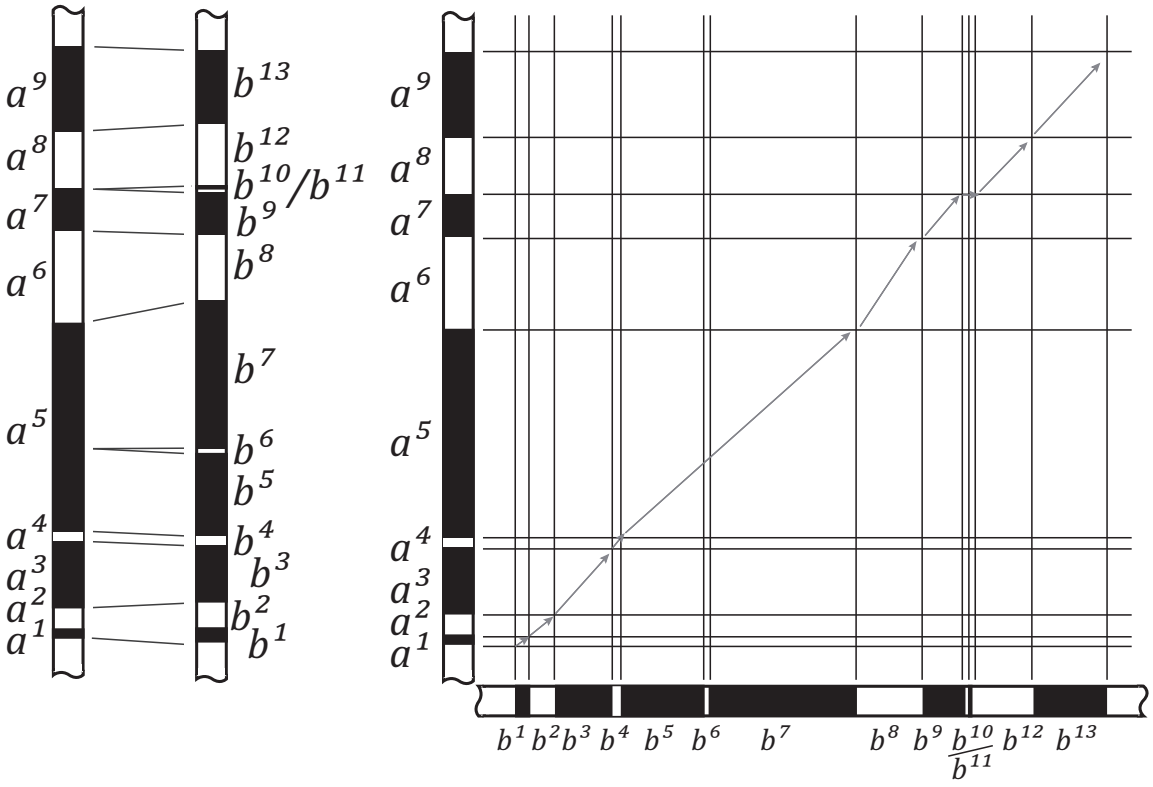

FIGURE 4.4 – Correlation between two polarity columns and associated correlation path in the DTW table displaying gaps (chrons b^{10} and b^{11}) and "one to many correlation" (chrons a^5, b^5, b^6 and b^7)

a^1 to a^9 and chrons noted from b^1 to b^{13}, respectively. The correlation between the two columns can be represented as a path $CP(\mathbf{a}, \mathbf{b}) = [cp_1, \ldots, cp_i, \ldots, cp_k]$ in a $2D$ diagram (Fig.4.4) where cp_i is an element of the path. In the example presented in Fig. 4.4 $CP(\mathbf{a}, \mathbf{b})$ is noted :

cp_1	cp_2	cp_3	cp_4	cp_5	cp_6	cp_7	cp_8	cp_9	cp_{10}	cp_{11}
a^1	a^2	a^3	a^4	a^5	a^6	a^7	$\emptyset$	$\emptyset$	a^8	a^9
b^1	b^2	b^3	b^4	b^5 b^6 b^7	b^8	b^9	b^{10}	b^{11}	b^{12}	b^{13}

Four different configurations may arise : (1) two units are well correlated (i.e. diagonal arrow in the diagram noted $cp_i = (a^f, b^g)$; (2) a polarity zone in column **a** is missing in column **b** (i.e. vertical arrow noted $cp_i = (a^f, \emptyset)$) ; (3) a polarity chron in column **b** is missing in column **a** (i.e. a horizontal arrow noted $cp_i = (\emptyset, b^g)$) ; and (4) a polarity zone of **a** (respectively **b**) is associated to several polarity chrons of **b** (respectively **a**, see the correlation of chrons a^5 in Fig. 4.4). This last configuration will be addressed in section 4.3.1.5.
A cost is associated to each of these first three configurations. The best correlation between the two columns is the one for which the sum of the individual costs of all successive configurations is minimal. The cost of the correlation $CP(a_i, b_j)$ between column **a** from a^1 to a^i and column **b** from b^1 to b^j, $C(i, j)$ is recursively computed as follows :

$$C\left(a^i, b^j\right) = \min \begin{bmatrix} c(a^i, b^j) + C\left(a^{i-1}, b^{j-1}\right) \\ g(a^i) + C\left(a^{i-1}, b^j\right) \\ g(b^i) + C\left(a^i, b^{j-1}\right) \end{bmatrix} \tag{4.1}$$

where $c(a^i, b^j)$ is the cost of a correlation (called a match and noted $cp_l = (a_i, b_j)$) between two units and $g(a^i)$ and $g(b^i)$ are the costs of an extra unit (called a gap) in column **a** (noted $cp_l = (a_i, \emptyset)$) and column **b** (noted $cp_l = (\emptyset, b_j)$), respectively. Applying Eq. (4.1) from $i = 1$ to 9 and $j = 1$ to 13 yields the minimum cost correlation between columns **a** and **b**.

4.3.1.5 Specification to magnetostratigraphy

In the following section, we present how the DTW algorithm has been improved in order to achieve correlations between a given magnetic polarity column and the GPTS. Let **a** denote the polarity column established from paleomagnetic sampling and analyses, and **b** the polarity reference scale.

Cost computation We first assume that the reference scale **b** is complete, meaning that each polarity change a^i recorded in the polarity column **a** must be correlated to a polarity change in the reference scale **b**. Therefore, we set the cost of a gap in the studied polarity column to be equal to the infinity : $g(a^i) = \infty$.

The cost $c(a^i, b^j)$ of a match between a polarity chron (of the reference scale **b**) and a polarity zone (of the polarity column **a**), is considered only if the two considered units have

the same polarity. Moreover, the cost of a match is designed to minimise local variations of the accumulation rate.
Let $t(a^i)$ refer to the thickness, in meters, of the i^{th} polarity zone recorded in the studied polarity column, $p(a^i)$ its polarity, $d(b^j)$ the duration of the j^{th} polarity chron of the reference scale and $p(b^j)$ its polarity. When the correlation between a^i and b^j is evaluated within the DTW algorithm, the correlation $CP(a^{i-1}, b^{j-1})$ is known. Let u and v be the last two units correlated before a^i and b^j :

$$\begin{array}{c} CP(a^{i-k}, b^{j-l}) = [cp_1, \ldots, cp_k] \\ (u, v) = cp_{k-l} \text{ where } u, v \neq \emptyset \\ \text{with } l \text{ as close as possible to 1} \end{array} \tag{4.2}$$

The match cost between a^i and b^j, is defined by :

$$\begin{array}{lll} \textbf{if } p(a^i) \neq p(b^j) & c(a^i, b^j) = \infty & \\ \textbf{else} & c(a^i, b^j) = 1 - \left(r^1/r^2\right) & \text{if } r^1/r^2 > 1 \\ & c(a^i, b^j) = 1 - \left(r^2/r^1\right) & \text{if not.} \\ \text{where,} & r^1 = t(a^i)/d(b^j) & \\ \text{and,} & r^2 = t(u)/d(v) & \end{array} \tag{4.3}$$

The use of a ratio in the cost function ensures that compared values are dimensionless. This cost function can be computed under the assumption that the accumulation rate is locally stationary in the two considered chrons. Due to discrete sampling, the thickness of a polarity zone in the studied section is not exactly known. Moreover, error is proportionally more important for thin polarity zones than for large ones. Uncertainty on the thickness of small polarity zones is managed by multiplying the match function by a correction factor $k(a^i)$:

$$k(a^i) = log\left(1 + \frac{min\left(t(a^i), t(a^{i-1})\right)}{\bar{t}(\mathbf{a})}\right) \tag{4.4}$$

where $\bar{t}(\mathbf{a})$ is the mean thickness of polarity zones on the studied section.
The cost of a gap in the reference scale $g(b^j)$ is computed as the ratio between the duration of the considered chron $d(b^j)$ and the mean duration of chrons of the reference scale $\bar{d}(\mathbf{b})$. It corresponds to the cost of an un-sampled, non-recorded (i.e non-deposition) or eroded polarity zone on the polarity column. It is therefore computed as $g(b^j) = d(b^j)/2\bar{d}(\mathbf{b})$ and respects the intuitive idea that non-sampled or non-preserved polarity zones are preferentially the smallest ones.

Gap management Most of the time, when a polarity change has not been sampled or preserved in the sediments, the resulting polarity column may display a polarity interval which actually includes two or more chrons of the reference scale (see correlation between chrons a^5 and b^5, b^6 and b^7 in Fig.4.4). Waterman and Raymond Jr. [1987] introduce the "one to many matching" possibility in the DTW algorithm. In this case, one unit of a

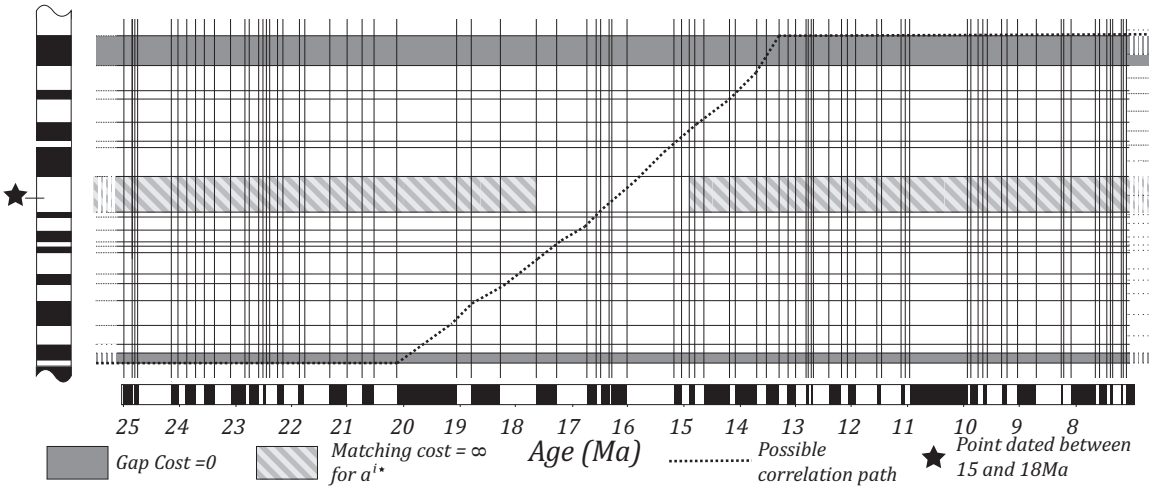

Figure 4.5 – DTW table for correlation between a polarity column (vertical) and the polarity reference scale (horizontal). Cells on which matching and gap costs are computed to manage extremities of the polarity column are displayed in dark grey. Cells on which matching and gap costs are computed to constrain correlation with dated point of the polarity column are displayed in light grey.

column may be correlated to several units of the second column. However, assuming that the magnetic polarity reference scale is complete implies that the "one to many matching" can only occur in one way, between one polarity zone of the studied polarity column and several chrons of the reference scale. Let $mg\left(a^i, [b^{j-1}, b^j, b^{j+1}]\right)$ denote the cost of a "one to many match" between polarity zone a^i of the polarity column and chrons b^{j-1}, b^j and b^{j+1} of the reference scale. If the polarity of a^i, b^{j-1} and $b^j + 1$ are the same, the "one to many" correlation is considered and

$$\begin{gathered} mg\left(a^i, [b^j - 1, b^j, b^j + 1]\right) = c(a^i, b^{j-1,j+1}) + g(b^j) \\ \text{where } b^{j-1,j+1} \text{ is a chron with a duration} \\ d\left(b^{j-1,j+1}\right) = d(b^{j-1}) + d(b^{j+1}). \end{gathered} \tag{4.5}$$

Management of borders A given polarity column observed in a sediment section contains only few units with respect to the reference scale. Therefore, in the DTW algorithm many gaps should arise at the polarity column extremities (Fig.4.5). Let's consider a polarity column **a** with its first polarity zone called a^1 and its last called a^n to be correlated to the reference scale noted **b**. As proposed by Smith and Waterman [1980] these extremities issues are managed by setting $g(b^j) = 0$ in Eq.4.1 if $i = 1$ or $i = n$.

Constraining the correlation using independent dating Some additional dating information derived from biostratigraphy (*e.g.* Charreau et al. [2009a], Sen [1986]), cosmonucleid isotopes (*e.g.* Hu et al. [2011]), palinology (*e.g.* Dupont-Nivet [2008]), *etc.*,

may enable to independently constrain the ages of a stratigraphic section. However, such independent age constraints will only be valid at a specific stratigraphic depth. Let $a^{i\star}$ be the i^{th} polarity zone of the polarity column where one has independently dated the sediment between 15 and $18Ma$ (Fig.4.5). The matching cost function is thus transformed to $c(a^{i\star,b^j}) = \infty$ if polarity chron b^j is older than $18Ma$ or younger than $15Ma$. This ensures that polarity zone $a^i\star$ is correlated to reference chrons dated between 15 and $18Ma$.

Best and n-best correlations Within the DTW algorithm, the cost of a match between a given polarity zone and a chrons (a^i and b^j) must be calculated independently from the correlation of the other units ($CP(a^{i-1}, b^{j-1})$). Our matching function (Eq.4.3) does not respect this condition. Therefore, to ensure the finding of the minimum cost correlation $CP(\mathbf{a}, \mathbf{b})$, the DTW algorithm is modified to output the k correlations $[CP(a^i, b^j)]^k$ between a^1 to a^i and b^1 to b^j built from modified version of equation 4.1 :

$$\left[C\left(a^i, b^j\right)\right]^k = \min^{\mathrm{k}} \begin{bmatrix} c(a^i, b^j) + \left[C\left(a^{i-1}, b^{j-1}\right)\right]^k \\ g(a^i) + \left[C\left(a^{i-1}, b^j\right)\right]^k \\ g(b^i) + \left[C\left(a^i, b^{j-1}\right)\right]^k \end{bmatrix} \tag{4.6}$$

where $\left[C\left(a^i, b^j\right)\right]^k$ are costs associated to the k correlations $\left[C\left(a^i, b^j\right)\right]^k$.
Tests carried out on various polarity columns show that if k is large enough, the optimal correlation is found (for example $k > 1,000$ ensures finding the minimum cost correlation between a polarity column of 25 polarity zone and a GPTS of 290 chrons).
Furthermore, this new version of the DTW algorithm computes not only the minimum cost correlation but also the n best correlations of a polarity column, offering insight into uncertainty in dating and accumulation rates estimation. As for the minimum cost correlation, a number k of computed correlations should be large enough to ensure finding the n minimum cost ones ($k > 20,000$ correlations are output to obtain the $n = 10,000$ minimum cost one in example presented in section 4.3.1.6).
Tests carried out on synthetic data sets (columns of 7 polarity zones are correlated to a 25 polarity chrons reference scale) where all possible correlations can be computed (125,423 in this case) show that the correlation costs follow an exponential distribution for the better half of the correlation. In a basic magnetostratigraphic problem (a 25 units polarity column to correlate to a reference scale covering the past 150My, *i.e.* 290 polarity chrons) the number of possible correlations reaches 10^{30} which is technically impossible to compute. Therefore only a few percent of the possible correlations can be done which we call the n best correlations. As presented above, $k > n$ correlations should be computed to ensure finding the n best correlations. If k is too low, the costs distribution does not exhibit an exponential distribution, indicating that the n output correlations do not represent the real n minimum cost ones. k can then be increased until the cost histogram honours the exponential function for realisation 1 to n.

Statistical analysis of the n best correlations The relationship between the cost of a correlation and its rank, considering only the n best (n being low when compared to

the total number of possible correlation) could be modelled by :

$$[CP(\mathbf{a},\mathbf{b})]^m \simeq \frac{1}{k_1} ln\left(k_2 \times m + k_1^{[CP(\mathbf{a},\mathbf{b})]^0}\right) \tag{4.7}$$

where, k_1 and k_2 are two constants greater than one, and $[CP(\mathbf{a},\mathbf{b})]^m$ is the cost of the m$^{\text{th}}$ best correlation. The cost-rank function computed for the study of the Xishuigou section (section 4.3.2.2h) is presented in Fig. 4.7. Two groups of correlations can be identified on the rank-cost function : (i) a first group, corresponding to the first hundred correlations in which the correlation cost increases rapidly with the rank ; (ii) a second group, called cost plateau, where the cost gently increases with the rank. Tests carried out on short synthetic polarity columns show that the second group actually includes about half of the entire possible correlations. We define "interesting correlations" as the correlations with a cost close to the minimum one and which therefore can be considered as likely. The first group actually corresponds to this definition of "interesting correlation".
Analysing the n best correlations of a polarity column offers an insight into uncertainties on sediment dating and resulting conclusions (accumulation rate, ...). A statistical analysis of uncertainty in a magnetostratigraphic study requires a number n of correlations large enough to ensure that all interesting correlations has been output. A qualitative evidence that all "interesting correlations" have been considered is the presence of a plateau for the cost-rank function (*e.g.* as observed in Fig. 4.7h).

Visualization of the n best correlations A visual and intuitive representation of the possible correlations (10,000 for the magnetostratigraphic column we studied) is a useful tool for the understanding of magnetostratigraphic uncertainties. Here, we propose a visualisation method of the n best correlations based on a representation of the dating weighted density. For each polarity zone a^i of the studied polarity column, its mean age is computed on each of the n best correlations $[CP(a^i, b^j)]^n$ and plotted on a depth-time diagram. We propose the contribution w_i of each dating $CP_i(\mathbf{a},\mathbf{b})$ to be inversely proportional to its cost $C_i(a,b)$:

$$w_i = 1 - \frac{C_1(\mathbf{a},\mathbf{b}) - C_i(\mathbf{a},\mathbf{b})}{C_1(\mathbf{a},\mathbf{b}) - C_n(\mathbf{a},\mathbf{b})} \tag{4.8}$$

A kernel smoother [Wand and Jones, 1995] is then applied to this set of weighted points, resulting in a representation of the alternative correlations where their relative probability is represented by the normalised weighted density map (Fig.4.6).

4.3.1.6 Validation proposed approach

The proposed approach is tested on two synthetic polarity columns designed to evaluate how non-stationary accumulation rate, erosion, faulting events and incomplete sampling are managed by the algorithm.

Synthetic column description A first synthetic polarity column (Fig.4.6 A) is built from the GTPS using a non-stationary and non-constant accumulation rate between polarity chrons *C3A.2n* to *C5Ar.2r*. Chrons *C3An.2n* to *C4Ar.1r** and *C4Ar.1r** to *C5r.3r-1n* were modified using accumulation rates drawn independently from a distribution law U $[0.06, 0.23]$ mm/yr while chrons *C5r.3r-1n* to *C5Ar.2r* were modified using a law U $[0.37, 0.63]$ mm/yr. The second synthetic polarity column (Fig.4.6 B) is designed to check whether or not our method enables us to manage un-sampled, eroded or faulted polarity zones. Two modifications are made on the first synthetic polarity column : (i) the reverse chron *C4r.1r* is suppressed, resulting in a normal polarity zone with a thickness equal to the cumulated thickness of polarity zones *C4n.2n*, *C4r.1r* and *C4r.1n* ; (ii) a gap of up to 1Ma is added by "eroding" completely the chron *C5n.2n* and partially the chron *C5r.1r* yielding a reverse polarity zone with a thickness equal to the thickness of chron *C5n.1r* and the remaining part of *C5r.1r*.

Result analysis Correlation results can be analysed via the minimum cost correlation (dash line in Fig.4.6) but also using the statistical distribution of the n best correlations.

Minimum cost correlation

The minimum cost correlation computed on the first synthetic column exactly reproduces the expected correlation. These results show that our correlation method manages non-stationary sediment accumulation rates. The correlation computed on the second synthetic polarity column is consistent with the way we built it. The un-sampled polarity chron (*C4r.1r*) is well recognised by the algorithm and results in a one to many correlation in the DTW table. The erosion occurring in chrons *C5n.2n* and *C5r.1r* is partially well identified. Contrary to a one to many correlation (*i.e.* chons c of the polarity column correlated with *C4r.1r*, *C5n.1r* and *C5n.2n*), the algorithm outputs an erosion of chron *C5n.1r* and *C5n.2n*.

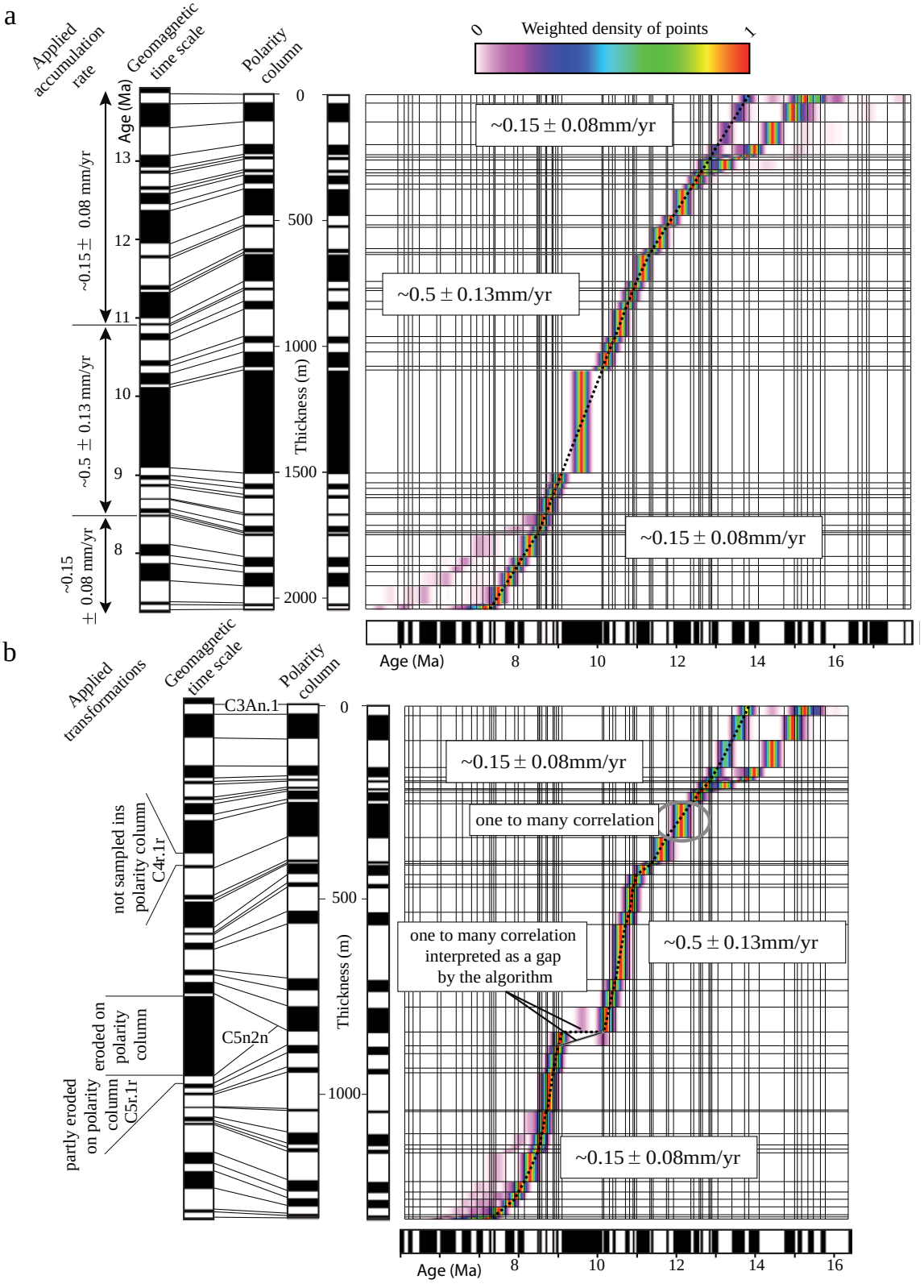

FIGURE 4.6 – Caption on next page.

FIGURE 4.6 – Correlation test with a polarity column where accumulation rate is not stationary (A) and where some chrons are not sampled or eroded (B). Dashed lined correspond to the minimum cost correlation of each case.

N best correlation

The probability density plot of the 10,000 best correlations of the two synthetic polarity columns are presented in Fig. 4.6. The quality of the resulting solutions is similar for the two columns. Dating of the central part of the polarity column (from 300m to 1600m and from 250m to 1000m for the first (Fig.4.6a) and the second polarity column (Fig.4.6b)) does not display major variation around the minimum cost correlation and attests a good confidence on the given ages in this part. At the point where the result of a faulting event has been mimicked in the second synthetic polarity column, variations arise around the minimum cost correlation, suggesting a possible missing polarity zone. Two other variations appear at the top of both polarity columns. In a real case, these variations may lead to alternative interpretations in terms of accumulation rates as presented in section 4.3.3.

4.3.2 Application to recent magnetostratigraphic analyses in Central Asia

4.3.2.1 Central Asia a key area for tectonics, climate and resources in Asia

Central Asia is constituted by several large and very active mountain ranges including the Tianshan, the Qilianshan, the Kunlun Shan, *etc.* All these ranges dominate the topography over thousands of metres with some summits higher than 7km. While originally formed during a long-lived Paleozoic to Mesozoic history of subduction/collision of several continental blocks (*e.g.* Windley et al. [1990]), their high present topography attests to an intense and younger deformation : all these ranges were uplifted and reactivated under the India-Asia collision [Tapponier and Mohar, 1979]. Therefore, since the collision started 55Ma ago [Patriat and Achache, 1984], this region has played a key role during the deformation of the Asian continent accommodating up to 40% of the whole convergence between India and Asia. Moreover, intense deformation and tectonics in this area has probably strongly impacted the Asian and global climate, yielding a strong aridification of Central Asia [Fluteau et al., 1999]. The material eroded and shed from these uplifting mountains fills several large intracontinental basins (Tarim, Qaidam, Junggar) where thick and continuous sedimentary deposits have recorded tectonic and climate changes. Thanks to numerous tectonic wedges and large river entrenchments, thick and continuous sedimentary sections are now well exposed at the toes of these mountain ranges, enabling the analyses of sediments for tectonics, climate change, natural resources, textitetc. However, due to their continental origin, these sediments are poorly dated *via* classic biostratigraphic method, which greatly inhibits our ability to stratigraphically correlate different sections or to place temporal bound on tectonic and climate processes. Therefore during the past decades, magnetostratigraphy has been the technique of choice to better constrain the de-

positional ages of these series and numerous studies have been published in international journals. However, subjective magnetostratigraphic correlations sometimes yield controversial ages because several authors may propose several correlations for the same section. Consequently, the interpretation and conclusions derived from these controversial ages are open to debate. Two examples of conflicting interpretation will be discussed and treated below.

4.3.2.2 The Xishuigou section

The Xishuigou section is located in NE Tibet in the Subei area. In this section three authors have proposed three different magnetostratigraphic correlations yielding depositional ages that vary by about 20Ma. Gilder et al. [2001] first dated the section between 26Ma and 19Ma (Fig.4.7) while later Yin et al. [2002] correlated the same section from 33.5 to 27, and Wang et al. [2003] from 20 to 9Ma. These contrasting results are very puzzling as they lead to conflicting interpretations. It is nevertheless very important to better assess the depositional ages in this section as they bear on tectonics and climate change linked to the NE Tibet uplift.

We first output the 10,000 minimum cost correlations considering all magnetic polarity changes identified in Gilder et al.'s first column. Output correlations are presented in Fig. 4.8. The minimum cost correlation dates the Gilder et al.'s column from reference polarity chron *C5n.1n* to *C5Er* which is equivalent to the age proposed by Wang et al. [2003]. This also holds for the 10 best ones. The first solution equivalent to Gilder et al.'s interpretation is the 1171st with a cost of 10.33 and a weight of 0.27, which do not let it appear in the weighted density plot. Based on the correlation rules described above, this interpretation may thus be interpreted as improbable. The solution proposed by Yin et al. [2002] does not appear in the 10,000 minimum cost correlations output. The analyses of the density plot show two alternative solutions of the top of the polarity column. The most probable one indicates an accumulation rate decrease at ca. 13 Ma.

When looking at differences between our computed correlations and the interpretation proposed by Wang et al. [2003] it appears that : (i) we found no faulting event as interpreted by Wang et al. [2003] at polarity zone g ; (ii) in our results, 12 polarity chrons are missing which represent about 50% of the whole reference chrons for the considered period. Given the sampling density, this is unlikely. Such a large discrepancy may suggest that unknown events in the reference scale may have been identified in the Gilder et al's column as suggested by these authors [Gilder et al., 2001]. Therefore, we performed a second test where short polarity zones b and 11 supported by only two paleomagnetic samples are not considered. Results presented in Fig. 4.7c show that the minimum cost correlation (with a cost of 6.67) is then exactly the same as the interpretation proposed by Gilder et al. [2001]. The 10 best correlations are also in the same range of age. The first output correlation comparable to the interpretation proposed by Wang et al. [2003] is the 248th one with a cost of 7.94998. The weighted age density plot shows that the two alternative correlations proposed by Gilder et al. [2001] are the most probable. Then two other groups of probable

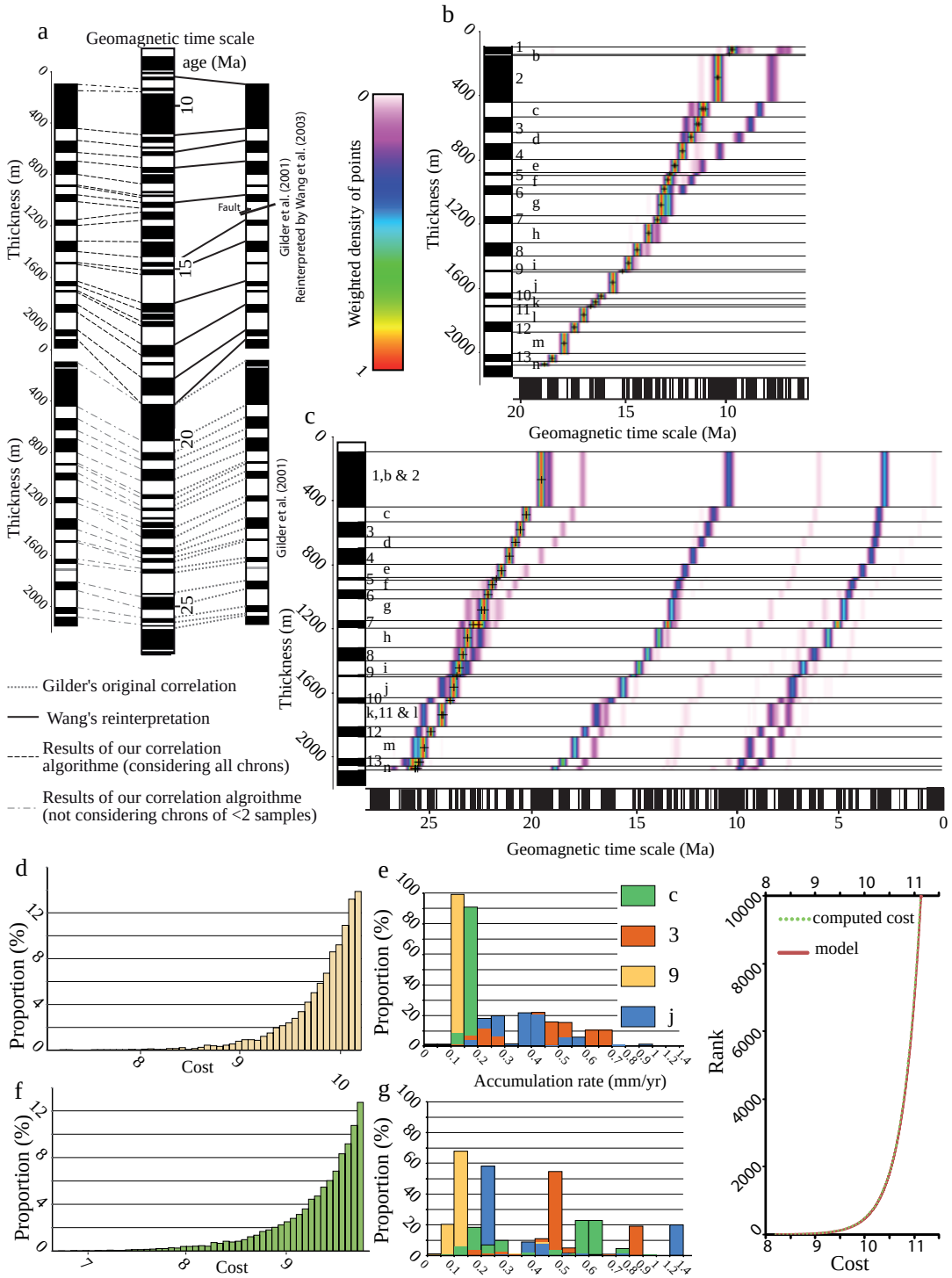

FIGURE 4.7 – Caption on next page.

Figure 4.7 – Correlation results for the Xishuigou section. (a)Comparison between correlation proposed by Gilder et al. [2001], [Wang et al., 2003] and minimum cost correlation computed considering all polarity changes sampled by Gilder et al. [2001] and only polarity zones supported by more than 2 samples. (b) and (c) weighted density age versus depth plot of the 10,000 bests correlations computed considering all polarity zones (b) and only polarity zones supported by at least two samples (c). (d) and (e), related cost distribution for the 10,000 best correlations. (e) and (g) related weighted accumulation rate distribution at polarity zones c, 3, 9 and j. (h) cost-rank function for the 10,000 best correlations considering all sampled polarity changes. The proposed model is computed thanks to equation 4.7 with $k_1 = ln(14.7)$ and $k2 = 10^9$.)

alternative solutions appears : one group corresponding to the interpretation proposed by Wang et al. [2003] and one between 2.5 Ma et 10 Ma. The solution proposed by Yin et al. [2002] is not reproduced in the computed 10,000 best correlations.
From these results we conclude that, when loose polarity zones b and 11 are removed, the most probable correlation dates the section from chrons *C6n* to *C7Ar**. Although the correlation proposed Wang et al. [2003] remains possible, no faulting event seems to be justified in the absence of other observation.

4.3.2.3 The Yaha section

In the Yaha section located in southern Tianshan, two authors also have proposed different correlations with the reference scale. Charreau et al. [2006] established the first magnetostratigraphic column which they correlated to the reference scale from 12.5 to 5.2Ma and, later, thanks to complementary sampling above the first section, from 12.5 to 1.7Ma [Charreau et al., 2009b]. The sedimentation rates derived from this correlation show a stepwise acceleration at 11Ma which authors relate to enhanced uplift in the Tianshan mountains. Huang et al. [2006] challenge this view and correlate Charreau et al's first bottom section from 9 to 2Ma which yields accelerated sedimentation rates at 7Ma, concluding that the Tianshan underwent intense deformation at this time. Despite some clues indicating that Huang's proposition was probably invalid [Charreau et al., 2008] and the fact that the upper section has been sampled since, the debate may remain open. The approach presented here enables us to decipher which correlation is the most probable following rules described in section 4.3.1.3 (fig.4.8). The analysis of the 10,000 best correlations confirms the interpretation proposed by Charreau et al. [2009b]. The minimum cost correlation faithfully reproduces Charreau et al's correlation with a small variation on the top on the polarity column and the 10,000 best correlations all show an accumulation rate acceleration between 10 and 11 Ma.

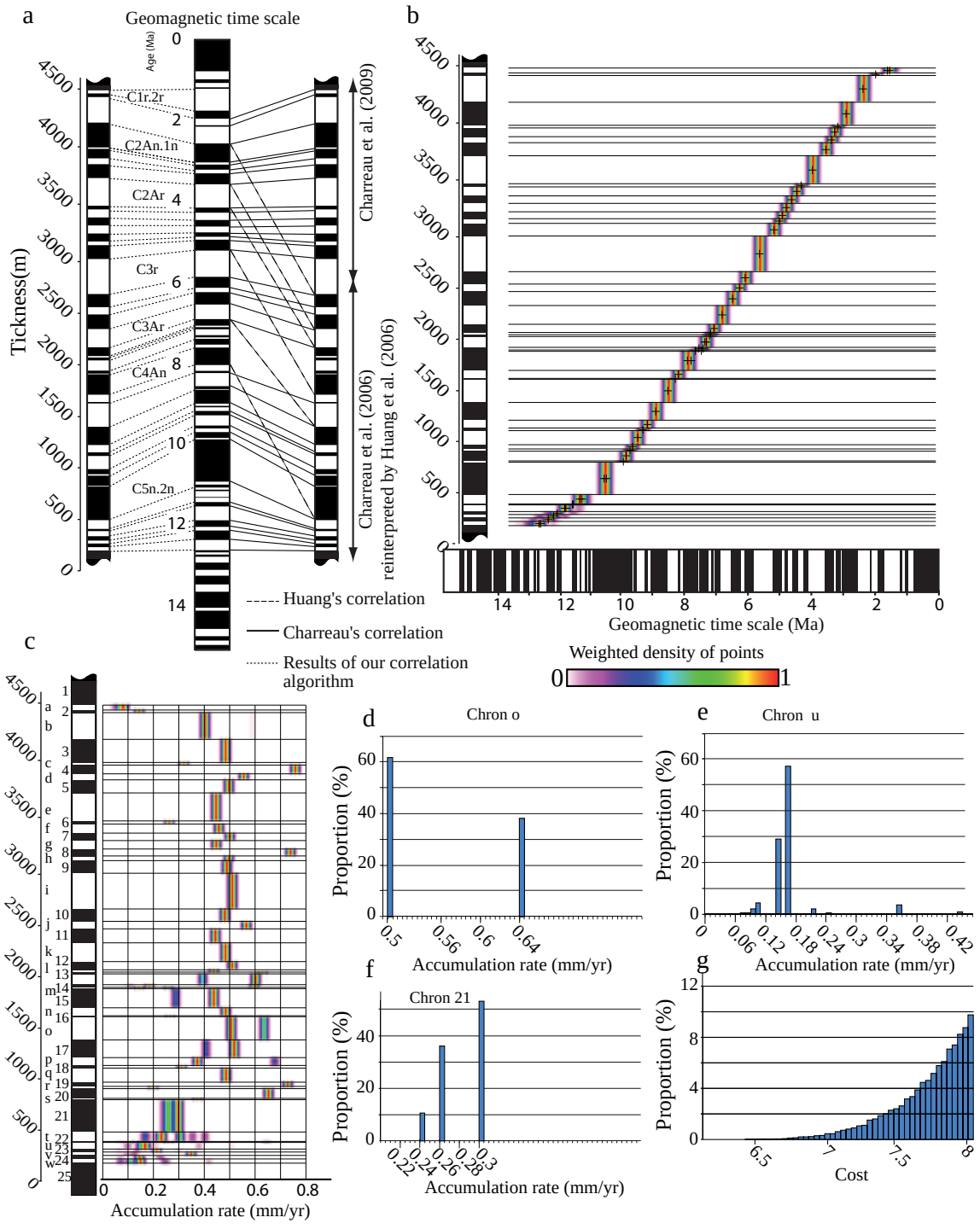

FIGURE 4.8 – Caption on next page.

Figure 4.8 – Magnetostratigraphic correlation of the Yaha section. (a) Comparison between correlations proposed by [Charreau et al., 2009b], Huang et al. [2006] and the minimum cost correlation. (b) Weighted density age versus depth plot of the 10,000 bests datings. (c) Weighted density plot of instantaneous accumulation rate. (d), (e) and (f) Histogram of accumulation rates weighted by correlation cost for chron o, u and 21. (g) Cost distribution of the 10,00 bests correlations.Magnetostratigraphic correlation of the Yaha section. (a) Comparison between correlation proposed by Charreau et al. [2009b], Huang et al. [2006] and the minimum cost correlation. (b) Weighted density age versus depth plot of the 10,000 bests correlations. (c) Weighted density plot of instantaneous accumulation rate. (d), (e) and (f) Histogram of accumulation rates weighted by correlation cost for polarity zones o, u and 21. (g) Cost distribution of the 10,000 bests correlations.

4.3.3 Certainty and uncertainty on sediments age and accumulation rates

Magnetostratigraphic data and correlation confidence. Evaluating the degree of confidence in a given magnetostratigraphic correlation is critical. It depends on the sampling density and the uncertainty degree of the polarity column correlation to the GPTS. The sampling density and its ability to ensure identification of all the polarity zones recorded in the studied section can be evaluated via s jackknife test [Tauxe and Gallet, 1991]. Uncertainty about the correlation mainly originates from : (i) the number of recorded magnetic polarity zones in the studied section and (ii) the distortion of the recorded signal. For example, a succession of three polarity zones may correlate to many parts of the GPTS while a column of fifty polarity zones, recorded in sediment deposited under constant accumulation rate, will yield a unique dating solution. In contrast, non-stationary accumulation rate, faulting event, erosion, *etc.* may lead to complex polarity columns that are difficult to correlate to the GPTS. A significant problem in magnetostratigraphy is to evaluate whether the information content of a section is sufficient to date rocks with enough confidence. From the set of realisations, a possible criterion for evaluating this aspect could be to look at the spread for the age of each polarity zone (e.g., standard deviation, interquartile range) or the number of modes of the age distribution for each polarity zone. Taking the average over all polarity zones of age standard deviations or interquartiles as a criterion seems a viable way to assess the significance of the correlations. For example, 10,000 realisations of a three- polarity zones section would undoubtedly yield a very large average age spread, meaning that we don't have enough information to deduce anything. Data are in this case considered as non-informative. Conversely, for a longer section, this average dispersion should decrease. An argument against such a procedure is that the method forces alternative solutions to be considered, hence artificially increases the spread when the number of realisations is large. However, as pointed out in Section 4.3.1.5 the correlation cost reaches a plateau when the number of computed correlations is high. Hence the weight (Eq.4.8) of unlikely realisations tends to zero. The use of the weighted standard deviation allows computing a factor characterising the capability of a column to provide dating with confidence. The

weighted standard deviation for a given polarity zone sd_w^c is defined by :

$$sd_w^2 = N' \times \frac{\sum_{i=1}^{N} w_i \times (x_i - \bar{x_w})^2}{(N'-1) \times \sum_{i=1}^{N} w_i} \tag{4.9}$$

where N is the number of realisations, N' the number of realisations with a non-zero weight w_i, x_i the age of the polarity zone and $\bar{x_w}$ the mean age of the polarity zone considering the N realisations. The mean value of the weighted standard deviation $\bar{sd}_w$ can be computed considering all polarity zones of the considered column. Following results are obtained for the Xishuigou section and the Yaha section :

- $sd_w^c = 0.03Ma$ for the Yaha section (Fig.4.8b).
- $sd_w^c = 0.72Ma$ for the Subei section considering all sampled reversals (Fig. 4.7b).
- $sd_w^c = 7.82Ma$ for the Subei section considering only the polarity zones supported by at least 2 samples (Fig. 4.7d).

A high sd_w^c suggests that the data available for the magnetostratigraphic correlation are non-informative and thus that additional data coming from other dating methods (*e.g.*, palynology, cosmogenics) should be used to better constrain the correlation.

Sampling biased and accumulation rate uncertainty From detailed accumulation rates, one may quantify subsidence, sedimentary fluxes (*e.g.* Métivier et al. [1999]) or reconstruct past erosion rates (*e.g.* Charreau et al. [2011]). Evaluating the uncertainty on accumulation rates is therefore critical to better manage these calculations. Even in the Yaha section, though good confidence exists on the correlation to the GPTS, significant uncertainties on instantaneous accumulation rates remain. Fig. 4.8c displays a weighted density plot of instantaneous accumulation rates, computed as the depth-time density plot (see section 4.3.1.5) from the 10,000 best correlations of the Yaha polarity column to the GPTS. Figs. 4.8d, e and f presents the histogram of accumulation rate calculated for polarity zones o, u and 21 respectively, calculated for each of the 10,000 correlations and weighted by each correlation cost. From these diagrams, it turns out that the accumulation rate is most uncertain for the bottom part of the polarity column where multimodal distributions are observed (polarity zones 21 to w). For example, in polarity zone u, it ranges between 0.07 mm/yr and 0.35 mm/yr, with a mode of 0.16 mm/yr. Accumulation rates calculated for polarity zone 21 are comprised between 0.24 mm/yr and 0.3 mm/yr. Above, the uncertainty decreases with accumulation rates varying between 0.5 and 0.64 mm/yr for polarity zone o.

The observed instantaneous accumulation rate is dependent on the thickness assigned to a polarity zone. Since the thickness of a given polarity zone is derived from the depth variation of the magnetic direction, discrete sampling should also yield the uncertainty on the exact position of the magnetic polarity change. This uncertainty could be quantified. Let d_a^1 and d_b^1 denote the depth of two successive samples of opposite magnetic orientation between which lies one of the two limits of the considered polarity zone is and d_a^2 and d_b^2 the depth of the two samples defining the second limit of the polarity zone. We note

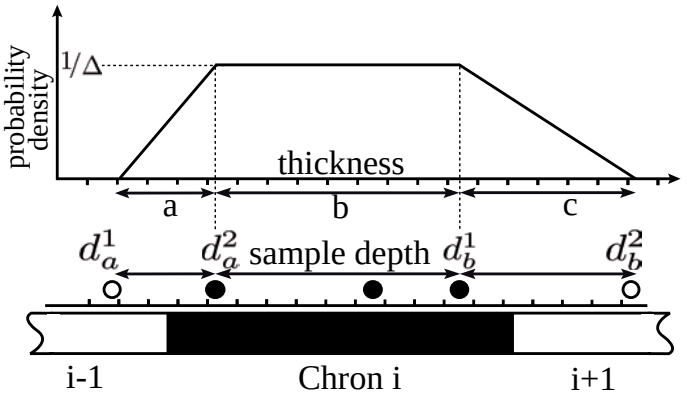

FIGURE 4.9 – Thichness probability density function $t(x)$ of polarity zone i computed from depth of samples d_a^1, d_b^1, d_a^2, and d_b^2 and distance separating these samples a, b and c.

$\Delta = max(|d_a^1 - d_b^1|, |d_a^2 - d_b^2|)$ and $\delta = min(|d_a^1 - d_b^1|, |d_a^2 - d_b^2|)$. The probability density function of the polarity zone thickness $t(x)$ (Fig. 4.9) may be taken as :

$$t(x) = \begin{pmatrix} 0 \text{ if } x < |d_b^1 - d_a^2| \\ 0 \text{ if } x > |d_a^1 - d_b^2| \\ x - d_a^2 + d_b^1/\Delta \cdot \delta \text{ if } x \in \left[|d_b^1 - d_a^2|, |d_b^1 - d_a^2 + \delta|\right] \\ 1/\Delta \text{ if } \text{ if } x \in \left[|d_b^1 - d_a^2 + \delta|, |d_b^1 - d_a^2 + \Delta|\right] \\ -x - d_a^1 - d_b^2/\Delta \cdot \delta \text{ if } x \in \left[|d_b^1 - d_a^2 + \Delta|, |d_a^1 - d_b^2|\right] \end{pmatrix} \quad (4.10)$$

Errors on chron thickness have a particular impact on the instantaneous accumulation rates computed on thin chrons. Examples of its impact can be observed on figure 4.8c where abrupt variation of the accumulation rate on thin chron (c, 4, 6 and 8 for instance) are questionable. In those cases, the thickness probability density function should be used to better evaluate uncertainties on accumulation rates. Moreover, uncertainty on chron thickness could also impact the dating. The corrective cost computed thanks to the equation 4.4 allows us to handle uncertainty on chron thickness. However it does not take into account the probability density function of chron thickness and thus does not allow to propagate it down to the accumulation rate. A way to propagate the chron thickness uncertainty down to the accumulation rate would be : (i)build n polarity columns sampling possible thicknesses of each chron ; (ii) correlate the n columns to the GPTS using the proposed approach ; (iii) compute weighted age and accumulation rate density plots from the correlations of the n columns. However, this approach, based on a simple sampling of the chron thickness, requires to generate and correlate a substantial number of polarity column and is not applicable in practice. Additional research is thus required to develop an optmized methodology.

Other sources of uncertainty in sediment dating and accumulation rate estimation come from the GTPS itself. Agrinier et al. [1999] proposed a probabilistic representation of chron age in the GPTS. This representation should be used to incorporate GPTS uncertainty on

sediment dating. However, we consider this uncertainty is low as compared to bias induced by the non stationary accumulation rate, fault, erosion and sampling strategy and, to a lesser extent, sediment compaction rate.

Conclusions

The present paper introduces a new method for correlating a given magnetostratigraphic column to the GPTS with systematic and explicit rules (or cost function, see section 4.3.1.5). Uncertainties on magnetostratigraphic correlations interpreted by geologists come from characteristics of the sedimentary record (accumulation variability, fault or erosion) but also from the subjectivity of such an interpretation. The proposed numerical approach does not claim to be objective, because correlation rules proposed in section 4.3.1 are also subjective. However these correlation rules are explicitly and mathematically expressed and can be discussed, whereas a hand made correlation cannot be evaluated without additional external constraints on the age of rocks (such as fossil, pollen fission track ...) .
The two main improvements of our method are : (i) its ability to handle, in the stratigraphic record, potential gaps either due to non sampling, sedimentary hiatus (non-deposition and/or erosion) or faulting and non stationary and variability of sediment accumulation ; (ii) the possibility to compute and analyse not only the most probable correlation but also the n best correlations of a section.
The main flaw of our technique is that we assume all polarity changes recorded in a studied sedimentary section are known in the GPTS. In particular cases, when short term chron or local sediment re-magnetization occur, this limitation may represent obstacle to a good correlation. However, such debatable chrons are supported only by few samples and represent thin chron on the sedimentary section. Since our correlation method manages gaps well, debatable chrons could be ignored in the correlation computation and thus automatically managed by adding a gap if they are actually identified in the GPTS.
The proposed correlation method offers a different approach to magnetostratigraphic studies. A large view of possible correlations of a given polarity column can be computed in a short amount of time (about 2 hours for the Yaha section when the entire GPTS is considered). A statistical study of sediment deposition age and related accumulation rate is thus possible. Moreover, the method can shed new light on hand made deterministic correlations by providing alternative solutions.

This work was performed in the frame of the GOCAD research project. The companies and universities members of the GOCAD consortium are acknowledged for their support.

4.4 Études complémentaires : analyse de la fonction coût

Le nombre de datations possibles, considérant la méthode de corrélation proposée, est trop important pour permettre de calculer l'ensemble des possibles lors d'une étude type. En effet, entre une section comprenant 25 inversions et une colonne de référence de 290 inversions (cas similaire à la section Yaha), le nombre de corrélations possibles est de l'ordre de 10^{30}. Compte tenu des temps CPU et de la place mémoire nécessaire pour calculer un grand nombre de corrélations, seul un nombre restreint de corrélations peut être calculé (20000 dans les études présentées). Afin d'estimer le nombre limite de modèles de datation nécessaire à ce que que l'ensemble des corrélations "intéressantes" soient prises en compte, nous proposons d'analyser l'ensemble des possibles dans un cas simple : la corrélation d'une colonne synthétique de 7 inversions avec une colonne de référence de 25 inversions. Quatre colonnes synthétiques sont construites en attribuant à chaque chron une épaisseur issue d'un tirage aléatoire dans une distribution uniforme entre 0 et 200 mètres. L'ensemble des corrélations possibles entre les colonnes synthétiques et la colonne de référence réduite (125 423 dans chacun des 4 cas) est ensuite calculé et analysé suivant les caractéristiques de la fonction rang-coût (Fig.4.10) et de la distribution des coûts (Fig.4.11).

La fonction rang-coût L'évolution du coût d'une corrélation en fonction de son rang est un paramètre clés de l'évaluation de la méthode de corrélation proposée. La figure 4.10 amène plusieurs commentaires :

- La fonction rang-coût est similaire pour l'ensemble des quatre colonnes synthétiques utilisées ;
- Elle présente un comportement à l'origine (Fig.4.10 B) similaire à la fonction rang-coût calculée pour la colonne de Xishuigou (Fig.4.8 h) ;
- Un plateau de valeur est atteint près de la 1000^{me} corrélation. Le coût entre la 1000^{me} et la 80000^{me} corrélation évolue relativement peu ;
- Le coût des corrélations au delà du 80000^{me} rang croie ensuite fortement.

Le paramètre le plus important de la fonction rang-coût est son comportement à l'origine. On constate que le coût y évolue très rapidement et ainsi, les corrélations "intéressantes", c'est-à-dire avec un coût proche du coût minimal, sont groupées dans les 500 à 1000 premières réalisations. Cette constatation justifie que lors d'une étude type, seul le calcule d'un nombre restreint de corrélations (c'est-à-dire permettant d'atteindre le plateau de couts) soit nécessaire afin prendre en compte l'ensemble des corrélations "intéressantes".

La distributions des coûts Les coûts de l'ensemble des corrélations possibles pour la colonne 4 (Fig.4.10) montrent une distribution log-normale dont la médiane vaut 29,45 et le mode 28. Ainsi les corrélations correspondant aux deux premiers quartiles montrent une distribution exponentielle. La méthode proposé en section 4.3.1.3 pour déterminer le nombre k de corrélations nécessaires pour obtenir les n corrélations de moindre coût est basée sur cette observation.

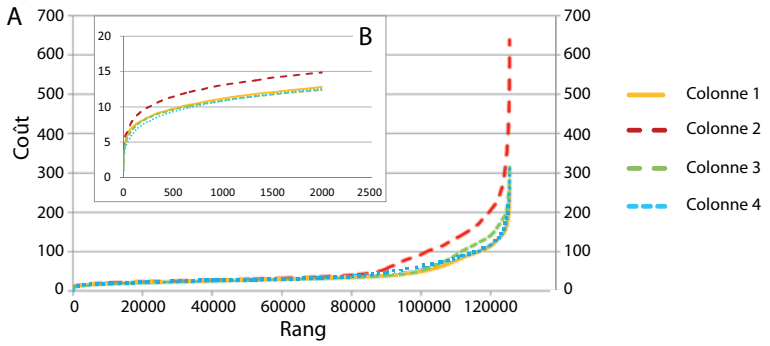

FIGURE 4.10 – Coût en fonction du rang de la corrélation pour les 125 424 réalisations possibles (A) entre une colonne de 7 inversions et une colonne de référence de 25 inversions. (B) Zoom sur les 2000 premiers modèles.

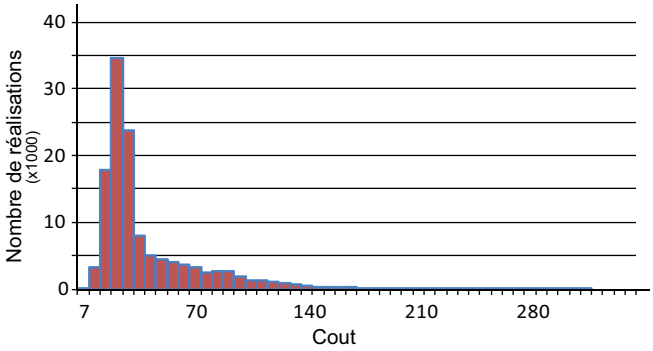

FIGURE 4.11 – Distribution des coûts de corrélation pour la colonne 1, Fig.4.10

4.5 Perspectives

La méthode présentée dans l'article précédent constitue une première étape vers une gestion des incertitudes associées à la datation des roches par magnétostratigraphie. Cependant, comme énoncé en section 4.3.3, la méthode de corrélation proposée ne prend que partiellement en compte les incertitudes liées à la qualité de l'échantillonnage. Une meilleure intégration des incertitudes résultant d'un échantillonnage discret constituerait une plus value pour la gestion des incertitudes, notamment sur les taux d'accumulation instantanés.
En effet, même si leurs effets sur la qualité des datations nous semblent mineurs, les taux d'accumulations de sédiments calculés à partir des corrélations automatiques sont fortement variables au niveau des chrons les plus fins (l'erreur relative étant plus grande pour les chrons les plus fins considérant un même pas d'échantillonnage, *c.f.* Fig.4.9). La méthode actuelle considère la position des inversions comme étant médiane entre deux échantillons de polarité différente. Il en résulte la construction et la datation d'une colonne déterministe. Afin de prendre en compte les incertitudes sur les épaisseurs de chron, une méthode simple consistant à construire un grand nombre de colonnes de polarités dont on tire aléatoirement la position des inversions (compte tenu de la position des échantillons) peut être envisagée. Les colonnes de polarités ainsi construites pourront ensuite être corrélées et l'ensemble des résultats utilisés pour déterminer les incertitudes sur l'âge des roches et les taux d'accumulation. De plus, les corrélations calculées sont comparables en ce qui concerne leurs coûts (même nombre d'inversions, âge et taux d'accumulation proches). Une étude statistique similaire à celle présentée en section 4.3.3 est alors envisageable en prenant cette fois en compte les corrélations issues du set de colonnes de polarités généré.
Compte tenu des temps de calcul nécessaires (environ 2 heures pour calculer les 10 000 meilleures corrélations entre une colonne de 25 inversions et une référence de 190 inversions), une étude intégrant les incertitudes sur les épaisseurs de chrons, et donc nécessitant de calculer les 10 000 meilleures corrélations pour un grand nombre de colonnes de polarités, n'est pas envisageable en l'état. Un moyen de réduire les temps de calcul de manière significative est de restreindre la zone d'étude en terme d'âge des roches. En effet, l'âge approximatif des roches peut être connu *a priori* (que ce soit par méthode indirecte ou en appliquant la méthode de corrélation que nous proposons). Dans ce cas, la colonne de référence passe de plus de 190 inversions à moins de 50, pour une étude similaire a celles présentées en section 4.3.2, et les temps de calcul sont alors de l'ordre de la dizaine de minutes par colonne.

Conclusions générales

Ce mémoire de thèse présente une nouvelle manière d'appréhender le problème des corrélations stratigraphiques. Dans ce travail, l'algorithme de déformation temporelle dynamique et ses variantes doivent être considérés comme des outils servant à relier un ensemble de règles de corrélations et un ensemble de données. Le choix de cet algorithme de base reste une considération d'ordre technique et c'est l'utilisation d'une méthode systématique, automatique et stochastique pour construire un ensemble de modèles de corrélations stratigraphiques qui peut être questionnée. Tout d'abord, l'approche que nous proposons, même si elle s'appuie sur des concepts de stratigraphie établis de longue date, introduit des changements dans la manière d'aborder la stratigraphie d'une zone d'étude. Ensuite, la notion d'ensemble de corrélations possibles découlant de l'utilisation de cette méthode stochastique nécessite de positionner nos travaux vis-à-vis des méthodes de modélisation de réservoirs existantes (méthodes inverses ou d'échantillonnage des incertitudes).

Sur la chaîne de construction d'un modèle stratigraphique

Les travaux réalisés au cours de cette thèse offrent une alternative à la méthode classique de construction de modèles stratigraphiques. Dans une approche de stratigraphie séquentielle, construire un modèle stratigraphique nécessite : (i) d'identifier les lithofaciès ; (ii) de décrire les environnements de dépôt associées à chaque lithofaciès ainsi que leur position dans le paléopaysage (profondeur de dépôt ...) ; (iii) de définir les unités stratigraphiques ; (iv) et de corréler les unités interprétées entre les différents puits disponibles. Ces étapes ne sont pas indépendantes, la construction d'un modèle stratigraphique est en fait une suite de tests d'hypothèses. Les corrélations de séquences stratigraphiques relie entre les puits des surfaces isochrones remarquables délimitant les unités de dépôt. Ainsi, construire une corrélation revient à construire un paléopaysage, lui-même utilisé pour définir les environnements de dépôt auxquels se rattachent les différents lithofaciès identifiés. Au delà de l'aspect laborieux d'une telle démarche, c'est la quantité et la diversité des informations et concepts à prendre en compte pour construire un modèle stratigraphique qui peut poser problème et générer des incohérences dans le modèle final. C'est en ce sens que Borgomano et al. [2008] proposent une règle trigonométrique simple liant les paléoangles définis par les corrélations des séquences stratigraphiques et les épaisseurs de ces séquences (section 1.3.2.1). Cette règle simple permet de valider ou non *a posteriori* les corrélations stratigraphiques construites et/ou les profondeurs de dépôt assignées à chaque faciès (les paléoangles étant déterminés à partir de la profondeur de dépôts des sédiments).

L'approche que nous proposons diffère de la méthode classique puisqu'il s'agit de générer

automatiquement des modèles de corrélations à partir de règles explicitement établies (et formulées mathématiquement). Ainsi, toute incohérence entre description faciologique et définition des unités stratigraphiques d'une part, et corrélation stratigraphique d'autre part, est interdite. La validation du modèle de corrélation passera alors par l'analyse de la structure tridimensionnelle des unités corrélées. Suite à cette analyse, soit le modèle stratigraphique sera validé par le géologue (compte tenu d'observations ou de connaissances non intégrées dans les règles de corrélation) ; soit les règles de corrélation (e.g. : la carte paléogéographique, voir la section 1.3.2.2) devront être revues ; soit l'interprétation des séquences stratigraphiques et/ou des lithofaciès devra être reformulés.

En magnétostratigraphie, la méthode proposée autorise à considérer un grand nombre de corrélations possibles. Dans ce cas, les corrélations générées ne mènent pas à une nouvelle interprétation des unités magnétostratigraphiques ni même à la remise en question des règles de corrélation. Elles donnent au géologue une vue d'ensemble des corrélations possibles et cohérentes et doivent le guider dans la recherche de nouveaux indices réduisant ces incertitudes.

Sur l'intégration de corrélation stratigraphique stochastique dans une étude de réservoir

Les récentes avancées méthodologiques en modélisation de réservoir ont élargi le champ d'investigation de l'espace des incertitudes. Alors qu'au début des années 1990 l'échantillonnage des incertitudes pour un modèle de réservoir s'appuyait essentiellement sur les simulations géostatistique de propriétés pétrophysiques, et/ou des faciès, dans une grille stratigraphique à géométrie et topologie constantes, les derniers développements en géomodélisation permettent de se concentrer entre autres, sur les incertitudes dues à : la géométrie des failles (*eg.* Lecour et al. [2001] et des horizons stratigraphiques (*eg.* Goff [2000], Corre et al. [2000]) et à topologie des réseaux de failles (*eg.* Cherpeau et al. [2010]).

Les travaux présentés dans ce mémoire s'inscrivent dans la continuité de ces développements méthodologiques puisque nous nous intéressons ici à la topologie des horizons stratigraphiques. Comme suggéré dans le chapitre 2, les incertitudes sur les corrélations stratigraphiques affectent fortement les modèles dynamiques. Cependant, même si ces nouvelles méthodes de construction de modèles géologiques permettent de mieux échantillonner l'espace des incertitudes, et ainsi de s'approcher de la réalité géologique, il en résulte une multiplication des modèles à prendre en compte. L'utilisation de règles de corrélations définies par des concepts de stratigraphie (notamment séquentielle ou sismique comme proposé dans les chapitres 1 et 3) permettent dans un premier temps de limiter les modèles générés à ceux acceptables d'un point de vue géologique. De plus, l'approche hiérarchique proposée dans le chapitre 1 peut permettre de générer, dans un premier temps, des modèles à faible résolution stratigraphique, validés ou infirmés *a posteriori* par

des données indirectes, comme notamment les tests d'écoulement effectués au niveau des différents puits de production. Les modèles ainsi sélectionnés peuvent ensuite servir de base à la simulation de corrélations d'unités stratigraphiques d'ordre supérieur et ainsi se positionner dans une approche multi-résolution comme proposé par Scheidt et al. [2011].

Enfin, on peut supposer que deux modèles stratigraphiques visuellement «proches » auront une réponse à l'écoulement également proche. Les corrélations stratigraphiques entre n puits peuvent être représentées sous la forme d'un chemin au travers d'un tableau de dimension égale au nombre de puits considérés. Dans cette représentation, deux modèles stratigraphiques visuellement proches correspondront à deux chemins de corrélations également proches. Cette première constatation permet d'envisager la construction d'un espace dans lequel les modèles seront positionnés les uns par rapport aux autres en fonction d'une distance représentative de leur similarité. Afin de limiter la dimension de l'espace dans lequel sont représentés les modèles stratigraphiques, les axes de cet espace peuvent être construits en regroupant les puits utilisés sur un critère de proximité géographique. On peut ainsi espérer tendre vers une représentation des modèles de corrélation similaire à celle proposée dans le chapitre 4, c'est-à-dire couplant distance entre modèle stratigraphique et vraisemblance géologique de ceux-ci, en intégrant le coût de chaque corrélation. Cette représentation peut, à terme, permettre d'intégrer les corrélations stratigraphiques à des méthodes de sélection de modèles, de calage historique ou encore de quantification des incertitudes.

Bibliographie

E. Adams and W. Schlager. Basic types of submarine slope curvature. Journal of Sedimentary Research, 70(4) :814, 2000.

P. Agrinier, Y. Gallet, and E. Lewin. On the age calibration of the geomagnetic polarity timescale. Geophysical Journal International, 137(1) :81–90, 1999.

E. R. Ainsworth. Sequence stratigraphic-based analysis of reservoir connectivity : influence of depositional architecture a case study from a marginal marine depositional setting. Petroleum Geoscience, 11(3) :257–276, 2005.

E. R. Ainsworth, M. Montree, and S. T. C. Duivenvoorden. Correlation techniques, perforation strategies, and recovery factors : An integrated 3-d reservoir modeling study, Sirikit field, Thailand. AAPG Bulletin, 83(10) :1535–1551, Oct. 1999.

U. Baaske, M. Mutti, F. Baioni, G. Bertozzi, and M. Naini. Using multi-attribute neural networks classification for seismic carbonate fades mapping : a workflow example from mid-cretaceous persian gulf deposits. Geological Society, London, Special Publications, 277(1) :105–120, 2007.

W. Bashore, U. Araktingi, M. Levy, and W. J. Schweller. Importance of a geological framework and seismic data integration for reservoir modeling and subsequent fluid-flow predictions. In J. M. Yarus and R. L. Chambers, editors, Stochastic modeling and geostatistics : Principles, Methods, and Case Studies : AAPG Computer Applications in Geology 3, 1994.

C. Bond, A. Gibbs, Z. Shipton, S. Jones, and G. Stracher. What do you think this is ¿'Conceptual uncertainty"in geoscience interpretation. GSA TODAY, 17(11) :4, 2007.

J. R. F. Borgomano, F. Fourrier, S. Viseur, and L. Rijkels. Stratigraphic well correlations for 3D static modeling of carbonnate reservoirs. AAPG Bulletin, 92 :789–824, 2008.

P. Bouchet, P. Jacquemin, and J.-L. Mallet. Goscope project : Extracting geological structures from seismic data. In 22^{nd} Gocad Meeting Proceedings, 2002.

P. Bouisset and A. Augustin. Borehole magnetostratigraphy, absolute age dating, and correlation of sedimentary rocks, with examples from the paris basin, france. American Association of Petroleum Geologists Bulletin, 77(4) :569–587, 1993.

I. M. Brown. A new method for correlation of multiple stratigraphic sequences. Computers and Geosciences, 23 :697–700, 1997.

M. Bursik and G. Rogova. Use of neural networks and decision fusion for lithostratigraphic correlation with sparse data, Mono-Inyo Craters, California. Computers and geosciences, 32(10) :1564–1572, 2006.

R. Butler. Paleomagnetism : magnetic domains to geologic terranes. Blackwell Scientific Publications, Boston, 1992.

P. Calcagno, J. Chilès, G. Courrioux, and A. Guillen. Geological modelling from field data and geological knowledge : : Part i. modelling method coupling 3d potential-field interpolation and geological rules. Physics of the Earth and Planetary Interiors, 171 (1-4) :147–157, 2008.

S. Cande and D. Kent. A new geomagnetic polarity time scale. Journal of geophysical research, 97(B10) :13–917, 1992.

S. Cande and D. Kent. Revised calibration of the geomagnetic polarity timescale for the late cretaceous and cenozoic. Journal of Geophysical Research, 100(B4), 1995.

O. Catuneanu, A. Willis, and A. Miall. Temporal significance of sequence boundaries. Sedimentary Geology, 121(3-4) :157–178, 1998.

G. Caumon, A. Tertois, and L. Zhang. Elements for stochastic structural perturbation of stratigraphic models. Proc. EAGE Petroleum Geostatistics, Cascais (A02), 2007.

T. Charles, J. M. Guéméné, B. Corre, G. Vincent, and O. Dubrule. Experience with the quantification of subsurface uncertainties. In SPE Annual Technical Conference and Exhibition (SPE 68703), 2001.

J. Charreau, S. Gilder, Y. Chen, S. Dominguez, J.-P. Avouac, S. Sen, M. Jolivet, Y. Li, and W. Wang. Magnetostratigraphy of the Yaha section, Tarim Basin (China) : 11 Ma acceleration in erosion and uplift of the Tian Shan mountains. Geology, 34(3) :181–184, 2006.

J. Charreau, Y. Chen, S. Gilder, and L. Barier. Comment on "Magnetostratigraphic study of the Kuche depression, Tarim Basin, and Cenozoic uplift of the Tian Shan Range, Western China" Baochun Huang, John D.A. Piper, Shoutao Peng, Tao Liu, Zhong Li, Qingchen Wang, Rixiang Zhu [Earth Planet. Sci. Lett., 2006, doi :10.1016/j.epsl.2006.09.020]. Earth and Planetary Science Letters, 268(3-4) :325–329, 2008.

J. Charreau, Y. Chen, S. Gilder, L. Barrier, S. Dominguez, R. Augier, S. Sen, J.-P. Avouac, A. Gallaud, F. Graveleau, and Q. Wang. Neogene uplift of the Tian Shan Mountains observed in the magnetic record of the Jingou River section (northwest China). Tectonics, 28(2), 2009a.

J. Charreau, C. Gumiaux, J.-P. Avouac, R. Augier, Y. Chen, L. Barrier, S. Gilder, S. Dominguez, N. Charles, and Q. Wang. The Neogene Xiyu Formation, a diachronous prograding gravel wedge at front of the Tianshan : Climatic and tectonic implications. Earth and Planetary Science Letters, 287(3-4) :298–310, 2009b.

J. Charreau, P.-H. Blard, N. Puchol, J.-P. Avouac, E. Lallier-Vergès, D. Bourlès, R. Braucher, A. Gallaud, R. Finkel, M. Jolivet, Y. Chen, and P. Roy. Paleo-erosion rates in central asia since 9ma : A transient increase at the onset of quaternary glaciations ? Earth and Planetary Science Letters, 304(1-2) :85–92, 2011.

N. Cherpeau, G. Caumon, and B. Levy. Stochastic simulations of fault networks in 3d structural modeling. Comptes Rendus Geosciences, 342(9) :687 – 694, 2010. doi : 10.1016/j.crte.2010.04.008.

D. R. Collins and J. H. Doveton. Automated correlation based on Markov of vertical successions and walther's law. In Computers in geology—25 years of progress, pages 121–132, 1993.

B. Corre, P. Thore, V. de Feraudy, and G. Vincent. Integrated uncertainty assessment for project evaluation and risk analysis. In SPE Annual Technical Conference and Exhibition (SPE 65205), 2000.

A. Cox and R. Hart. Plate tectonics : How it works. Wiley-Blackwell, 1986.

G. De Bruin and E. Bouanga. Time attributes of stratigraphic surfaces, analyzed in the structural and Wheeler transformed domain. In 69th EAGE Conference & Exhibition, 2007.

C. Deutsch and L. Wang. Hierarchical object-based stochastic modeling of fluvial reservoirs. Mathematical Geology, 28(7) :857–880, 1996.

C. Deutsch, A. Journel, et al. GSLIB : Geostatistical software library and user's guide, volume 2. Oxford university press New York, 1998.

C. V. Deutsch. Geostatistical Reservoir Modeling. Oxford University Press, New York, NY, 2002. 376 p.

J. Doveton. Chapter 6 : Lateral correlation and interpolation of logs. In Geologic log analysis using computer methods, pages 127–150. Amer Assn of Petroleum Geologists, 1994a.

J. H. Doveton. Lateral correlation and interpolation of logs. In Geologic Log Analysis Using Computer Methods, pages 127–150, 1994b. ISBN 0891817018.

O. Dubrule and E. Damsleth. Achievements and challenges in petroleum geostatistics. Petroleum Geoscience, 7(S) :S1 – S7, 2001.

H.-C. K. M. Dupont-Nivet, G. Tibetan uplift prior to the eocene-oligocene climate transition : Evidence from pollen analysis of the xining basin. Geology, 36(12) :987–990, 2008.

P. Durand-Riard, G. Caumon, L. Salles, and T. Viard. Balanced restoration of geological volumes with relaxed meshing constraints. Computers & Geosccciences, 36(4) :441–452, 2010.

J. H. Fang, H. C. Chen, A. W. Shultz, and W. Mahmoud. Computer-aided well log correlation. AAPG Bulletin, 76(3) :307–317, 1992a.

J. H. Fang, H. C. Chen, A. W. Shultz, and W. Mahmoud. Computer-aided well log correlation (1). The American Association of Petroleum Geologists Bulletin, 76(3) :307–317, 1992b.

F. Fluteau, G. Ramstein, and J. Besse. Simulating the evolution of the asian and african monsoons during the past 30 myr using an atmospheric general circulation model. Journal of Geophysical Research D : Atmospheres, 104(D10) :11995–12018, 1999.

F. Fournier and J. Borgomano. Geological significance of seismic reflections and imaging of the reservoir architecture in the Malampaya gas field (Philippines). AAPG Bulletin, 91(2) :235–258, 2007.

F. Fournier, L. Montaggioni, and J. Borgomano. Paleoenvironments and high-frequency cyclicity from Cenozoic South-East Asian shallow-water carbonates : A case study from the Oligo-Miocene buildups of Malampaya (Offshore Palawan, Philippines). Marine and Petroleum Geology, 21(1) :1–21, 2004.

F. Fournier, J. Borgomano, and L. Montaggioni. Development patterns and controlling factors of Tertiary carbonate buildups : Insights from high-resolution 3D seismic and well data in the Malampaya gas field (Offshore Palawan, Philippines). Sedimentary Geology, 175(1-4 SPEC. ISS.) :189–215, 2005.

T. Frank, A. Tertois, and J. Mallet. 3d-reconstruction of complex geological interfaces from irregularly distributed and noisy point data. Computers & geosciences, 33(7) :932–943, 2007.

K. Fu. Digital pattern recognition. Communication and cybernetics. Springer-Verlag, 1980.

G. Fullen. A gentle guide to multiple alignment 2.03. `www.techfak.uni-bielefeld.de/bcd/Curric/MulAli/mulali.html`, 1997.

J. Gari. Modélisation stratigraphique haute résolution 3D de systèmes sédimentaires carbonatés : les affleurements de la marge carbonatée du Beausset d'âge Cénomanien à Coniacien moyen (Provence,France). PhD thesis, Université de Provence, Marseille, France, 2007.

S. Gilder, Y. Chen, and S. Sen. Oligo-Miocene magnetostratigraphy and rock magnetism of the Xishuigou section, Subei (Gansu Province, western China) and implications for shallow inclinations in central Asia. Journal of Geophysical Research B : Solid Earth, 106(B12) :30505–30521, 2001.

G. Glatzmaier and T. Clune. Computational aspects of geodynamo simulations. Computing in Science & Engineering, 2(3) :61–67, 2000.

G. Glatzmaier and P. Roberts. A three-dimensional self-consistent computer simulation of a geomagnetic field reversal. Nature, 377 :203–209, 1995.

J. Goff. Simulation of stratigraphic architecture from statistical and geometrical characterizations. Mathematical geology, 32(7) :765–786, 2000.

C. Griffiths and S. Bakke. Interwell matching using a combination of petrophysically derived numerical lithologies and gene-typing techniques. Geological Society, London, Special Publications, 48 :133, 1990.

J. Grötsch and C. Mercadier. Integrated 3-d reservoir modeling based on 3-d seismic : The Tertiary Malampaya and Camago buildups, offshore Palawan, Philippines. AAPG Bulletin, 83(11) :1703–1728, 1999.

J. Hladil, M. Vondra, P. Cejchan, R. Vich, L. Koptikova, and L. Slavik. The dynamic time-warping approach to comparison of magnetic-susceptibility logs and application to Lower Devonian calciturbidites (Prague Synform, Bohemian Massif). Geologica Belgica, 13(4) :385–406, 2010.

L. Holden, P. Mostad, B. Nielsen, J. Gjerde, C. Townsend, and S. Ottesen. Stochastic structural modeling. Mathematical geology, 35(8) :899–914, 2003.

J. A. Howell. A fortran 77 program for automatic stratigraphic correlation. Computers and Geosciences, 9(3) :311–327, 1983.

X. Hu, E. Kirby, B. Pan, D. E. Granger, and H. Su. Cosmogenic burial ages reveal sediment reservoir dynamics along the yellow river, china. Geology, 39(9) :839–842, 2011.

B. Huang, J. Piper, S. Peng, T. Liu, Z. Li, Q. Wang, and R. Zhu. Magnetostratigraphic study of the Kuche Depression, Tarim Basin, and Cenozoic uplift of the Tian Shan Range, Western China. Earth and Planetary Science Letters, 251(3-4) :346–364, 2006.

P. Kedzierski, G. Caumon, J.-L. Mallet, J.-J. Royer, and P. Durand-Riard. 3d marine sedimentary reservoir stochastic simulation accounting for high resolution sequence stratigraphy and sedimentological rules. In J. Ortiz and X. Emery, editors, Proc. eighth Geostatistical Geostatistics Congress, volume 2, pages 657–666. Gecamin ltd, 2008.

B. Koehrer, T. Aigner, and M. Poppelreiter. Field-scale geometries of Upper Khuff reservoir geobodies in an outcrop analogue (Oman Mountains, Sultanate of Oman). Petroleum Geoscience, 17(1) :3, 2011. ISSN 1354-0793.

F. Lallier, S. Viseur, J. Borgamano, and G. Caumon. 3d stochastic stratigraphic well correlation of carbonate ramp systems. In Society of Petroleum Engineers - International Petroleum Technology Conference, 2009.

M. Lecour, R. Cognot, I. Duvinage, P. Thore, and J.-C. Dulac. Modeling of stochastic faults and fault networks in a structural uncertainty study. Petroleum Geoscience, 7 : S31–S42, 2001.

V. Levenshteiti. Binary codes capable of correcting deletions, insertions, and reversals. In Soviet Physics-Doklady, volume 10, 1966.

L. Lisiecki and P. Lisiecki. Application of dynamic programming to the correlation of paleoclimate records. Paleoceanography, 17(4) :1049, 2002. ISSN 0883-8305.

L. Lourens, F. J. Hilgen, N. J. Shackleton, J. Laskar, and J. Wilson. Orbital tuning calibrations and conversions for the Neogene Period. In F. Gradstein, J. Ogg, and A. Smith, editors, A Geologic Time Scale 2004, pages 469–471. Cambridge University Press, Cambridge, 2004.

W. Lowrie and D. Kent. Geomagnetic polarity timescales and reversal frequency regimes. In J. Channell, D. Kent, W. Lowrie, and J. Meert, editors, Timescales of the Paleomagnetic Field, pages 117–129. AGU Geophysical Monograph Series 145, 2004.

J.-L. Mallet. Geomodeling. Applied Geostatistics. Oxford University Press, New York, NY, 2002. 624 p.

J.-L. Mallet, P. Jacquemin, and E. Labrunye. On the use of trigonometric polynomials in seismic interpretation. In 22^{nd} Gocad Meeting Proceedings, 2002.

O. Man. On the identification of magnetostratigraphic polarity zones. Studia Geophysica et Geodaetica, 52 :173–186, 2008. ISSN 0039-3169.

O. Man. The maximum likelihood dating of magnetostratigraphic sections. Geophysical Journal International, 185(1) :133–143, 2011.

F. Métivier, Gaudemer, Y., P. Tapponnier, and M. Klein. Mass accumulation rates in asia during the cenozoic. Geophysical Journal International, 137(2) :280–318, 1999.

R. Moyen, J.-L. Mallet, T. Frank, B. Leflon, and R. Jean-Jacques. 3D-parameterization of the 3D geological space - the GeoChron model. In Proc. European Conference on the Mathematics of Oil Recovery (ECMOR IX), 2004.

C. S. Myers and L. R. Rabiner. Comparative study of several dynamic time-warping algorithms for connected-word recognition. The Bell System Technical Journal, 60(7) : 1389–1409, 1981.

A. Neal, J. Sequence stratigraphy hierarchy and the accommodation succession method. Geology, 37(9) :779–782, 2009. cited By (since 1996) 0.

D. Neuhaus, J. Borgomano, J. Jauffred, C. Mercadier, S. Olotu, and J. Grötsch. Quantitative seismic reservoir characterization of an Oligocene–Miocene carbonate buildup :

Malampaya field, Philippines. In G. Eberli, J. Masaferro, and J. Sarg, editors, Seismic imaging of carbonate reservoirs and systems : AAPG Memoir 81, pages 169–183. 2004.

R. Olea. Expert systems for automated correlation and interpretation of wireline logs. Mathematical Geology, 26(8) :879–897, 1994.

R. A. Olea. Correlator 5.2 - a program for interactive lithostratigraphic correlation of wireline logs. Computers and Geosciences, 30(6) :561–567, 2004.

P. Patriat and J. Achache. India-eurasia collision chronology has implications for crustal shortening and driving mechanism of plates. Nature, 311(5987) :615–621, 1984.

J. Philip. Les formation calcaire à Rudistes du Crétacé Supérieur Provencal et Rhodanien : stratigraphie et paléogéographie. Bulletin du BRGM, 3 :107–151, 1974.

J. Philip. Late Cretaceous carbonate-siliciclastic platforms of Provence, southeastern France. Memoirs - AAPG, pages 375–375, 1993.

J. Philip. Sequences and Systems Tracts of Mixed Carbonate-Siliciclastic Platform-basin Setting : The Cenomanian-Turonian Stages of Province (southeastern France). In P. De Graciansky, T. Jacquin, and V. P.R., editors, Mesozoic and Cenozoic sequence stratigraphy of European Basins, volume 60, pages 387–396. Society of Economy and Paleontology Mineralogy Special Publication, 1998.

J. M. Philip and J. Gari. Late cretaceous heterozoan carbonates : palaeoenvironmental setting, relationships with rudist carbonates (provence, south-east france). Sedimentary Geology, 175(1-4) :315 – 337, 2005.

M. Sackin, P. Sneath, and D. Merriam. ALGOL program for cross-association of non-numeric sequences using a medium size computer. Kansas Geol. Survey Special Distribution Publ, 23, 1965.

A. O. Sales, E. C. Jacobsen, A. A. Morado, Jr., J. J. Benavidez, F. Navarro, and A. E. Lim. The petroleum potential of deep-water northwest Palawan Block GSEC 66. Journal of Asian Earth Sciences, 15(2-3) :217–240, 1997.

P. Samson, O. Dubrule, and N. Euler. Quantifying the impact of structural uncertainties on gross-rock volume estimates. In NPF/SPE European 3D Reservoir Modelling Conference (SPE 35535), 1996.

C. Scheidt, J. Caers, Y. Chen, and L. Durlofsky. A multi-resolution workflow to generate high-resolution models constrained to dynamic data. Computational Geosciences, 15 : 545–563, 2011.

W. Schlager. Fractal nature of stratigraphic sequences. Geology, 32(3) :185–188, 2004.

W. Schlager. Ordered hierarchy versus scale invariance in sequence stratigraphy. International Journal of Earth Sciences, pages 1–13, 2009.

A. Seiler, S. Aanonsen, G. Evensen, and J. Rivenæs. Structural surface uncertainty modeling and updating using the Ensemble Kalman Filter. SPE Journal, 15(4) :1062–1076, 2010.

V. J.-P. I. C. Sen, S. Magnetostratigraphy and biostratigraphy of the neogene deposits of kastellios hill (central crete, greece). Palaeogeography, Palaeoclimatology, Palaeoecology, 53(2-4) :321–334, 1986.

T. F. Smith and M. S. Waterman. New stratigraphic correlation techniques. Journal of Geology, 88(4) :451–457, 1980.

S. Suzuki, G. Caumon, and J. Caers. Dynamic data integration for structural modeling : Model screening approach using a distance-based model parameterization. Computational Geosciences, 12(1) :105–119, 2008.

P. Tapponier and P. Mohar. Active faulting and Cenozoic tectinics of the Tien Shan, Mongilia, and Baykal region. Journal of Geophysical Research, 84(B7) :3425–3459, 1979.

L. Tauxe and Y. Gallet. A jackknife for magnetostratigraphy. Geophysical Research Letters, 18(9) :1783–1786, 1991.

S. J.-H. A. Tauxe, L. Depositional remanent magnetization : Toward an improved theoretical and experimental foundation. Earth and Planetary Science Letters, 244(3-4) : 515–529, 2006.

P. R. Vail. Seismic stratigraphy interpretation using sequence stratigraphy. part 1 : Seismic stratigraphy interpretation procedure. In Atlas of Seismic Stratigraphy, volume 27, pages 1–10. AAPG, 1987.

P. R. Vail, J. R. M. Mitchum, R. G. Todd, J. M. Widmier, S. Thompson, J. B. Sangree, J. N. Bubb, and W. G. Hatlelid. Seismic stratigraphy and global changes of sea level. In C. E. Payton, editor, Seismic Stratigraphy – Applications to Hydrocarbon Exploration, pages 49–212. American Association of Petroleum Geologists Memoir 26, 1977.

P. R. Vail, F. Audemard, S. A. Bowman, P. N. Eisner, and C. Perez-Cruz. The stratigraphic signatures of tectonics, eustasy and sedimentology – an overview. In G. Einsele, W. Ricken, and A. Seilacher, editors, Cycles and Events in Stratigraphy. Springer-Verlag, Berlin, Heidelberg, 1991.

T. Van Hoek, S. Gesbert, and J. Pikens. Geometric attributes for seismic stratigraphic interpretation. The Leading Edge, 29 :1056–1065, 2010.

S. Viseur. Turbidite reservoir characterization : object-based stochastic simulation meandering channels. Bulletin de la Société géologique de France, 175(1) :11–20, 2004.

M. Wand and M. Jones. Kernel smoothing. Monographs on statistics and applied probability. Chapman & Hall, 1995.

X. Wang, B. Wang, Z. Qiu, G. Xie, J. Xie, Z. Will, D.and Qiu, and T. Deng. Danghe area (western Gansu, China) biostratigraphy and implications for depositional history and tectonics of northern Tibetan Plateau. Earth and Planetary Science Letters, 208(3-4) : 253–269, 2003.

M. S. Waterman and R. Raymond Jr. The match game : New stratigraphic correlation algorithms. Mathematical Geology, 19(2) :109–127, 1987.

W. Wei. Revised age calibration points for the geomagnetic polarity time scale. Geophysical research letters, 22(8) :957–960, 1995.

H. H. Williams. Play concepts-northwest Palawan, Philippines. Journal of Asian Earth Sciences, 15(2-3) :251–273, 1997.

B. Windley, M. Allen, C. Zhang, Z. Zhao, and G. Wang. Paleozoic accretion and cenozoic redeformation of the chinese tien shan range, central asia. Geology, 18(2) :128–131, 1990.

A. Yin, P. Rumelhart, R. Butler, E. Cowgill, T. M. Harrison, D. A. Foster, R. V. Ingersoll, Q. Zhang, X.-Q. Zhou, X.-F. Wang, A. Hanson, and A. Raza. Tectonic history of the Altyn Tagh fault system in northern Tibet inferred from Cenozoic sedimentation. Bulletin of the Geological Society of America, 114(10) :1257–1295, 2002.

S. P. Zoraster. Curve alignment for well-to-well log correlation. Proc. SPE Annual Technical Conference and Exhibition, pages 2805–2808, 2004.

Corrélation stratigraphique stochastique de puits

Résumé

La corrélation entre les différents puits disponibles des unités stratigraphiques identifiées correspond à l'une des premières étapes de la construction d'un modèle de sous-sol. Les horizons stratigraphiques construits définissent, de part leur géométrie et leur topologie, l'architecture stratigraphique du sous-sol guidant simulations géostatistiques des propriétés réservoirs et des faciès. Cependant, la faible qualité et/ou quantité des données disponibles ainsi que la complexité de la mise en œuvre des concepts sédimentologiques utilisés pour construire un modèle de corrélation rendent cette étape incertaine. Afin de gérer et d'échantillonner ces incertitudes, une méthode stochastique de corrélation stratigraphique est proposée. Cette méthode se base sur le développement de règles de corrélation, assises sur des concepts sédimentologiques ainsi que sur les connaissances *a priori* de la zone étudiée. Cette méthodologie est appliquée à la corrélation de séquences stratigraphiques de la de marge carbonatée, d'âge Crétacé Supérieur, du bassin Sud-Provençal. Dans cette optique, deux règles de corrélations, basées sur la cohérence des paléoangles et sur une représentation de la paléotopographie construite *a priori* sont définies. L'étude de la répartition des faciès dans les différents modèles de corrélations générés indique que les incertitudes sur les corrélations stratigraphiques conduisent à envisager plusieurs scenarios de compartimentation de réservoir. Une étude liant corrélations stratigraphiques, simulations d'écoulement et géophysique est menée sur le champ de gaz de Malampaya. Dans ce cas, des unités diagénétiques sont corrélées afin de construire différents modèles statiques et dynamiques de ce réservoir. Cette étude permet de montrer un fort contrôle stratigraphique sur la répartition de l'écoulement alors que l'imagerie séismique semble moins affectée. L'étude de dépôts fluviaux deltaïques au niveau du bassin de la mer du Nord sert de base au développement de règles de corrélations intégrant des informations issues de l'imagerie séismique. Ces nouvelles règles de corrélations permettent de mieux contraindre le problème de corrélations stratigraphique lorsque les sédiments enregistrés au niveau des puits montrent une forte cyclicité. La magnétostratigraphie est une autre source d'information permettant d'étudier l'histoire du remplissage et de la déformation de bassins sédimentaires. Le développement de règles dédiées à cette discipline, et l'utilisation de celles-ci sur des séries sédimentaires himalayennes, permet d'appréhender les incertitudes sur l'âge des sédiments ainsi que sur les paléo-taux d'accumulation de sédiments.

Stochastic stratigraphic well correlation

Abstract

Stratigraphic correlation consists in linking boundaries of correlative units between wells or outcrops over a given study area, and is therefore one of the first steps of the characterization of the subsurface geometry, supporting geostatistical modeling of static reservoir properties. However, this early step is subject to uncertainties, since stratigraphic well correlation is constrained only by sparse observations (wells and outcrops), low resolution information coming from geophysics, regional knowledge and geological concepts. The Dynamic Time Warping (DTW) algorithm serves as a base for the development of a generic method stochastically performing stratigraphic correlation between units identified on available wells. The proposed method relies on the definition of correlation rules that are applied using the available data and some regional knowledge, according to the way stratigraphic units are defined. An application to the Cretaceous southern Provence carbonate basin has been performed using correlation rules based on paleo-angles and the theoretical architecture of the depositional environment. The computation of vertical proportions of facies on numerous models generated from the stochastic correlations of sequence stratigraphic units indicates that the uncertainties on the stratigraphic correlation impact the compartmentalization of the modeled reservoirs. The impact of stratigraphic correlation uncertainties on fluid flow behavior is assessed through the example of the Malampaya diagenetic carbonate reservoir. Diagenetic units are correlated on the basis of their wireline log signature and diagenetic types. Different models are generated from the stochastic well correlations, and the corresponding water saturation profiles are computed. They show different displacement patterns, indicating a stratigraphic control of the dynamic property, which contrasts with the synthetic seismic model constructed from the corresponding geomodel. Magnetostratigraphic correlation is another way to study sedimentary basin deposition and deformation history. Adapting the DTW algorithm to magnetostratigraphic data, we generate dating models of Himalayan deposits, for which conflicting interpretations are proposed in the literature. This allows managing the associated accumulation rates uncertainties.